Pipe and Ductwork Progress Tracking using 3D Sensing Technologies

by

Adrien Guillemet

A thesis
presented to the University of Waterloo
in fulfillment of the
thesis requirement for the degree of
Master of Applied Science
in
Civil Engineering

Waterloo, Ontario, Canada, 2012

AUTHOR'S DECLARATION

I hereby declare that I am the sole author of this thesis. This is a true copy of the thesis, including any required final revisions, as accepted by my examiners.

I understand that my thesis may be made electronically available to the public.

Abstract

Automated construction progress tracking is becoming critical to efficient and effective construction management. More and more construction companies are putting aside the old way of tracking progress, which was mainly based on foremen daily reports and visual inspections, and are adopting 3D sensing technologies as a new and modern way of tracking progress. Technologies such as 3D laser scanners (LADARs) are investigated as a means to acquire comprehensive 3D point-cloud data which can then be studied by management to determine the progress of construction. Although being much more accurate and efficient than visual inspections, this new progress tracking approach can be improved by applying object recognition algorithms that enable an automated progress tracking. This new approach has been investigated by other researchers, but only for progress tracking of structural elements. This study focuses on mechanical objects such as pipes and ducts, which would give the progress tracking a better level of detail and a wider scope. The investigation is carried out on a field database acquired during the construction of the Engineering VI Building at the University of Waterloo. It was found that the laser scanning technology is a suitable method for acquiring point-clouds of pipes and ductwork, and also that the object recognition algorithm used in this study allows a progress tracking as well as a quality tracking of the HVAC system installation.

Acknowledgements

I wish to express my sincere gratitude to Dr Carl T. Haas, my supervisor, for his effective guidance and moral support throughout the course of this study, at work as well as in everyday life. I am also grateful to Dr Ralph Haas, Dr Jeffrey West and Dr Mahmoud Ahmed for their help and support.

I also acknowledge and thank Dr. Frédéric Bosché for his collaboration. The assistance of my fellow graduate students Yelda Turkan, Arash Shahi, Afrooz Aryan and Antony Chettupuzha, as well as the undergraduate students Rida Abdull and Yazan Chaban, who collaborated on publications and/or contributed to the field data collection, is also deeply appreciated.

I would like to thank Gary Caldwell for allowing and enabling the data field acquisition on the Engineering VI Building necessary for this study.

A big thanks to Sylviane Wignacourt from Ecole Centrale de Lille for helping me getting into the MSc program at the University of Waterloo.

And finally, thanks to my family for letting me go and explore the world by myself.

Table of Contents

List of Figures

List of Tables

Chapter 1
Introduction

1.1 Background and motivation

Progress tracking in the construction industry is a huge part of construction management. Today's methods to track the progress on site are mostly conducted visually and manually (Schaufelberger, 2002), time-consuming, and may impact the quality of the progress estimations (Kiziltas et al., 2005). Additionally, those methods are not accurate and are prone to human errors that eventually lead to missed data or approximations. This research studies the advantages that the laser scanning technology has to offer to construction management in terms of data accuracy and time consumption in the progress tracking process.

The use of this technology is increasing in the construction industry (Greaves and Jerkins, 2007), however the data acquisition output is not used to automatically track the progress of construction. This thesis presents a comprehensive study of the performance of the laser scanning technology in a construction site environment on the campus of the University of Waterloo, Ontario, Canada.

Although progress tracking using 3D laser scanning technology has already been conducted by Bosché (2008) and Turkan (2012), who investigated tracking of large physical components such as floors, beams and columns, this research focuses on much smaller elements such as ducts and pipes, thus extending progress tracking in construction even further.

1.2 Objectives

Using 3D Laser scanning technology as a means to acquire point-clouds of construction sites to track the progress is a relatively new idea that needs to be further investigated. Two objectives can be drawn from this idea:

(1) The primary objective of this research is to establish the viability of using the 3D laser scanning technology to perform 3D data acquisitions of the construction site at different stages of construction.

(2) The secondary objective is to demonstrate that the algorithm Bosché (2008) can be applied to pipe and ductwork progress tracking.

1.3 Methodology

The research consists of several sequential phases. First, the problem is defined and relevant literature is reviewed. The second phase deals with field trials and data acquisition to test the technology. Thirdly, the data collected on the field is analyzed to evaluate the pipe and ductwork tracking system. And finally, conclusions are drawn and recommendations are made to conclude the study.

1.4 Thesis organization

The thesis is organized as follows:

Chapter 2 introduces some background knowledge on different technologies used as of today in construction management and progress tracking, as well as the theory behind the object recognition algorithm that is used in this study.

Chapter 3 deals with the data acquisition performed with the laser scanning technology. The different characteristics of the laser scanner are described in detail, as well as the method of acquisition and the data acquired.

Chapter 4 presents the object recognition software used in this study and the different manual necessary tasks performed on the data to make it ready for usage by the software.

Chapter 5 describes the results of the object recognition analyses performed on the data.

Chapter 6 draws conclusions and makes recommendations for future research.

Chapter 2
Background and Literature Review

2.1 Need for sensing in construction management

Until recently, progress tracking was only performed through visual inspections and foreman daily reports. Inspectors were selected and trained to ensure that work met contract schedule and specifications. Checklists were developed and distributed to the inspectors so that they did not overlook critical items. A log was at their disposal to report any deficiency that was then discussed during the weekly meeting (Schaufelberger, 2002). Monitoring progress was an extensive manual operation that required intense labor relying on personal judgment with a high probability of incomplete and inaccurate reports. In the early 2000's, the Architectural-Engineering-Construction/ Facility Management (AEC/FM) industry recognized the urgent need for quick and accurate project progress assessment, therefore the way of monitoring progress by visual inspection had to be reinvented and automated.

In recent years, many researchers came to realize the potential of several new technologies designed in the mid 1990's for automated monitoring. Among those technologies are: Radio Frequency Identification (RFID), Global Positioning System (GPS), Ultra-Wide Band (UWB), photogrammetry, and Laser Detection and Range tracking (LADAR). Research has shown that all these technologies had the potential to improve significantly productivity and savings.

2.2 Sensing technologies for material and progress tracking

2.2.1 RFID

Since Rodriguez and Jaselskis (1994) had been using bar coding as a means to track materials on a construction site, focus was cast upon the new RFID technology capable of achieving the same task but without the need for direct line of sight between tag and sensor (Razavi, 2008). An RFID tag transfers radio frequency waves that enable the reader device to locate the tag position in 2 or 3 dimensions. Line of sight is not required, it can therefore be used in cluttered environments (e.g., temporary structures, stored equipment, walls, etc.). Each tag has a unique ID which allows the system to track every item independently from the others, however the tag number cannot identify between different replicates of an available item. There are two types of tags available: passive and

active. Passive tags have no battery and their read range is short, on the other hand active tags are battery powered and benefit from a higher read range. The update rate for this technology is hourly or daily based and it is sufficient for applications such as inventory management. Recently the application of RFID-based sensing systems has been investigated in construction material tracking and supply chain management. The size of such sensors is large and the weight is heavy. Also, the cost increases in order to have higher positioning accuracy. Song (2006) studied using the RFID technology to automatically track pipe spools in lay down yards.

2.2.2 GPS

Similar achievements were made by researchers working on the GPS technology. GPS is a global navigation satellite system that requires an unobstructed line of sight to four or more GPS satellites to provide location information. Its widespread availability is an advantage for this technology. In a case where very accurate data is required, higher installation and maintenance costs are involved. The GPS technology produces accurate coordinates enabling the tracking of materials with substantial rapidity. The system also enables construction progress estimation, mining, landslide monitoring, etc. However, the application of GPS is restricted to outdoor uses as its signal is altered by multipath effects in indoor environment.

2.2.3 UWB

Any signal with a relative bandwidth larger than 20% or absolute bandwidths greater than 500 GHz is considered as an UWB signal. The use of UWB technology in real-time tracking of construction materials and resources is becoming more valuable because of the rising competition between construction companies, more accurate work performance demand, budget restrictions and tighter schedules. UWB is therefore investigated as the technology for indoor material monitoring, as well as workforce tracking, and equipment positioning (Teizer et al. 2008). UWB provides a large coverage area and a real-time data collection capability that can be used for safety management. The main advantages for UWB systems are: low power, low cost, precise positioning with high data rate and very low interference with other available wireless systems. However, some challenges are associated with UWB systems. Because of the very large bandwidth occupancy UWB systems, it is necessary to have a regulation in order to avaoid interference between different users. Another problem is the lack of standards which the industry agrees to make the UWB devices interoperable. And although UWB

promises a low-cost technology, low-power operation, resolving the interference may increase the cost of the technology.

2.2.4 Photogrammetry

Photogrammetry is the art and science of deriving accurate measurements of real world objects from imagery. Although photogrammetry has been studied and applied for centuries, many of its core principles and methodologies have been developed over the last two centuries (American Society of Photogrammetry, 1980). In particular, aerial photogrammetry was used extensively in the 20th century because of the importance of measuring topographies for a variety of reasons that range from strategic military to real estate and environment conservation considerations. Close range photogrammetry usually refers to that branch of photogrammetry wherein the distance between the object and the camera is less than 300 meters. Close range photogrammetry has been applied in a wide variety of disciplines including manufacturing, medical, sport, biology, zoology, preservation of cultural heritage sites, aerospace and forensic sciences. Within the civil engineering domain it has been used for structural monitoring (Fryer et al., 2007), deformation measurements (Niederöst et al., 1997), concrete crack measurements (Liang-Chien et al., 2006), project progress tracking (Golparvar-Fard et al., 2009, El-Omari et al., 2008). Research initiatives are being conducted to determine the suitability of photogrammetry for automated construction progress monitoring (Ahmed and Haas, 2010). The availability of high resolution and relatively inexpensive digital cameras, comprehensive photogrammetry software packages and powerful but relatively inexpensive computing processors has meant that reasonably accurate close range photogrammetry can now be conducted for significantly lower costs than traditional analog methods.

2.2.5 Laser scanning technology definition

The terrestrial three dimensional laser scanning technology, also named LADAR (Laser Detection and Ranging), is an imaging technology expanding in use since the 90's, that is used as an efficient tool to acquire 3D point clouds. Laser scanners are based on two main technologies: (1) time-of-flight or pulse-based, and (2) phase-based (Jacobs, 2008). Pulse-based scanners send a laser pulse in a narrow beam toward an object and then estimate the distance to the object based on the time the pulse takes to be reflected from the object back to the scanner. Phase-based scanners measure the distance to the object by calculating the phase shift in a continuously emitted and returned sinusoidal wave as the wave hits the object. Pulse-based scanners can be used for long-range applications up to 1 km,

while phase-based scanners are better suited for low-range applications up to 50 m (Jacobs, 2008). The development of this technology over the years enables users with a wide range of applications by accurately acquiring three dimensional data for a whole construction scene (Stone and Cheok, 2001). The acquired data is represented by a point cloud where every point contains coordinate information regarding its position in space. The generated point cloud represents every object surface within visible range. The LADAR technology was considered by many as the top technology to capture project point clouds with accuracy and speed (Cheok, 2000). These 3D point clouds can be considered as an end product or can be used for further purposes such as the creation of as-built CAD models for progress tracking and quality control.

LADAR technology has proved to be valuable for construction managers to help them on many tasks such as material tracking, progress monitoring, quality control and facility/infrastructure management (Akinci and Anumba, 2008). On the same aspect, Golparvar-Fard et al. (2009) note that such a tool allows managers to remotely explore the construction site and be used for contractor coordination purposes. Huber et al. (2010) are studying the laser scanning technology for analyzing surface flatness, quality assurance, floor plan modeling and recognition of building components. Measurement of deterioration for infrastructure is also being investigated: tunnels (Qui and Wu, 2008, Biddiscombe, 2005), bridges (Park et al., 2007), and freeways (Yen et al., 2008). Researchers are using the possibilities offered by the LADAR technology to monitor landsliding and any soil deformation measurement. Lijing and Zhengpeng (2008) show that the technology offers an advantage over traditional methods of surveying that overlook minor local deformations. All of these examples show the large range of applications that cover the laser scanning technology today, and this variety of applications involves a need for a reliable and cost effective method of point cloud acquisition of construction sites.

Greaves and Jerkins (2007) show that the market for the three dimensional laser scanning hardware and software as grown exponentially in the last decade. However, the technology is not used to its full potential as it is merely used to extract dimensions. Automatic object recognition techniques from 3D laser scans have been developed for project management and quality control applications. Recent developments in object-based recognition techniques enable the retrieval of 3D computer-aided design (CAD) objects from laser-scanned data (Bosché & Haas, 2008, Bosché et al., 2008, Bosché et al., 2009). In Bosché's method, the 3D model of the scanned environment is used as-priori knowledge for recognizing objects from the scanned 3D point clouds. In this method, the 3D model is utilized to

identify the relative position of the object to be recognized from the scanned point cloud. Therefore, the object recognition system has a-priori expectations of where to find each element, given that the 3D model and the scanned point cloud are correctly registered together.

2.2.6 Selecting the 3D imaging approach

As explained by Ahmed et al. (2011), photogrammetry and laser scanning technologies both have advantages and disadvantages. Many factors have to be considered when choosing between the two technologies such as: (1) purchasing cost, (2) training time, (3) point-cloud resolution, (4) portability, (5) lighting, (6) constraining environmental and weather conditions recommendations, (7) eye safety distances and health issues and (8) data processing time. Habib et al. (2004) and El-Omari et al. (2008) proposed approaches integrating photogrammetry and laser scanning, which would be the ideal situation. However in this study, the choice was made to use only the laser scanning technology for reasons including point-cloud resolution, data processing time and the ability to perform point-cloud acquisition in poorly lighted spaces.

2.3 Object recognition

2.3.1 Previous object recognition approaches

Some object recognition methods already exist, but they all have one major issue: they all operate on single objects in controlled environments, while this study considers a multitude of objects (e.g., pipes and ducts). Also, some of those methods, if applied to this research, would fail because of their non-discriminative approach, on the other hand the method developed by Bosché (2009) estimates the location of where the object should be, thus simplifying the approach.

2.3.2 Object recognition approach used in this research

The approach used here is based upon Bosché and Haas (2008), Bosché et al. (2010) and Turkan et al. (2012) which recognizes 3D objects in point clouds. The 3D objects are all contained within a single 3D CAD model called the "3D as-planned model", while the point clouds are obtained by using the 3D laser scanning technology and referred to as the "as-built" model. Therefore, Bosché (2009) compares the 3D as-planned model with the as-built model by matching the objects of the former with the points of the latter. Occlusions that could appear on either 3D model objects or non 3D

model objects (e.g. temporary structures, stored equipment, workers) are mostly a non issue as the approach typically proves to be robust enough to deal with them.

In a nutshell, the system requires (1) the conversion of both 3D as-planned model and as-built point-cloud into open-source formats, and then goes on with (2) a Manual coarse registration, (3) a Model fine registration, and finally (4) the Object Recognition itself. The different steps are further developed below.

2.3.2.1 Format conversion

The information contained within the 3D as-planned model and the as-built point-cloud must be fully accessible for this approach to be effective. However, 3D CAD models are stored in protected CAD engine formats such as (DXF), (DWG), (DGN); and point-clouds in (FWS). This explains the need to convert the 3D CAD model and as-built point-cloud into open-source formats. The 3D CAD model needs to be converted into a triangulated mesh format. The (OBJ) format approximates the 3D objects surfaces by a triangulated surface and leaves out the information of color, texture and other common CAD model attributes. It is important to note that in Bosché (2009), the triangulated mesh format used is not (OBJ) but STereoLithography (STL). However the (OBJ) format is the format used in this study because of software compatibility issues, as the software used in the format conversion only exported in (OBJ). As for the as-built point-cloud, it needs to be converted into an ASCII file: the (ASC) format is used in this study.

2.3.2.2 Manual coarse registration

The coarse registration is the operation that is performed to place the 3D as-planned model and the as-built point-cloud in the same coordinate system. This step is performed with a n-point registration approach by manually picking at least 3 pairs of matching points between the 3D as-planned model and the as-built point-cloud. Several software packages enable this operation; among those are Trimble™ RealWorks® (2007), and Faro Scene® (2007). However, the coarse registration does not prove accurate and reliable enough to be used as such, as only a few pairs of points were chosen. A second registration is necessary to improve the result of the coarse registration. This second registration is referred to as “fine registration”.

2.3.2.3 Fine registration

This step is performed by using an optimization algorithm that uses the results from the coarse registration and then locally searches for a better one. This step is referred to as "fine registration". A robust Iterative Closest Point (ICP) algorithm was specially developed for this system to perform the fine registration of a 3D model of a building under construction with a laser scan. The transformation (translation, rotation) is iteratively revised to minimize the distance between the as-built point-cloud and the 3D as-planned model using a least square optimization tool (Bosché, 2009). The steps are described below.

2.3.2.3.1 Selection of points in the as-built

All of the points contained within the as-built can be used for registration. However this selection is time consuming, which triggered the implementation of a robust data sampling algorithm that significantly reduces the processing time without jeopardizing the accuracy of the system.

2.3.2.3.2 Calculation of matching points in the 3D as-planned model

For each point within the 3D as-planned model, now in (OBJ) format, is calculated the closest of the orthogonal projections of the as-planned point on the object's triangulated facets. This method rejects the points with no orthogonal projection on any of the object's facets, which translate into rejecting the points at the borders of the objects. The Point Matching Algorithm is further detailed in Section 2.2.2.3.5.

2.3.2.3.3 Error metric

The error metric is defined as the Mean Square Error (MSE) of the Euclidian distance between pairs of matched points. Also, to ensure the robustness of the metric, points are rejected when:

(1) The Euclidian distance between two matched points is larger than a threshold τ_D. τ_D is adjusted at each iteration k with the formula:

$$\tau_{Dk}=\max\{2\sqrt{MSE_{k-1}};\varepsilon_{const}\}$$

where MSE_{k-1} is the MSE obtained at the (k-1)th iteration, and ε_{const} is a constant distance that can be interpreted as the maximum distance at which objects with dimensional deviation should be searched

for. In the results presented in this study, ε_{const}=50 mm. This value is chosen to be (i) large enough not to fail to recognize objects due to sensor inaccuracies; (ii) large enough not to fail to recognize objects that are built at a position up to 50 mm away from their expected position; but (iii) small enough not to mismatch *Data* and *Model* points corresponding to different objects.

(2) The angle between the normal vectors to two matched points is larger than a threshold τ_A. In the results presented in this study τ_A=45° as a default value.

2.3.2.3.4 Termination criterion

The iterative process is stopped when the MSE improvement between the current and previous iterations is smaller than 2 mm^2.

2.3.2.3.5 Point matching algorithm

Several matching strategies have been proposed in the past. The three main matching strategies are: (1) point-to-point (Besl and McKay, 1992), (2) point-to-plane (Chen et al., 1992) and (3) point-to-projection (Blais et al., 1995). Although the first two startegies generally result in more accurate registrations (Park et al., 2003, Rusinkiewicz et al., 2001), the third algorithm however, enables faster calculations at each iteration. The point-to-point matching algorithm is the algorithm used in this study with point rejection and acceleration techniques to decrease the computer time processing.

The algorithm calculates for each scanned data point, P_D, a matching model point, P_M that is the closest of the orthogonal projections of P_D on the CAD model's triangular facets. Acceleration techniques can be used to quicken the procedure by narrowing down the set of facets among which the closest projection is.

Distance-based outlier rejection is commonly applied in ICP algorithms, and is applied here with the threshold τ_D. As illustrated in Figure 1, a frustum can be constructed for each as-built point, centered on the point's scanning direction (ray), and with opening spherical angles equal to:

$$\alpha_\varphi=\alpha_\theta=2 \arctan (\tau_D/P_D.\rho)$$

where $P_D.\rho$ is the range of the given as-built point P_D. This point's frustum has the following characteristic: if the distance between the point and its orthogonal projection on a facet is lower than τ_D, then the facet must intersect the frustum. The other important characteristic is that the facets of

construction project 3D CAD models are naturally grouped into at least three hierarchical groups: single facet, object and model, as shown in Figure 2 below.

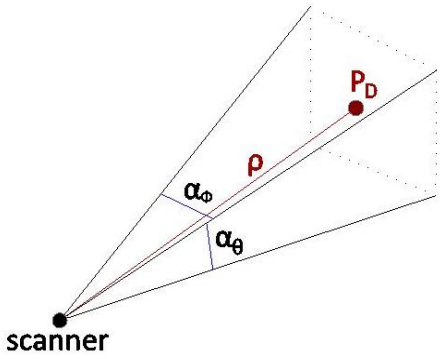

Figure 1: Frustum of a data point, P_D

Based on these observations, the following method to accelerate the designed point-to-point algorithm was developed by Bosché (2008). First, a Bounding Volume Hierarchy (BVH) is calculated for the project 3D CAD model where each bounding volume is the frustum of a facet hierarchical group, as identified in Figure 1. Then, back-facing culling and frustum culling are performed to remove all the facets from the BVH on which no matching point can possibly be found. Finally, for each scanned as-built point, its frustum is calculated as described above. The facets on which the matching as-planned point may be found (i.e., on which the orthogonal projection should be calculated) are identified by going through the model's BVH. They are the facets whose frustums intersect the as-built point's frustum. The BVH, back-facing and frustum culling depend on the registration, (i.e., location of the scanner), so they must be recalculated each iteration of the fine registration algorithm. However, they enable a significant acceleration of the algorithm despite the necessary recalculations.

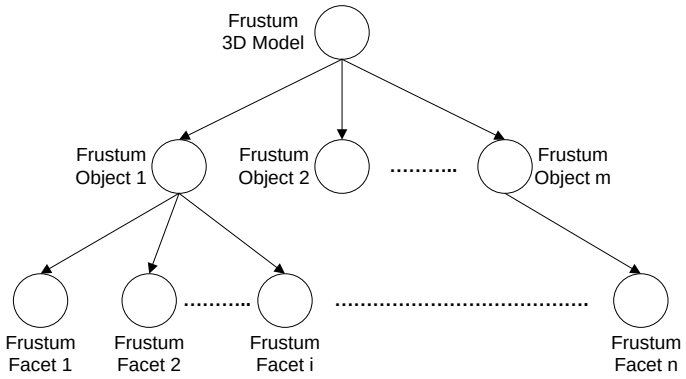

Figure 2: Facet hierarchical groups in a 3D CAD model

2.3.2.4 Object recognition

At the end of the registration process, the 3D as-planned model and the as-built point-cloud are optimally registered. The analysis of the as-built point cloud can then lead to the recognition of the object itself using the recognition metric defined in (Bosché et al., 2009). For each object, its recognized surface, $Surf_R$, is calculated based on the number of recognized points, their distances to the scanner and the scan's angular resolution. If $Surf_R$ is larger than or equal to $Surf_{min}$, then the object is considered recognized; it is not otherwise. Both $Surf_R$ and $Surf_{min}$ are calculated as a function of the scan's angular resolution. Thus the object recognition metric used here is invariant with the scan angular resolution and the distance between the scanner and the object. Detailed information can be found in (Bosché et al., 2009).

Chapter 3
Data Acquisition

The automated pipe progress tracking approach presented in this study is investigated with a comprehensive as-built point-cloud database from a building under construction. This chapter gives information about the construction site, the characteristics of the laser scanner used, the field data acquisition, and the data collected.

3.1 Construction site: Engineering VI building

The fieldwork program of this research was conducted on a construction site on the campus of the University of Waterloo. The Engineering VI Building is a new 5-storey 100,000-square-foot building designed to house the Chemical Engineering Department of the University, was a perfect fit for this study: indeed, a chemical facility like this building provides a large number of pipes and ducts designed to collect and evacuate chemical fumes from the different labs of the building, or to provide water and gas to those labs. Figure 3 and 4 show the Engineering VI building.

Figure 3: Design drawing of Engineering VI (Courtesy of Aecon®)

Figure 4: Engineering VI under construction, University of Waterloo

3.2 Data acquisition equipment

3.2.1 Faro Laser Scanner

The laser scanner that is used in this study is a FARO Laser Scanner LS 840 HE, shown in Figure 5. This scanner is considered an advanced surveying and spatial imaging sensor that uses the time-of-flight technology to determine the distance of objects from its mirror, and allows the collection of millions of points with a high spatial resolution. Table 1 shows the technical specifications of the laser scanner.

Table 1: Technical specifications of Faro Laser Scanner LS 840 HE

Range	0.6m to 40m
Resolution	Up to 700,000,000 points
Measurement Speed	120000 Hz
System Distance Error	+/-3mm at 20m
Laser power	20mW
Wavelength	785nm
Beam Divergence	0.025 mrad
Beam Diameter at exit	3mm, circular
Vertical Field of view	320°
Horizontal Field of view	360°
Weight	14.5kg
Ambient Temperature	+5° / +40°

Figure 5: Faro Laser Scanner LS 840 HE

3.2.2 Utilization of the equipment

3.2.2.1 Total station

The scanning process implies the setup of the laser scanning station, in Figure 6, with all its necessary equipment. The list of all the required items is shown in Table 2.

Table 2: Laser scanning station items

Item	Components
Laser scanning kit	-laser scanner -tripod -wires -user guide
Targets	-spheres -paper targets
Safety perimeter kit	-poles -tape
Laptop	
Power source	

Figure 6: Laser scanning station

3.2.2.2 Use of targets

Since 3D laser scanners are instruments that can only sense what is in their field of view, multiple scans are necessary to cover all the invisible angles from the point of view of the laser scanner at its first location, hence the use of targets to enable the user to register the scans later on. Thus, the targets are used as common reference points between the different scans to be able to register them all together as described in Section 3.5.2.2.

In theory, the requirement for the use of the targets is that a minimum of 3 targets must be common between 2 scans to be able to register them. Each of those targets suppresses one rotational degree of freedom between the scans. So it is also required that the 3 targets do not form a straight line which would leave out one rotational degree of freedom. It is advised to disperse the targets as much as possible in the scene to avoid any registering problem of that nature.

It is also advised to use more than 3 targets to avoid occlusions. Scanning a construction site implies a living scene where construction workers might be working at the exact location where the scan is being performed, which means that some of them might get in the way of the targets during the scan

acquisition, which would result in the loss of one of the 3 common targets and resulting in the impossibility to register the scans. This type of registering issue is called an occlusion. An occlusion can also be caused by a temporary structure being setup or moved between the laser scanner and the target. Thus, it is strongly recommended to use more than 3 targets to make sure than at least 3 of them will be visible in both scans. Five targets are usually enough to ensure the success of the registration later.

Another recommendation for the use of the targets is to communicate with the construction workers by explaining to them why it is extremely important that no target be moved or removed before the scans that are going to need those targets to be registered are performed. One moved target, even from a few centimeters may cause another registering issue.

Different kind of targets can be used:

(1) Spherical target: these targets are not always easy to position in the scene, especially at the early stages of the construction if the structure of the building under construction is only composed of concrete. Indeed, a spherical target uses a magnet as a means to be attached to a surface. Therefore, when no metallic surface is present on the site, then another type of target might be a better alternative, or a tripod can be used to position the sphere. The main advantage of this type of target is that it can be seen from every possible angle and still have the same form, therefore the target can be placed in the middle of the scene and thus reducing the number of scans. The spherical targets are shown in Figure 7.

Figure 7: Spherical targets

(2) Paper target: based on the difference of contrast between a white circle and a dark background, those targets can be positioned anywhere in the scene on a flat surface using some tape. They are easy to positioned, but can be hard to use for registration purposes if the angle from which they are seen is too big. Therefore, the user has to pay attention with this type of target compared to a spherical target. Also, these targets have to be placed on the sides of the scene, thus increasing the number of necessary scans. A paper target is shown in Figure 8.

Figure 8: Paper target

(3) Any flat surface: the software used for data processing purposes in this study, Faro Scene®, allows the user to use a flat surface anywhere in the scene to be used as a registering target. Therefore, if any of the registering issues listed above ever occurs, the user can use a wall, the floor, or the ceiling as a target.

Considering the different features, the number and the kind of targets used are completely dependent of the geometry of the scene as well as the materials composing the scene.

The number of targets at disposition is always critical. Indeed, with a laser scanning kit always comes with a set of spherical targets, but the set is only composed of a limited number of spherical targets. In that case, the use of the other targets is to be considered

A target can be shared between many scans if needed. Once a target has served its purpose for any given set of scans, it can be removed and reused between other scans. It is critical to identify which

target will not be useful again at its current location. To avoid that kind of issue, a scanning layout can prove useful.

3.2.2.3 Scanning layout

Developing a scanning layout before performing the scan can prove very useful. The scanning layout is a map of the facility that references the consecutive locations of the laser scanning station with the position of all the targets. This tool enables the user to make sure that all the targets are going to be visible from the point of view of the laser scanner and also that all the scans that are about to be acquired will have the proper number of targets to be registered with the others. It is also a practical way to ensure that no area is forgotten in the scans. It takes an experienced user to make the scanning layout obsolete. Such a user can foresee the upcoming locations of the future targets as well as the laser scanner's location.

3.2.2.4 Parameters

Before starting to perform the scan, different features can be adjusted such as the angle and the resolution of the scan. The resolution of the scan is the number of points contained in the acquired point-cloud. Table 3 and 4 respectively show the range of angle and the choices of resolution for the laser scanner.

Table 3: Angle parameters

Max vertical	+90°
Min vertical	-70°
Max horizontal	0°
Min horizontal	+360°

Table 4: Resolution and eye safety parameters

Resolution (number of points)	Eye Safety Distance (m)
7,000,000	0.3
11,000,000	0.7
28,000,000	1.0
44,000,000	1.3
175,000,000	2.5
700,000,000	4.9

It is to be noted that as the resolution goes, the safety perimeter around the scanner increases due to the longer exposition to the laser ray which increases the risk for eye damage. The construction site is a living environment where people work and walk through. Therefore, the resolution that is chosen needs to be sufficient for the purpose of the study but also respectful of the workers. A safety perimeter too large could cause frustration to the workers who now have to go around the perimeter by taking another route to get to their work station. Ultimately, their cooperation will be altered and targets could be removed.

3.2.2.5 Scanning

Once the parameters have been adjusted, the scan can be performed. The scan time differs with the resolution chosen as can be seen in Table 5.

The resulting data of the scanning process is called a point-cloud and contains geo-spatial information of the scanned environment in a Cartesian coordinate system with the value of the intensity of the laser beam back to the scanner. The intensity of the beam is proportional to the distance between the object and the laser scanner, thus enabling the software to calculate the distance.

Table 5: Laser scanner resolution specific characterizations

Resolution (number of points)	Scanning Time (min)	Number of points in the generated point cloud (Millions)
7,000,000	1.11	7
11,000,000	1.74	11
28,000,000	4.44	28
44,000,000	6.94	44
175,000,000	27.78	175
700,000,000	111.11	700

3.3 Laser scanning characteristics

3.3.1 Training / Expertise

The use of a laser scanner requires training on both on-site point-cloud acquisition and point-cloud data processing. A 3-day training session is offered at the purchase of the equipment to deal with data acquisition. However, a certain experience is required when it comes to identifying the laser scanner setup locations as well as the target locations to ensure that the acquired point-cloud can be related to other point-clouds. Experience is handy when it comes to being sure that such a problem will not occur. That experience is built up with time: a few weeks making those mistakes can provide that experience. An additional week of training is needed to acquire all the necessary experience to deal with point-cloud data processing by merging all the different point-clouds into one. That experience will include dealing with registration problems such as low-resolution target and target occlusion that are the major problems in the point-cloud creation process.

3.3.2 Portability

The portability of the laser scanning equipment is an important consideration. The technical sheet indicates that the laser scanner weighs 14.5kg, which does not include the additional equipment that is required, such as laptop, targets, extension cord, and what is needed to establish the eye safety distance perimeter around the scanner location. Carrying all this equipment is very time-consuming if

they are not stored directly on site, and even then at every change of laser scanner location the whole station must be relocated. Ultimately, the relocation of the station is as time-consuming as the scanning step in the whole data acquisition process, with 10 minutes each, mostly due to the laser scanning equipment poor portability.

3.3.3 Labor hours

Table 6 below shows the distribution of time consumption. These estimates were made from the average of 150 observations.

Table 6: Labor hours for data collection and processing

Activity	Time
Data acquisition training	3 days
Pre-processing software training	1 week
Calibration	N/A
Establishing the layout plan to scan	10min
Putting up the targets for registration	3min
Mobilizing the station	10min
Point-cloud acquisition	10min
Moving the station to next location	10min
Data pre-processing	5min

The data acquisition training is fairly quick and much easier compared to the pre-processing software training required to be able to merge together the different point-clouds using the targets. The calibration of the laser is not performed by the user due to the complexity and dangerousness of the technology.

The laser scanning process implies the deployment of the laser scanner station inside the building under construction due to its scanning range and precision. Once the area to scan has been determined, the positions of the successive stations must be planned. This decision is made by considering different factors, such as scanning range, desired precision and accuracy, and occlusions. When the scanning layout plan has been established, the last task to perform prior to mobilizing the scanning station is to determine the position of the registration targets. The targets must be positioned in the scanning environment by making sure that at least three of those targets will be in common between the first scan and the next. This process will ensure the success of the registration step which assembles the set of scans into one unique point cloud that represents the scanned area. Once all of the preliminary tasks have been performed, the station can be mobilized. A power source, which is usually available on site, is required to enable the laser scanner. At this point, the scanning process can be performed.

3.3.4 Constraints

There are a number of constraints associated with using these technologies on a construction site. The first package of constraints concerns the weather conditions during which the laser scanner is being used. The ambient temperature must be between 5°C and 40°C and the humidity non-condensing. The most important constraint of all is the eye safety distance concerning the laser beam: depending on the purpose of the laser scanner use (as-built data collection or progressing tracking data collection), a certain resolution is to be chosen prior to the scanning process. This choice will involve a different eye safety distance requirement. Establishing a safety perimeter around the laser scanner on the construction site can be challenging, keeping in mind that construction workers might be on site while scanning, which involves restricting their working area for the time of a scan collection. Another constraint is the target positions. For a point cloud to be useful, it has to be referenced into a known space coordinate system, which involves placing targets on scene that can be seen from another point cloud acquisition location. Point-clouds are usually acquired in a sequence on site before any data processing is done, which means that if a point-cloud in the middle of the sequence cannot be related to the others, a long time will be spent on manually merging those clouds into one common coordinate system. Thus, those targets sometimes have to be placed in difficult-access location and not to be removed until the two point-clouds have been acquired. The last practical constraint concerns the energy supply of the station which can be problematic at the early stages of construction.

The scene lighting is not a constraint for a laser scanning acquisition that relies on a laser beam travelling time such as the FARO LS 840.

3.4 Description of field data acquisition

The E6 Building was scanned from June 2010 to February 2011. It is important to note that no scan was performed between December 2010 and January 2011 because of the inability of the Faro Laser Scanner to function below 0°C. The building was finally enclosed in February 2011, hence the restart of the point-cloud acquisition.

3.4.1 First data acquisition

A first experiment was conducted in June 2010 to make sure that the technology chosen for the purpose of this study was in fact going to be efficient in performing scans of the building and processing of the scans to turn them into one single point-cloud of the whole building.

This series of scans was conducted when only the structure of the building was done, meaning that only the floor, the ceiling and the columns were completed. The state of the construction at that time was perfect to experiment with the technology and to learn how to use it properly without paying much attention to occlusions. One of the four staircases was used to connect the different floors together by performing scans from the inside of the staircase and making sure that targets from both floors are visible from the scanner's location, which is not always an easy task.

Much of the attention of the construction at that point was focused on the fifth floor, while floors below were less busy. This means that a lot of material and temporary structures were present on the fifth floor compared to the deserted floors below. This explains the decreasing number of scans performed for every floor going down the building as can be seen in Table 7. Because of the long range of the Faro Laser Scanner, only 3 scans were necessary to cover the empty first floor. Figure 9 shows two pictures of all the point-clouds registered together.

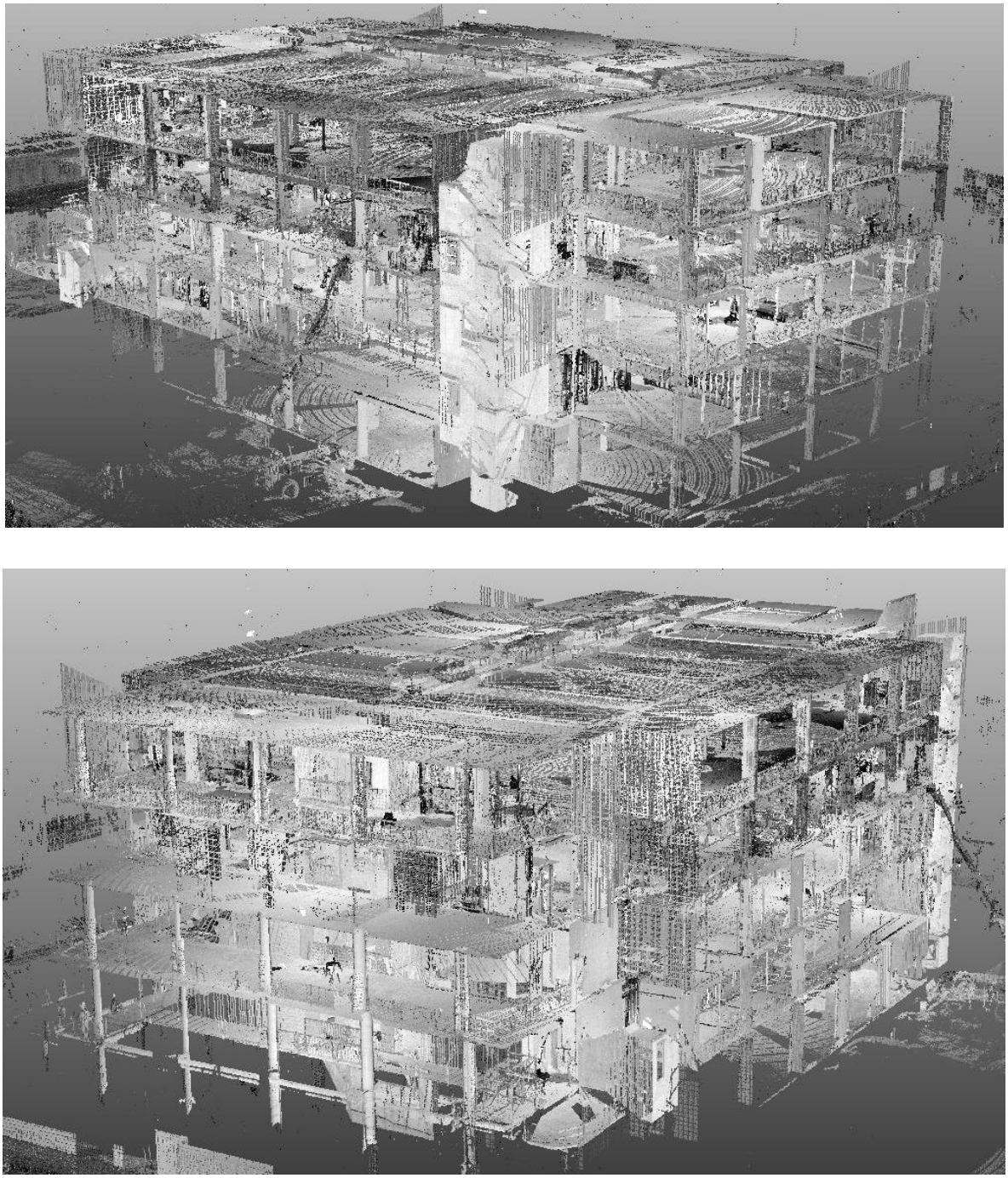

Figure 9: Ensemble of point-clouds performed on E6 Building

Table 7: Number of scans performed per floor

Floor	Number of scans
5th floor	11 scans
4th floor	8 scans
3rd floor	8 scans
2nd floor	8 scans
1st floor	3 scans

This experiment enabled the generation of a basic knowledge on how to use the laser scanning technology to create a point-cloud of a construction site.

3.4.2 Second data acquisition

Once the viability of the Faro Laser Scanner was proven for acquiring point-clouds, the second part of the data acquisition was conducted. This second set of data focused on particular areas of the Engineering VI Building, and aimed to acquire point-cloud data at different stages of construction. The attention of this study was focused on the service corridor of the fifth floor of the building because of the abundance of pipes coming from the lower levels and going all the way up to the penthouse (Figure 10). Those pipes, running through the service corridor at the center of the building, were the main focus of this study. The east and west wings of the fifth floor were also scanned. Figure 11 and 12 respectively show the service corridor at the beginning and at the end of the study.

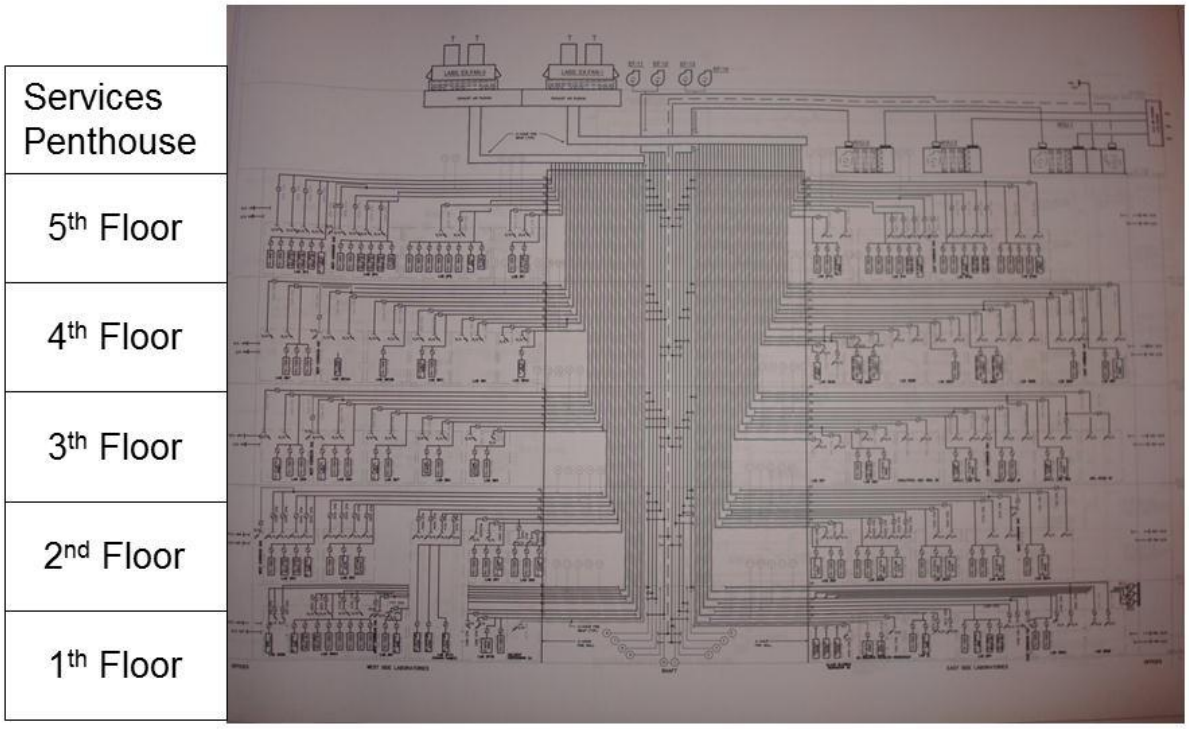

Figure 10: Elevation View of the Piping Network for Engineering VI Building

Figure 11: Service Corridor at the beginning of the study

Figure 12: Service corridor at the end of the study

All of the scans were collected from July 2010 to February 2011. Table 8 shows the schedule that was followed to perform the scans.

Table 8: Scanning schedule for second data acquisition

Location	Date
5th Floor, East wing	July 8th
	July 15th
	July 28th
	August 3rd
	August 4th
	August 6th
	August 9th
	August 11th
	August 13th
	August 18th
	August 19th
	August 23th
	September 2nd
	September 7th
	September 10th
	September 17th
	November 9th
5th Floor, West wing	July 16th
	July 27th
	July 29th
	August 6th
	August 10th
	August 13th
	August 16th
	August 20th
	September 10th
	September 17th
	September 24th
5th Floor, Service corridor	July 16th
	August 20th
	August 27th
	August 31th
	September 14th
	September 22th
	September 30th
	October 19th
	February 5th

3.5 Data pre-processing

3.5.1 Registration principle

The 3D laser scanner establishes a new coordinate system for every scan, and every point has coordinates in its coordinate system. However, in order to create one point-cloud out of all the as-built point-clouds acquired, it is necessary to ordinate them during a stage called "Registration". The purpose of the registration process is to properly position every point-cloud compared to the others. As a result, the registered output will be a giant point-cloud composed with all the acquired point-clouds properly placed within. After this operation, all of the point-clouds are located in the same Cartesian coordinate system.

There are 2 different methods to register the point-clouds:

(1) Without targets

(2) With targets

If the choice was made not to use any target, then the method implies positioning of the laser scanner at points with well-known coordinates. This method is rarely used in the industry because it can prove to be quite tricky: setting up the scanning station at a very precise point is overly prone to human error. Moreover, if the station is, only once, misplaced, then the whole scan sequence is in jeopardy. This is mostly why method (1) is so rarely used.

The target-based method is much more simple. A software called Faro Scene® was used in this study to achieve the target-based registration.

3.5.2 Faro Scene®

3.5.2.1 Memory RAM issue

Before starting to use Faro Scene® to register the targets, it is important to understand that processing point-clouds of millions of points requires a lot of memory (RAM). It is specified in the Faro Laser Scanner User Manual that 65MB RAM are required to process one million points. Consequently we can establish Table 9 with the required RAM memory for every resolution of scan.

Table 9: Number of points for every resolution

Resolution	Number of points in the generated point cloud (Millions)	Required Memory RAM
1/10	7	455 MB
1/8	11	710 MB
1/5	28	1.8 Go
1/4	44	2.8 Go
1/2	175	11.3 Go
1	700	45 Go

It is also important to know that 2 scans have to be loaded on Faro Scene® to register them, which means that twice the indicated memory RAM is required. This is why it is possible inside the software to specify the number of points the user wishes to load. That way any scan can be loaded at a reduced resolution onto Faro Scene® to be registered. The following figure shows how to reduce the number of uploaded points: it is now set to load an unlimited number of points, which means that the point-clouds will be loaded at their full resolution. This can be changed by entering a number after "Mio scan points" that specifies the number of millions of points to be loaded per scan. Figure 13 shows the menu on Faro Scene® to change the number of loaded points.

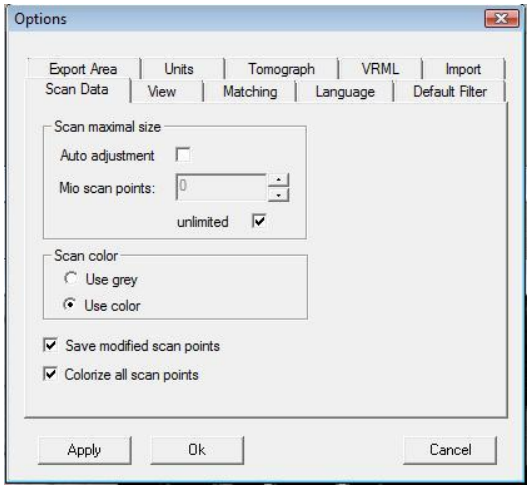

Figure 13: Loading the chosen amount of points

The only problem when a point-cloud is loaded at a reduced resolution is that a target located far away from the laser scanner on a scan might not be visible enough to be registered properly, which could potentially lead to an unregisterable point-cloud.

With that in mind, if more than 2 point-clouds have to be registered together,then it is strongly advised to work with only pairs of point-clouds that share 3 common targets.

3.5.2.2 Registering the targets

The registration phase starts with selecting the 2 scans sharing 3 targets, and that are ready to be merged into one single point-cloud. The targets that have been acquired during the scanning stage are to be named the same in every point-cloud and will serve as constraints for the registration. The user has to open the two point-clouds, locate the targets in common, and choose the type of target that was used in this point-cloud, as shown in Figure 14.

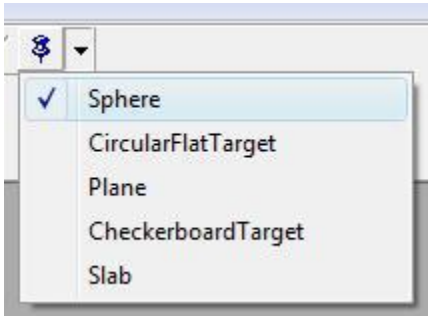

Figure 14: Registering the different kinds of targets

Then, the user names the 3 targets of the same way in the 2 point-clouds. One mistake on one of the names will lead to a registration failure, as well as a wrong acquisition of the targets during the scanning process, by range or occlusion. If the latter ever occurs, then the target has to be removed from the constraint list and another target must be created.

Once the naming is done and error-prone targets removed, the registration can start. The targets have now to be specified as references and the point-clouds placed around those references. Figure 15 shows the state of the browser after this stage.

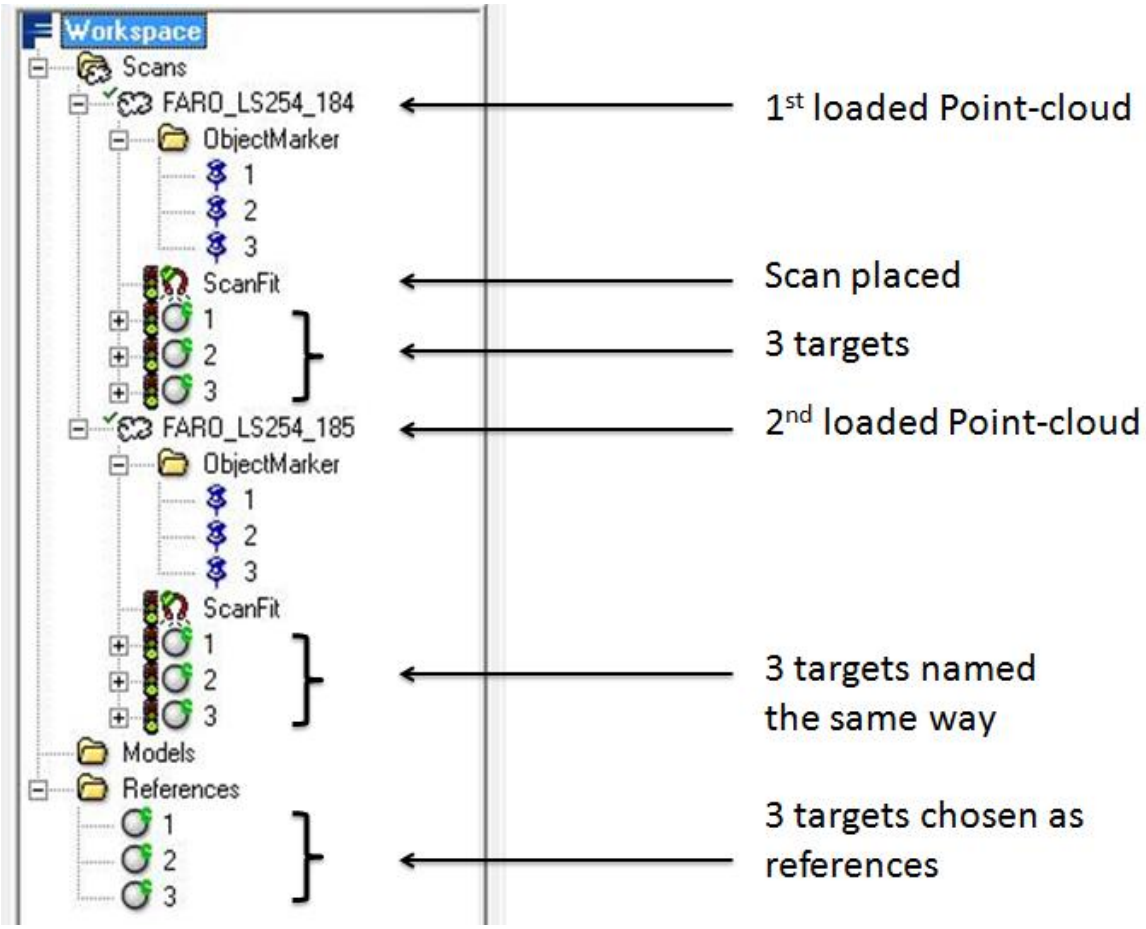

Figure 15: Data structure

Figure 16 shows two point-clouds that were acquired in the service corridor on the fifth floor. It shows the spherical targets hanging from plumbing pipes bearing the same names on both point-clouds. It also shows with a purple circle the location of the laser scanner from where the other point-cloud was taken. The location is calculated by the software once the targets have been registered. The point-louds are then registered and can be viewed with the 3D viewer as seen in Figure17. They can be unloaded to allow the use of the RAM for two other scans to be registered.

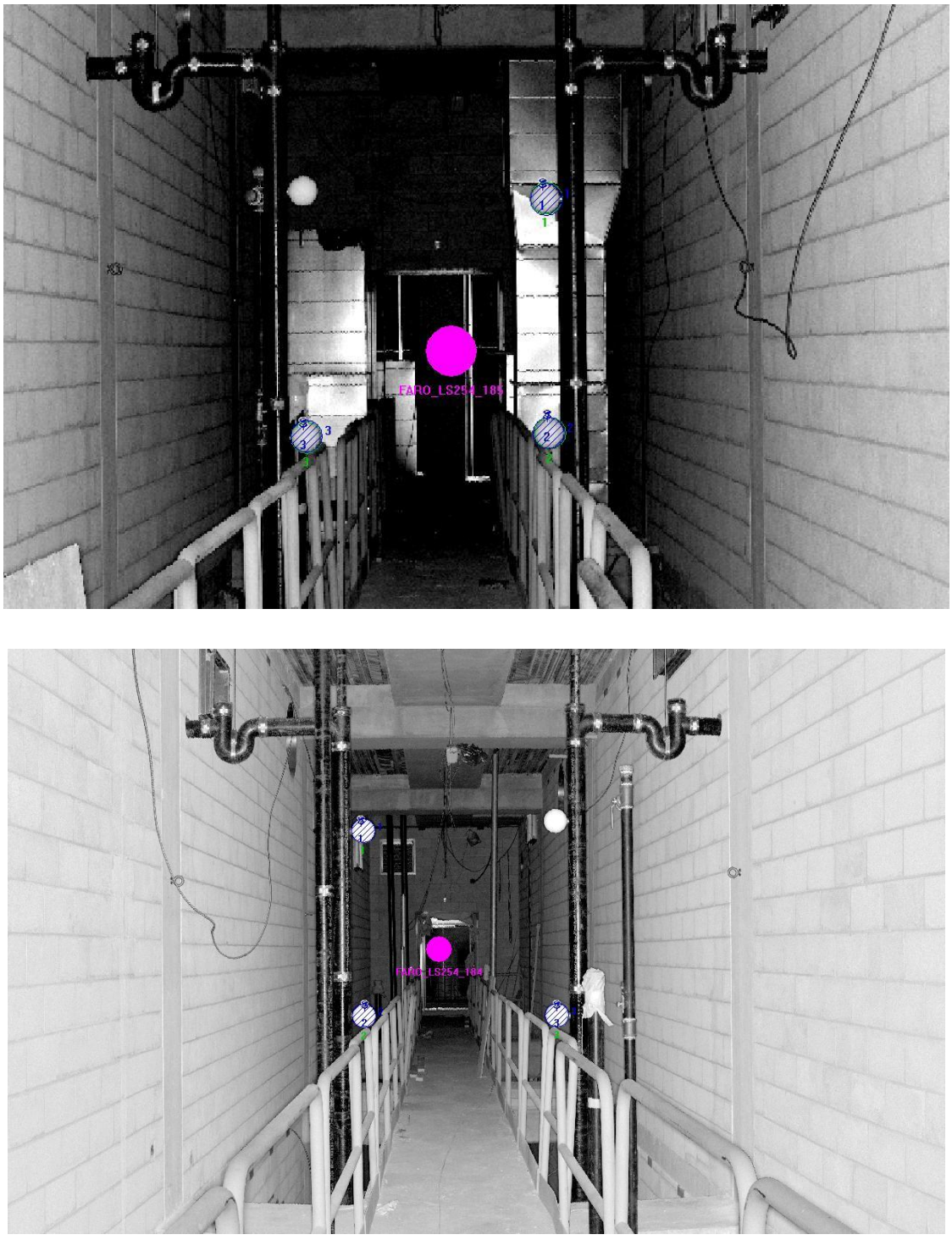

Figure 16: Views from the 2 laser scanner locations

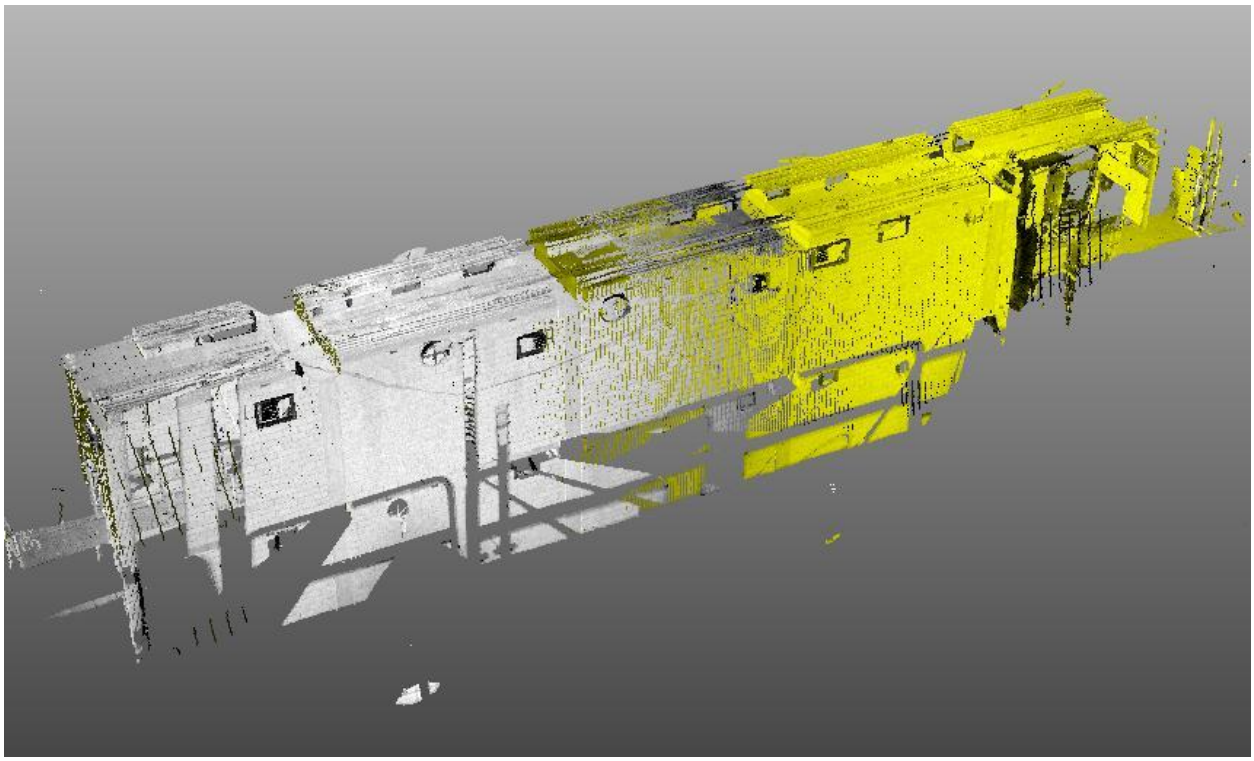

Figure 17: Two point-clouds, white and yellow, registered

Chapter 4
Registration Software and Object Recognition Software

This chapter presents the registration software and the object recognition software developed by Bosché (2008) that were used for this study. The data structure is first presented, followed by the summary of the necessary work that was performed on the as-built point-clouds and the as-planned data to respect the file formats required. In the end, the use of the two different programs is explained.

4.1 Data structure

The data must be organized as follows (the folder names in the brackets < > can be chosen as desired)

- > Folder: <Project>

    - > Folder: AsBuilt

        - > Folder <Scan> (for scan 1)

            - > File: ASCII File with point cloud 1 (.asc)

            - > File: ASCII File with scan 1 resolution (.asc)

            - > File: XML File with registration information (.xml)

        - > Folder <Scan> (for scan 2)

            - > File: ASCII File with point cloud 2 (.asc)

            - > File: ASCII File with scan 2 resolution (.asc)

            - > File: XML File with registration information (.xml)

        - > …

    - > Folder: AsPlanned

        - > File: OBJ

Figure 18 and 19 show screenshots of the directory structure. A description of each file type follows.

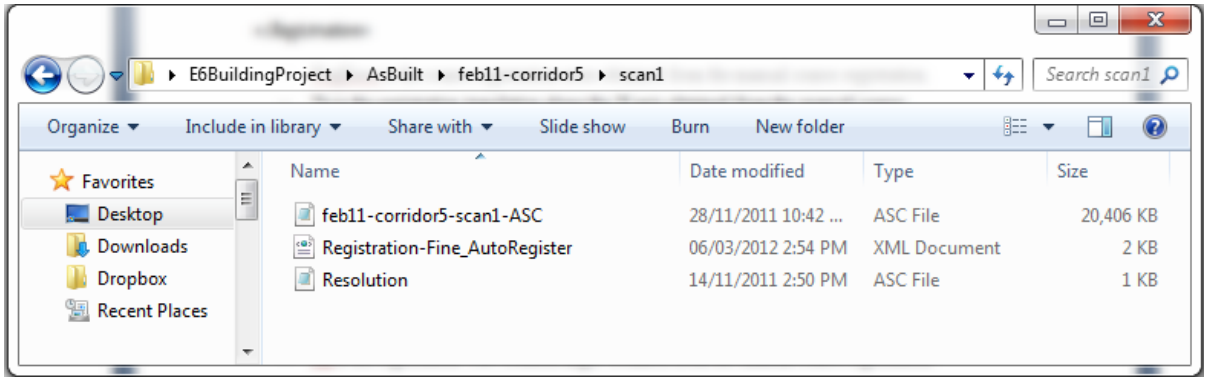

Figure 18: Directory structure, as-built folder

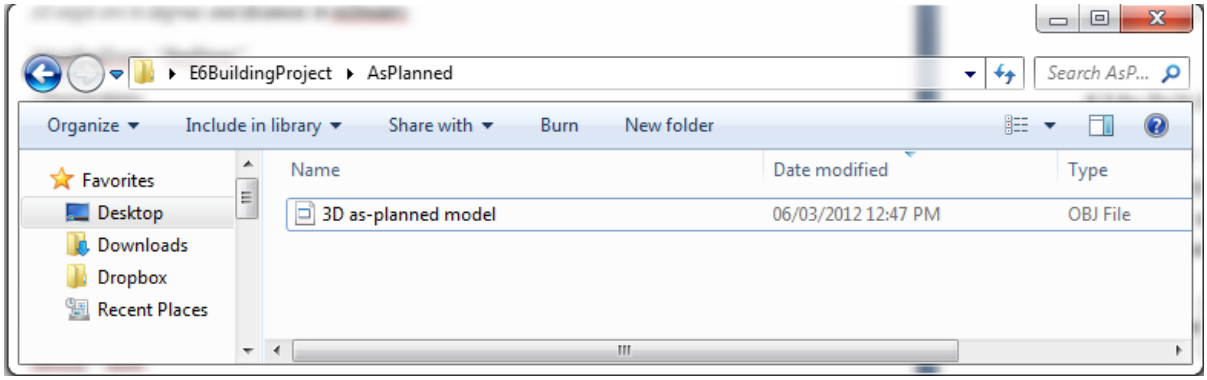

Figure 19: Directory structure, as-planned folder

Notes:

- The ASCII File containing the scan resolution information must contain “Resolution” in its name.
- The ASCII File containing the point cloud must NOT contain “Resolution” or “Position” in its name.

The reason for these naming constraints is to speed up the retrieval of the necessary files.

Point Cloud File: (Figure 20) This ASCII file is simply a list of points, one per line, and containing the position values X, Y, and Z.

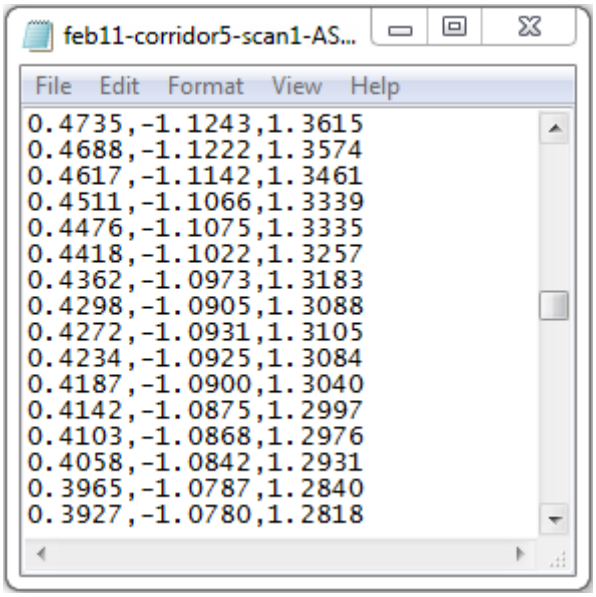

Figure 20: Point-cloud ASCII file

Resolution File: (Figure 21) This ASCII file contains the following three lines:

%in mm @ 100

Resolution Pan: "Rx"

Resolution Tilt: "Ry"

- Rx is the horizontal resolution.
- Ry is the vertical resolution.

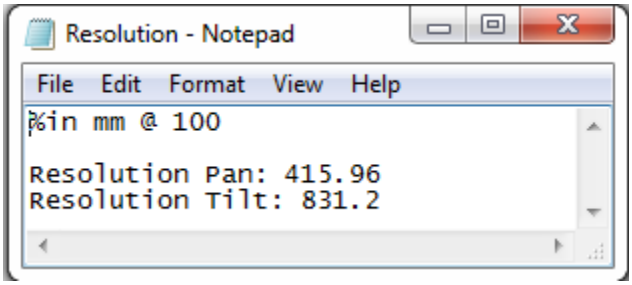

Figure 21: Resolution file

Registration File: (Figure 22) This is an ASCII file containing the following information.

MeanRegError: "RegError"

<Registration>

XDif: "Tx"

YDif: "Ty"

ZDif: "Tz"

RollDif: "Rroll"

PitchDif: "Rpitch"

YawDif: "Ryaw"

</Registration>

- RegError is the coarse registration error obtained from the manual coarse registration.
- Tx is the registration translation along the X axis obtained from the manual coarse registration.
- Ty is the registration translation along the Y axis obtained from the manual coarse registration.
- Tz is the registration translation along the Z axis obtained from the manual coarse registration.
- Rx is the registration Roll rotation angle obtained from the manual coarse registration.
- Ry is the registration Pitch rotation angle obtained from the manual coarse registration.
- Rz is the registration Yaw rotation angle obtained from the manual coarse registration.

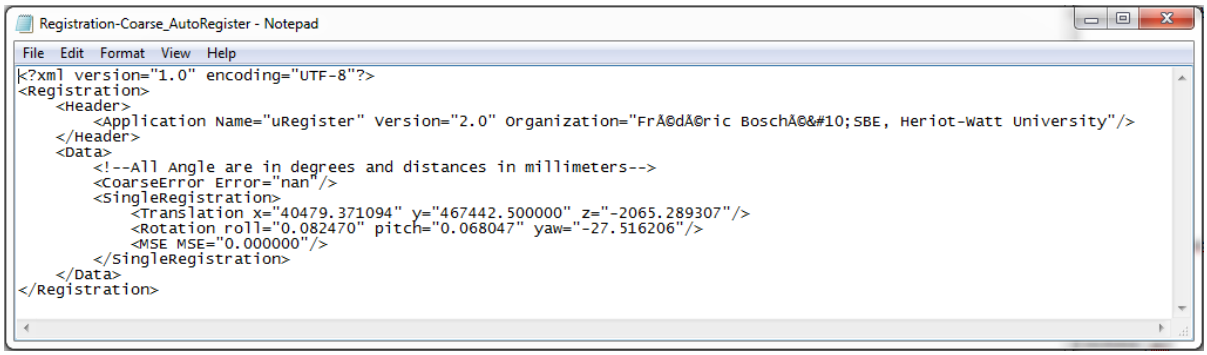

Figure 22: Registration file

4.2 As-built point-cloud format conversion

As explained in Chapter 3, once the point-clouds have been acquired, they had to be merged using the target-based registration technique in Faro Scene®. Now, as explained in Section 2.3.2.1, the data needs to be converted into an open-source format called (ASC). For this, the point-clouds will be subject to the following format conversion operations (Figure 23):

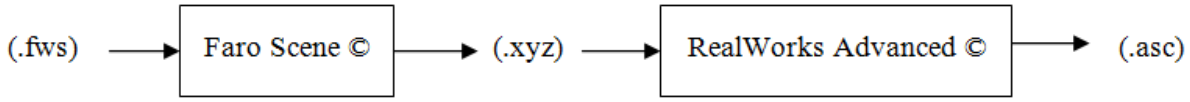

Figure 23: Data format conversion steps

A point-cloud acquired using a Faro Laser Scanner is by default in (FWS) format. Unfortunatly, this format is only useful in a Faro© environment, and needs to be converted into an open source format for the user to be able to use the point-cloud in Bosché (2008). Faro Scene® exports point-clouds into a variety of different formats but not into ASC, which creates the need for an intermediate format conversion between (FWS) and (ASC). The (XYZ) format is also an open source format and is used both as an export format by Faro Scene® and as an import format by Trimble™ RealWorks®, hence its presence into the format conversion process. Appendix A shows the different steps of the as-built point-cloud format conversion.

4.3 3D as-planned model format conversion

The 3D as-planned model needed to perform this study was missing for the purpose of this study, only the 2D drawings provided by Aecon© were at disposition. The 3D as-planned model had to be created from these drawings using AutoCAD 2012©. The electronic version of those drawings, which illustrates the pipes passing through the service corridor on the fifth floor of Engineering IV, are displayed below in Figure 24.

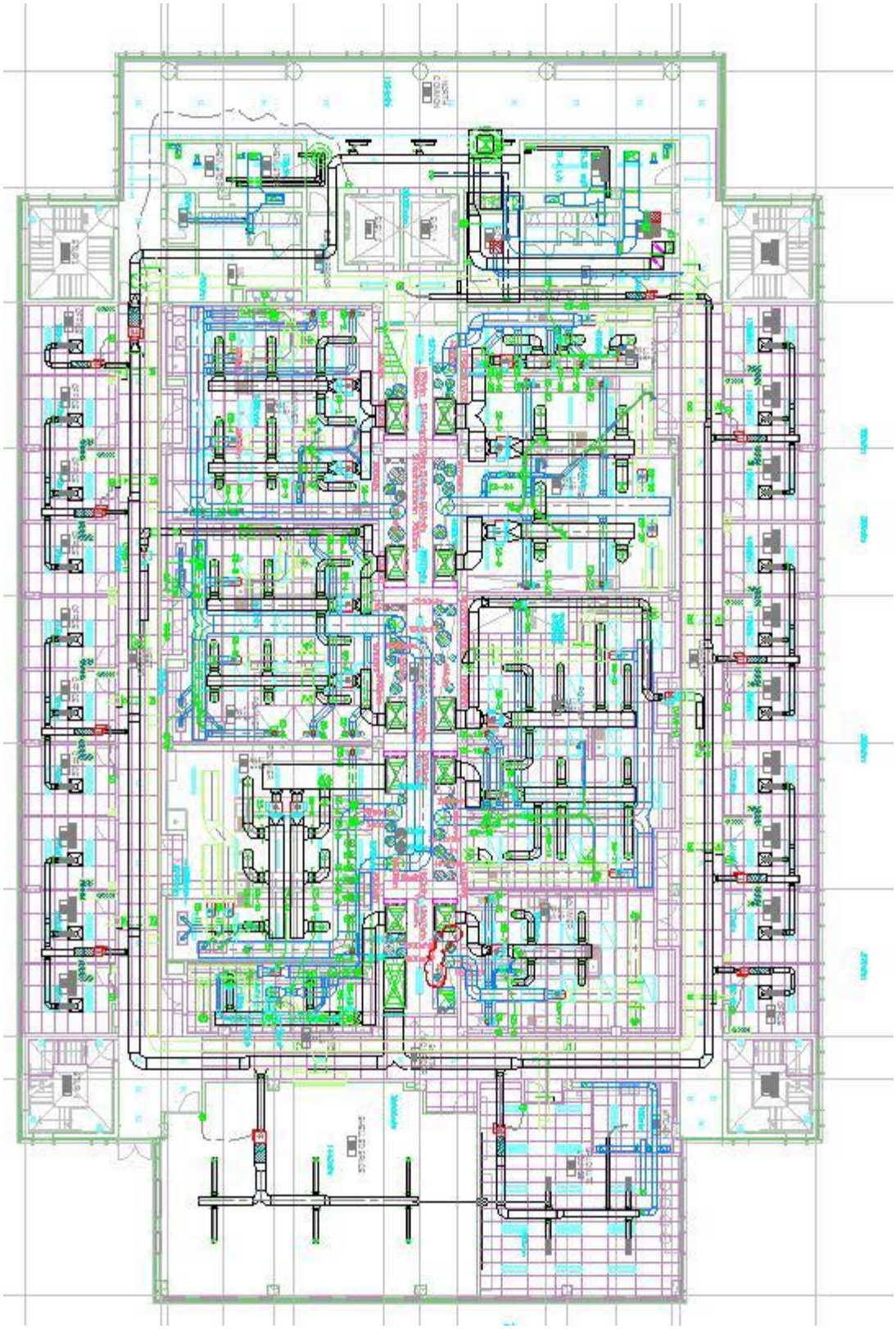

Figure 24: Drawings of HVAC systems - Engineering IV - fifth floor

AutoCAD 2012© was used to create the necessary 3D as-planned model from those drawings (Figure 25).

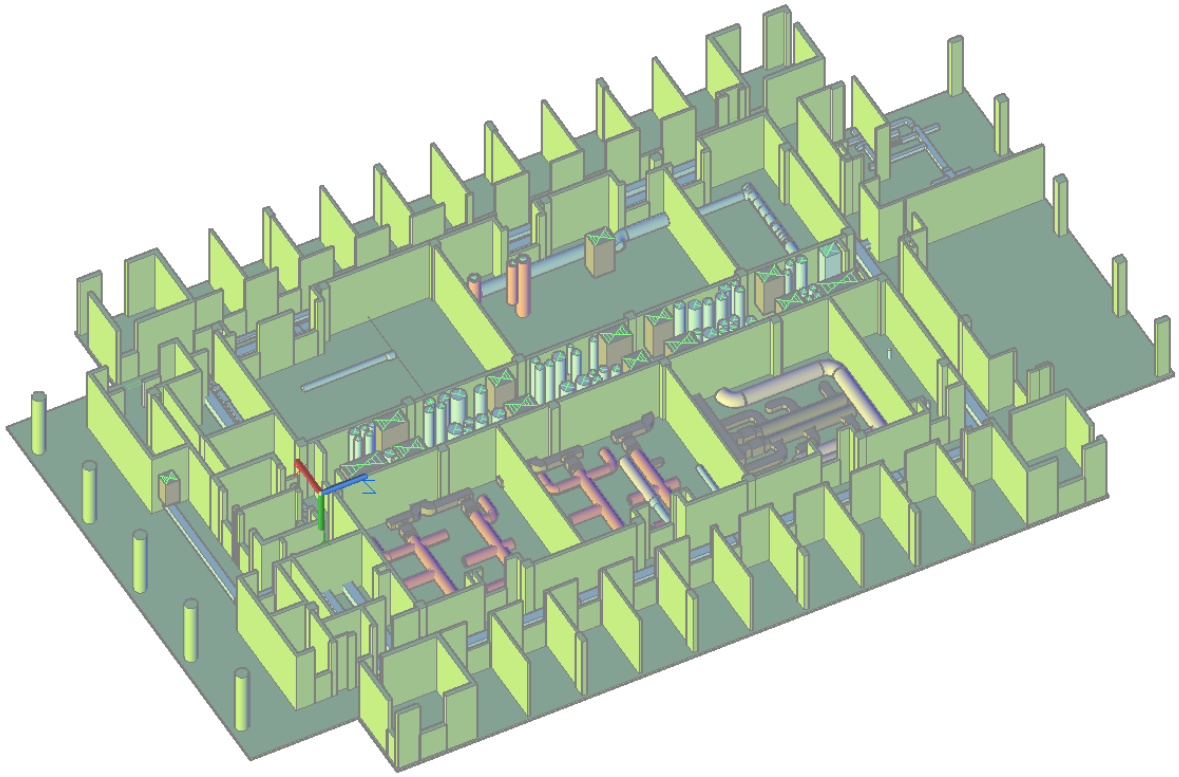

Figure 25: 3D As-planned model of Engineering IV - fifth floor – (DWG) format

Once the 3D as-planned model has been built from the drawings using AutoCAD 2012®, the format the model is in is DWG. A conversion from (DWG) to (OBJ) needs to be conducted for the model to be usable through Bosché (2008). Autodesk 3ds Max® was used to make the format conversion. Appendix B shows the import and export menus on Autodesk 3ds Max® as the were used to create the (OBJ) file.

4.4 Registration software

Once all of the files have been created and organized as described in Section 4.1, the registration software can be used to merge the coordinate systems of the as-built point-cloud and 3D as-planned model together. As explained in Section 2.2.2.2, a coarse registration has to be performed first, and three different planes (2 vertical, 1 horizontal) have to be selected on the 3D as-planned model and the as-built point-cloud each to be matched for the coarse registration. The walls and floor are used as

vertical and horizontal planes in this study. Figure 27 shows the selection of the planes. The left window shows the 3D as-planned model and the 3 planes that were selected for the coarse registration: 2 walls of the service corridor and the ceiling. And the right window shows the point-cloud and the selection of the same planes.

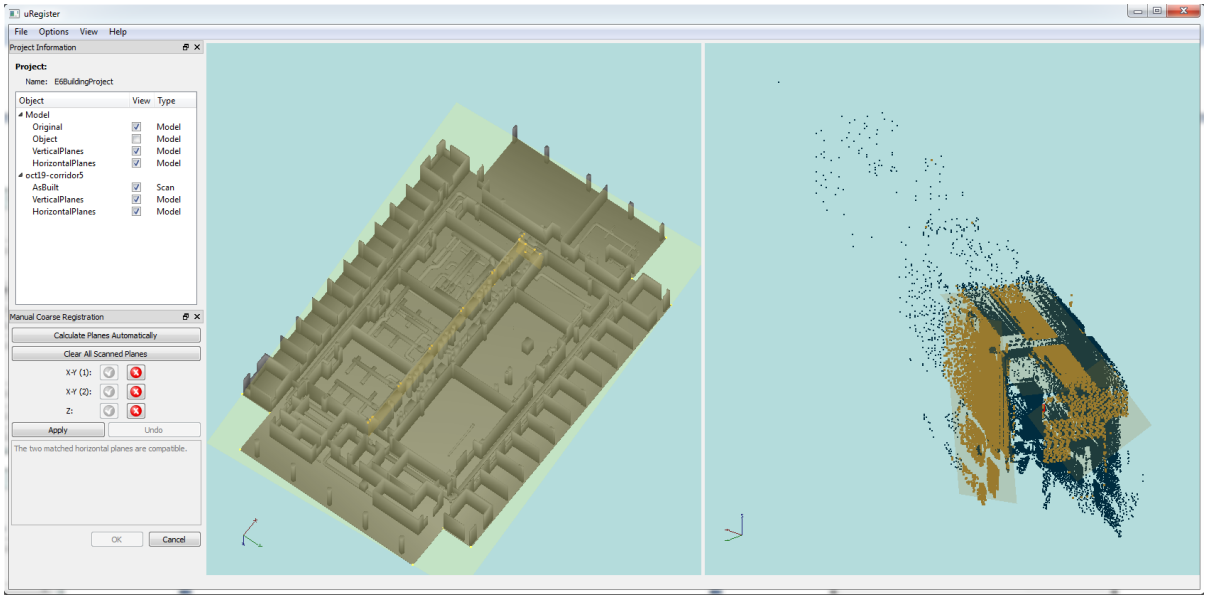

Figure 26: Coarse registration operation and result

Once the coarse registration is completed, a fine registration is performed as explained in Section 2.2.2.3. After the fine registration, the as-built point-cloud is inserted into the 3D as-planned model at its best calculated position, they are then both in the same coordinate system as shown in Figure 28. Appendix C shows the different steps and menus on the software to perform the registration.

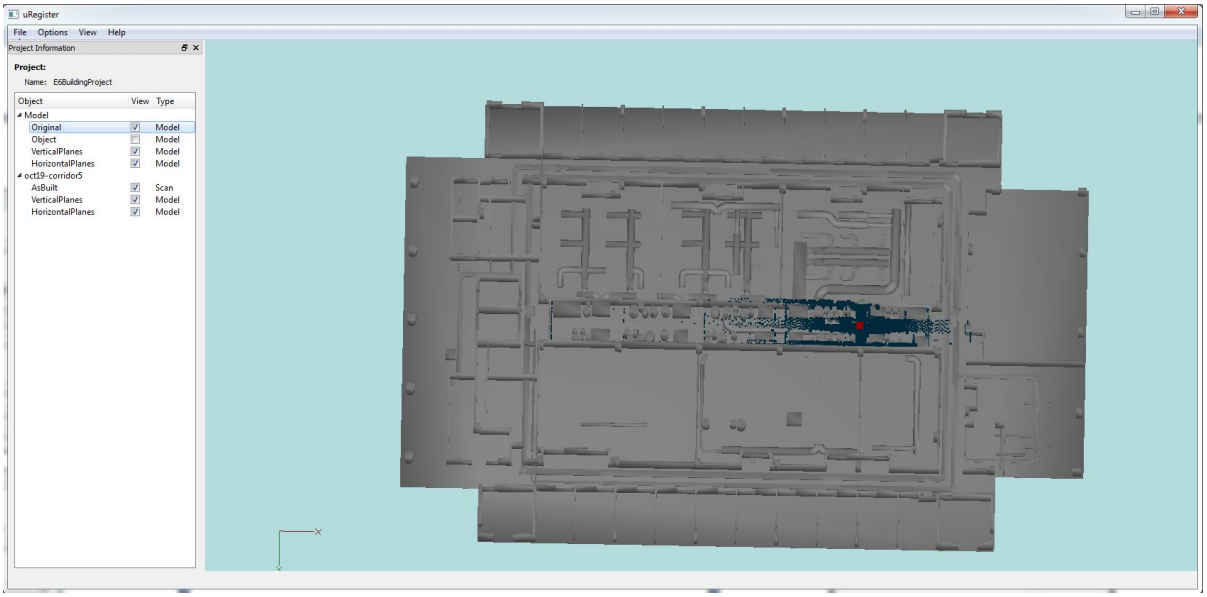

Figure 27: Output of the fine registration

4.5 Object recognition software

After that the registration is performed, the next step is to perform the object recognition as explained in Section 2.2.2.4.

The results of the object recognition process, as seen in Figure 29, are the original as-built point-cloud on top of the 3D as-planned model that has been colored depending on the following parameters:

(1) points recognized (colored in green and red) which constitute the points in the point-cloud that are located within 5 cm of a CAD object on the 3D as-planned model.

(2) points not recognized (colored in blue) which constitute the points in the point-cloud that are located more than 5 cm away from any CAD object on the 3D as-planned model.

The 5 cm limit is called the "construction error parameter". This parameter could only be set from 1 cm to 5 cm on the object recognition algorithm developped by Bosché (2008). The use of this parameter is discussed further in Section 5.3.4.

Appendix D shows the different steps and menus on the software to perform the object recognition.

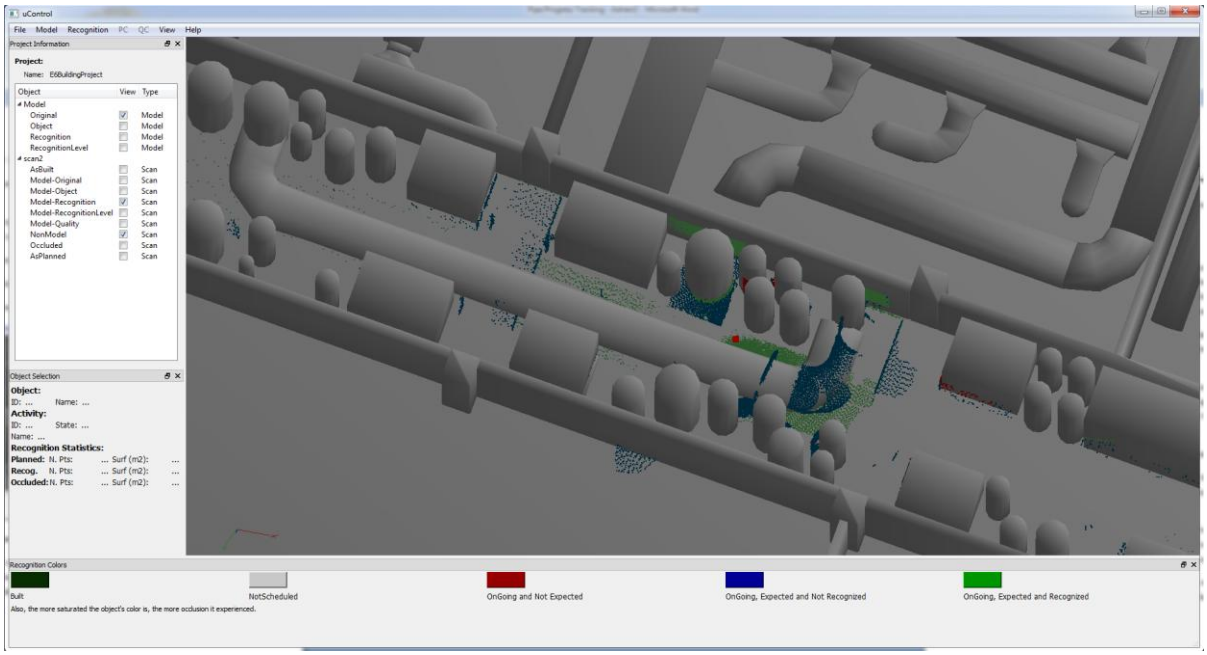

Figure 28: Results of object recognition

A detailed result of the study is available as an excel speadsheet, as shown in Figure 30, that lists the objects of the 3D as-planned model and whether or not they have been recognized. The list of object is created automatically by the algorithm, and every CAD objects is given an ID number. For the purpose of this study, only the column "Recognized" is used. This column gives a binary response to whether the object was recognized. Appendix E shows a more detailed Excel Spreadsheet example.

	A	B	C	D	E	F	G	H	I	J	K	L	M	N	O
1	RECOGNITION PARAMETERS:														
2															
3		RangeMax (m)	40.5692												
4		Unit Surf (m2)	0.000345746												
5		Nmin (pts)	10												
6		SurfMin (1 pt) (m2)	0.56905												
7		SurfMin (Nmin pts) (m2)	5.6905												
8															
9															
10															
11	RECOGNITION STATISTICS FOR ALL OBJECTS:														
12															
13	Element name	PCloud (pts)	MCloud (pts)	RCloud (pts)	OCloud (pts)	VSurf (m2)	PSurf (m2)	MSurf (m2)	RSurf (m2)	OSurf (m2)	Schedule_Status	Scan_Planned	Recognized	Recognition Percent	Occlusion Percent
14	Layer_M_HVAC_DUCT_EXHS	0	0	0	0	1.153124	0	0	0	0	1	0	0	0	0
15	Layer_M_HVAC_DUCT_EXHS	0	0	0	0	0.176239	0	0	0	0	1	0	0	0	0
16	Layer_M_HVAC_DUCT_RTUN	14	16	0	16	45.213875	1.93853	2.19118	0	2.19118	1	0	0	0	1
17	Layer_0	0	1	1	0	6.729351	0	0.350744	0.350744	0	1	0	0	0	0
18	Layer_7661A_5F_0_A_STRC	2923	5917	5596	228	186.330826	8.78422	19.2958	12.8667	5.92583	1	1	1	1	0.674599
19	Layer_M_HVAC_DUCT_EXHS	0	0	0	0	6.277836	0	0	0	0	1	0	0	0	0
20	Layer_7661A_5F_0_A_WALL	13188	45061	40553	2898	4081.356934	101.435	272.402	236.403	29.9103	1	1	1	1	0.294873
21	Layer_7661A_5F_0_A_WALL	255	470	433	11	171.933792	5.40681	12.581	9.9311	1.3903	1	0	1	1	0.257139
22	Layer_M_HAVC_INSULATION	13895	11301	958	2714	572.378845	97.0429	140.765	26.3478	69.2292	1	1	1	0.947297	0.713388
23	Layer_M_HVAC_DUCT_EXHS	0	1	1	0	1.569446	0	0.020353	0.020353	0	1	0	0	0	0
24	Layer_M_HVAC_DUCT_EXHS	0	0	0	0	3.202808	0	0	0	0	1	0	0	0	0

Figure 29: Excel spreadsheet results of object recognition

Chapter 5
Results of the Object Recognition

This chapter displays and analyzes the results of the object recognition process on the point-clouds.

5.1 Introduction

As explained previously, the service corridor of the fifth floor is the center of attention of this study. Figure 31 presents the drawing of the service corridor indicating the HVAC system. Nine different sets of scans were acquired on this part of the building as shown in Section 3.4.2. However, ducts and pipes started being installed in October 2010, which leaves only 2 useful sets of data for this study: October 19th 2010 (one scan) and February 5th 2011 (six scans).

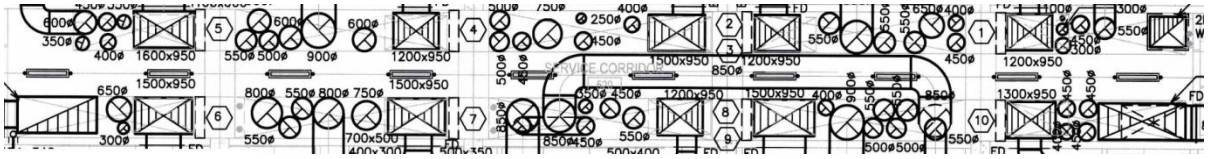

Figure 30: Arrangement of HVAC system in the fifth floor service corridor

The results for each scans presented in this chapter are organized as follows:

(1) A drawing presents a close-up view around the service corridor around the scanner location, which is represented by a yellow diamond. Red-colorized pipes represent the ducts and pipes that were built at the time of scanning.

(2) A screenshot near plan view (about 85° angle of incidence) of the object recognition result of the software with the 3D as-planned model and the as-built point-cloud. The point-cloud is colorized so as to represent the recognized points (green and red points) and the non-recognized points (blue points), as explained in Section 4.6.

(3) Another screenshot of the object recognition result of the software but with only the colorized as-built point-cloud so as to see the points on the point-cloud that were hidden by the objects in the 3D as-planned model.

(4) The drawings of the service corridor with colorized ducts and pipes depending on whether they were recognized (red), not recognized (blue), or wrongly recognized (green). As explained in Section 4.5, all of the objects on the 3D as-planned model are listed on an Excel spreadsheet and for each of

these objects the column “Recognized” indicates whether or not the object is recognized by the object recognition algorithm. An object highlighted in red (recognized object) received a value of 1 in the “recognized” column. An object highlighted in blue (not recognized object) received a value of 0 in the “recognized” column. An object highlighted in green (wrongly recognized) received a value of 1 in the “recognized” column when a value of 0 was expected because the object was not actually installed at the time of scan

The results presented in these figures (Figure 32 to Figure 59) are analyzed in Section 5.3.

5.2 Results of the different as-built point-clouds

5.2.1 October 19th, 2010

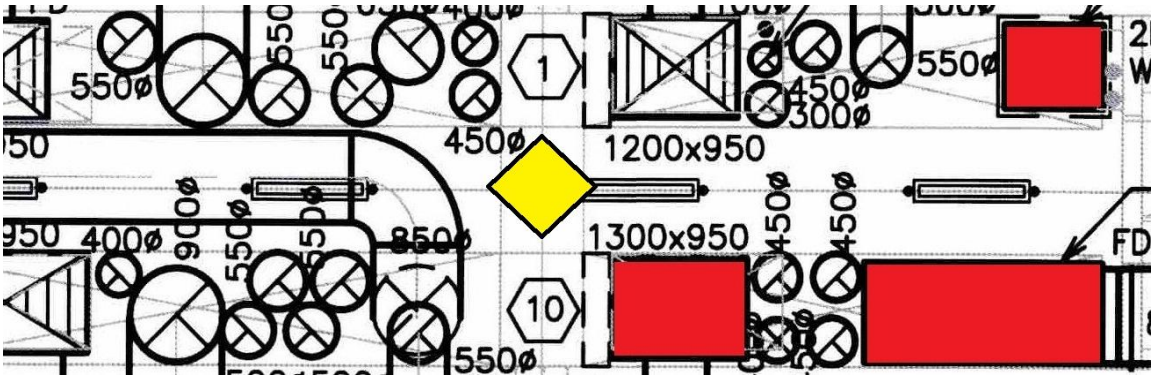

Figure 31: October 19th, 2010, objects built (indicated in red)

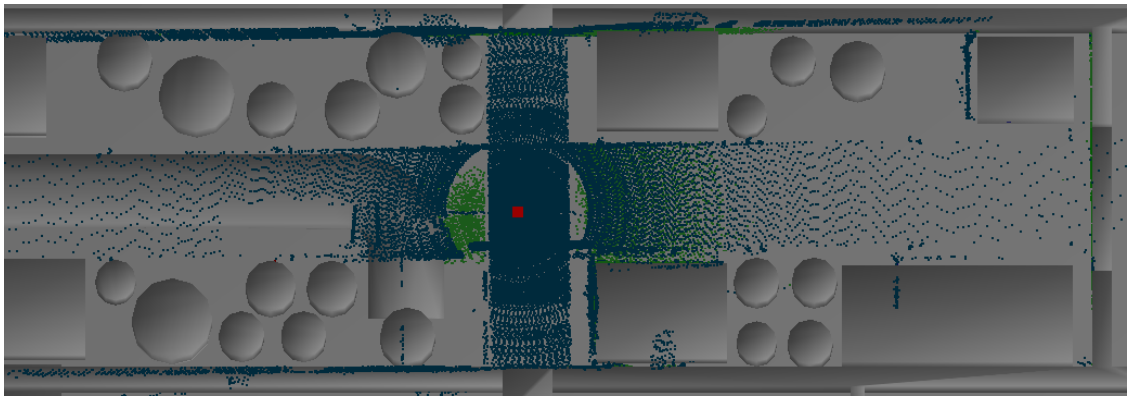

Figure 32: October 19th, 2010, 3D model and point-cloud after object recognition

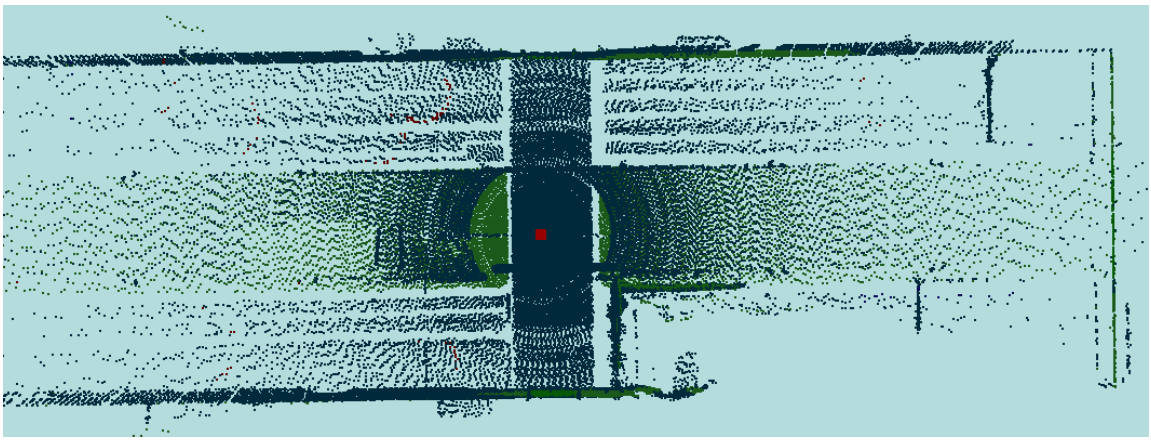

Figure 33: October 19th, 2010, point-cloud after object recognition

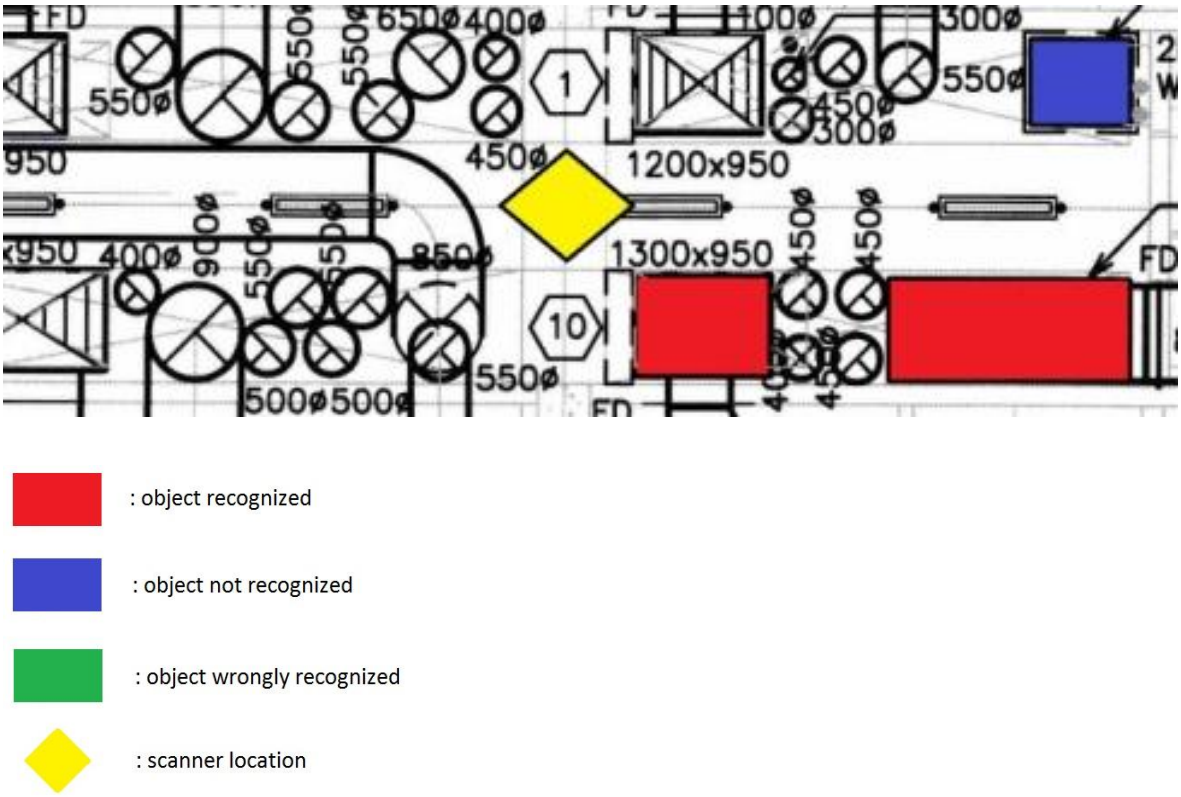

Figure 34: October 19th, 2010, object recognition results

5.2.2 February 5th, 2011, Scan 1

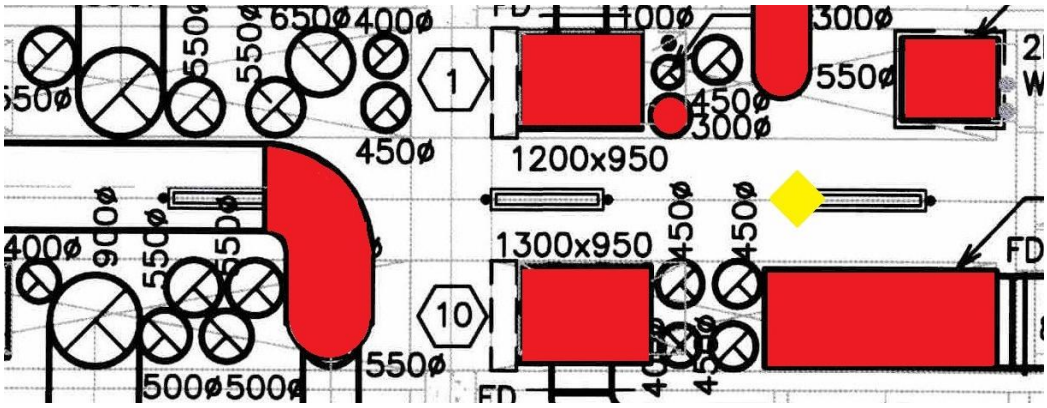

Figure 35: February 5th, 2011, Scan 1, objects built (indicated in red)

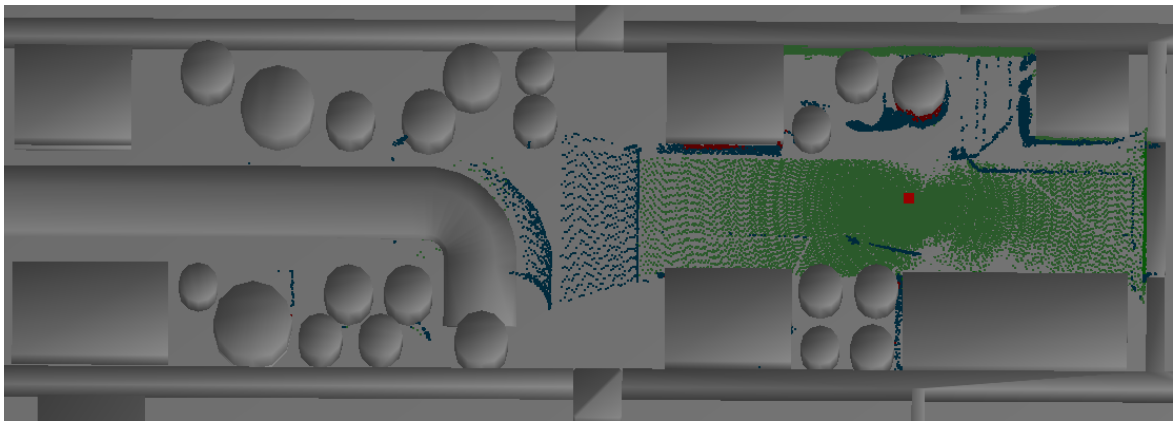

Figure 36: February 5th, 2011, Scan 1, 3D model and point-cloud after object recognition

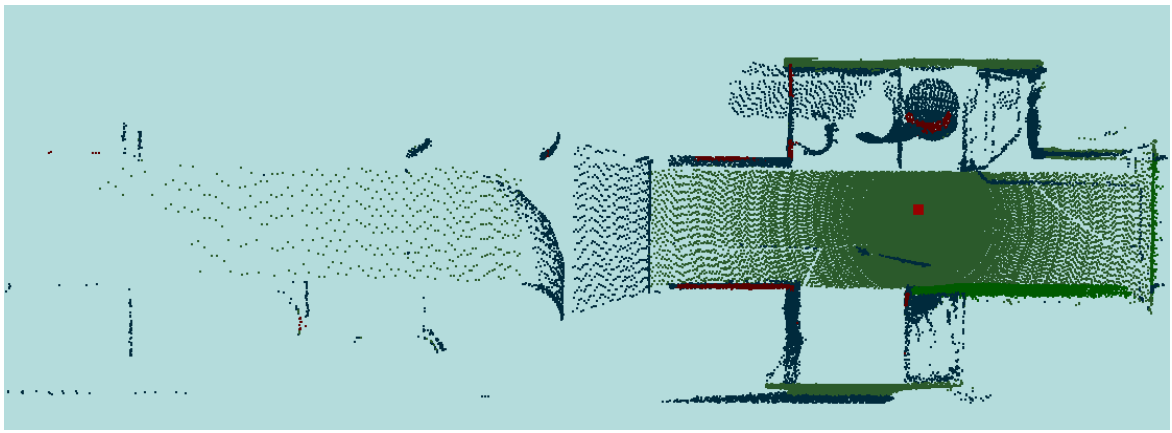

Figure 37: February 5th, 2011, Scan 1, point-cloud after object recognition,

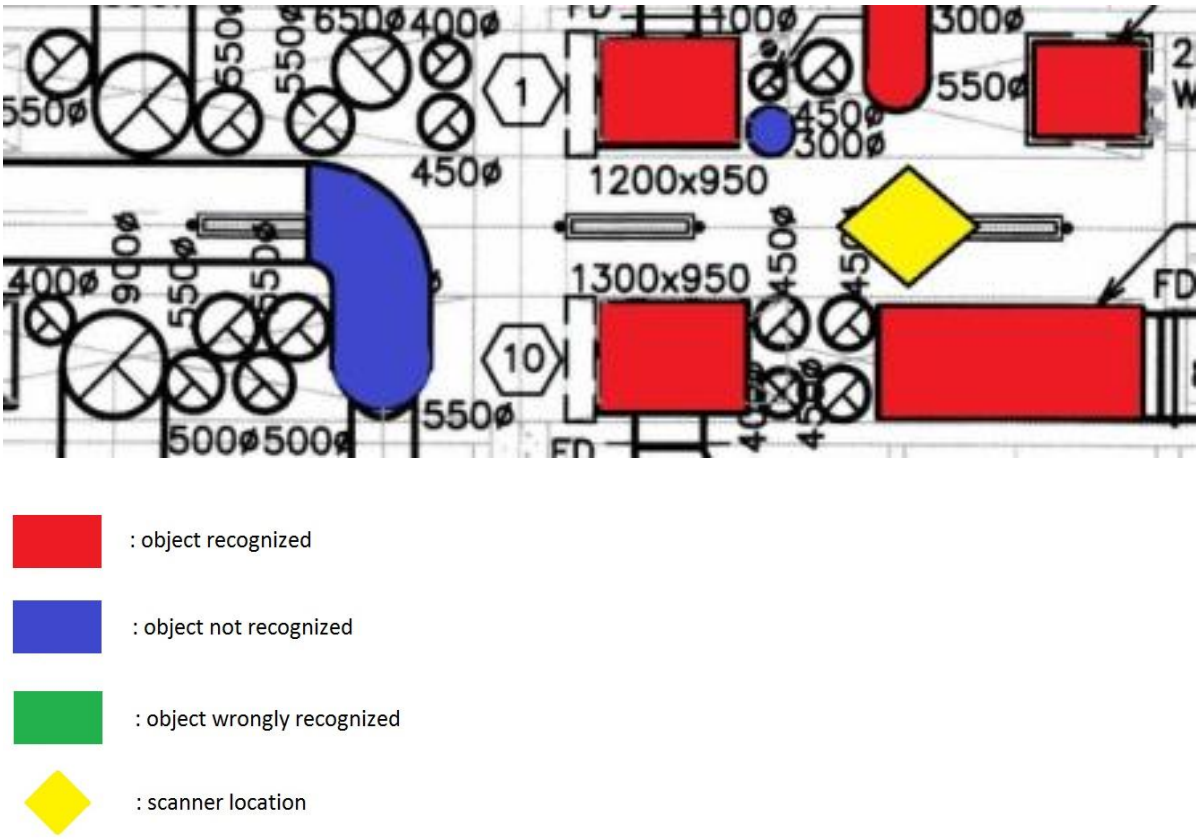

Figure 38: February 5th, 2011, Scan 1, object recognition results

5.2.3 February 5th, 2011, Scan 2

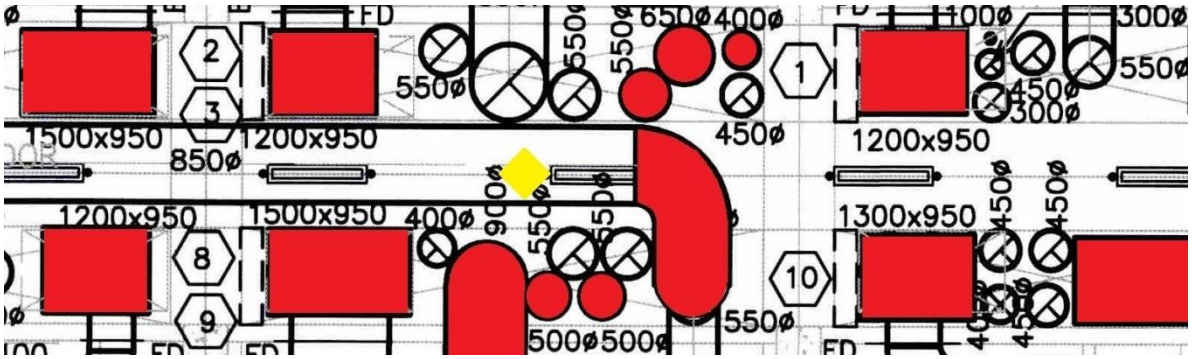

Figure 39: February 5th, 2011, Scan 2, objects built (indicated in red)

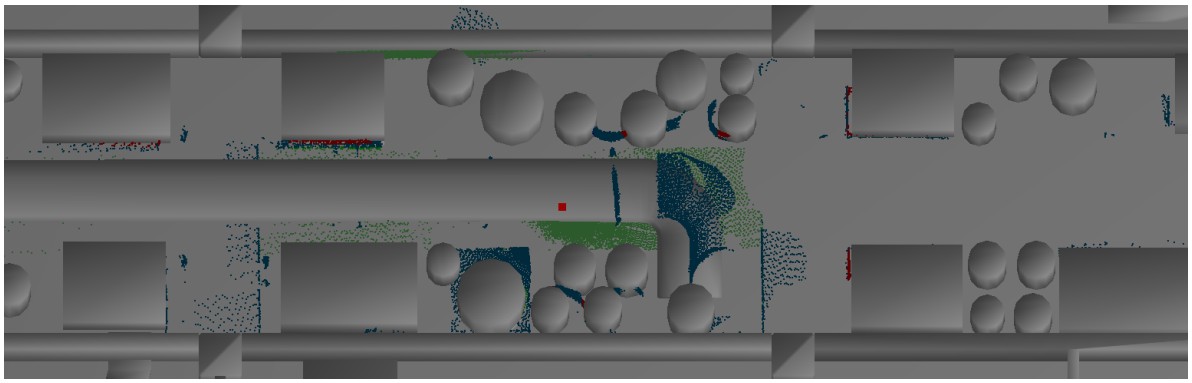

Figure 40: February 5th, 2011, Scan 2, 3D model and point-cloud after object recognition

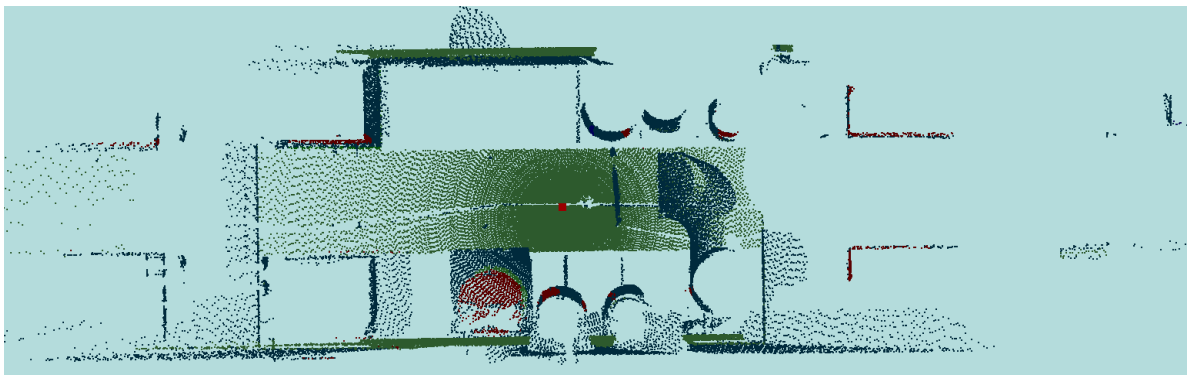

Figure 41: February 5th, 2011, Scan 2, point-cloud after object recognition

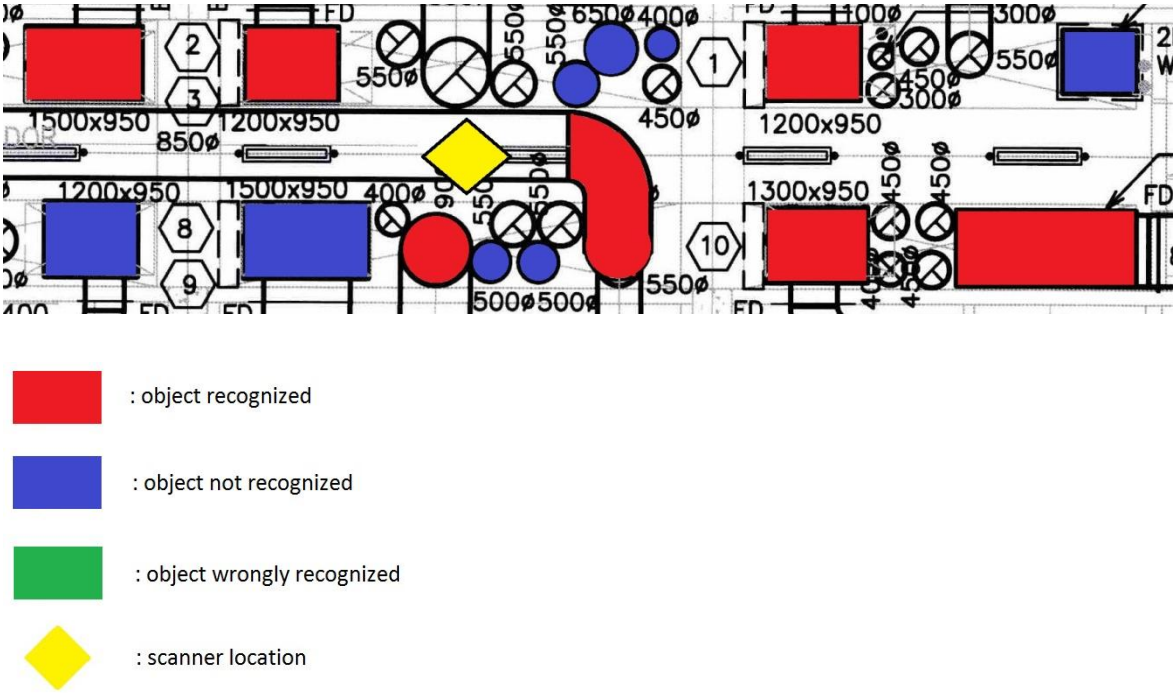

Figure 42: February 5th, 2011, Scan 2, object recognition results

5.2.4 February 5th, 2011, Scan 3

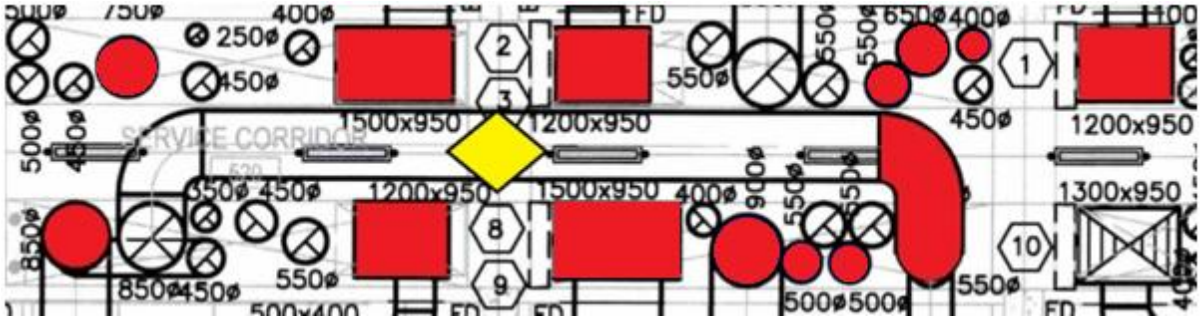

Figure 43: February 5th, 2011, Scan 3, objects built (indicated in red)

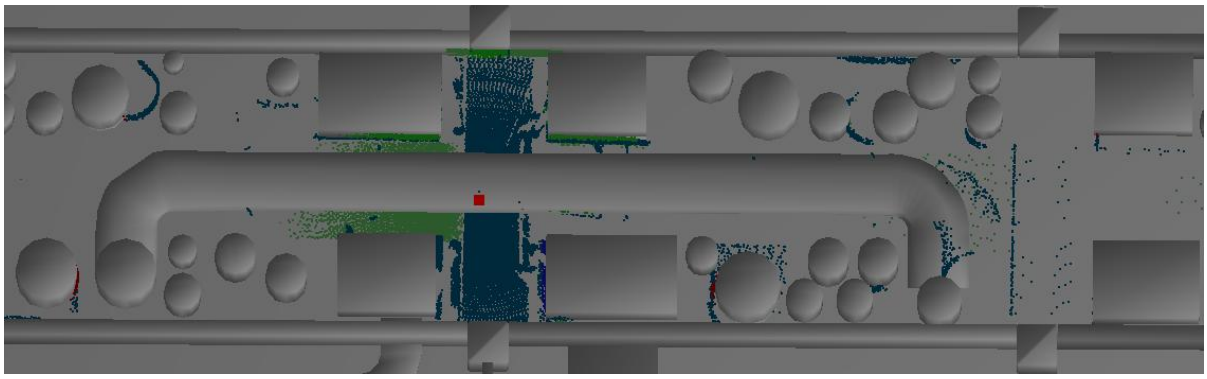

Figure 44: February 5th, 2011, Scan 3, 3D model and point-cloud after object recognition

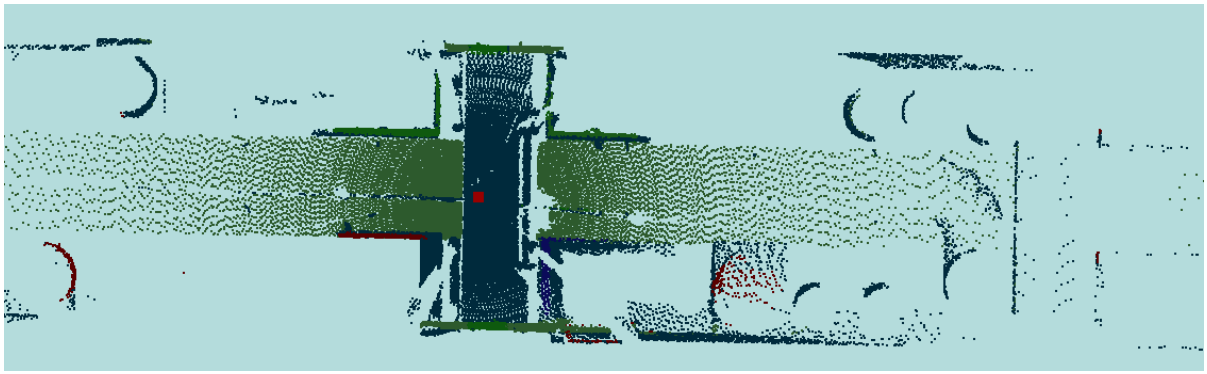

Figure 45: February 5th, 2011, Scan 3, point-cloud after object recognition

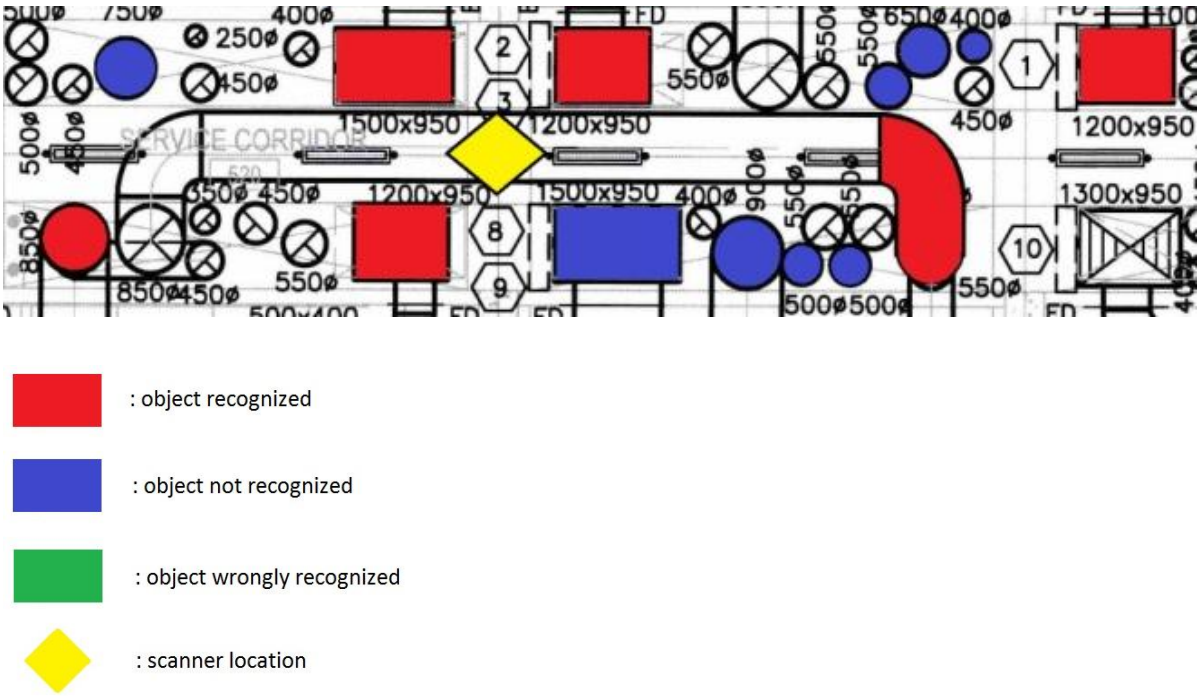

Figure 46: February 5th, 2011, Scan 3, object recognition results

5.2.5 February 5th, 2011, Scan 4

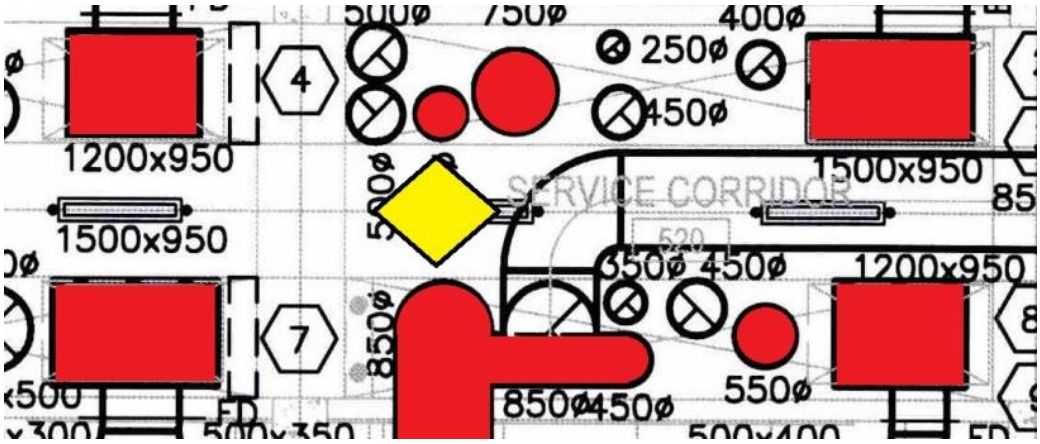

Figure 47: February 5th, 2011, Scan 4, objects built (indicated in red)

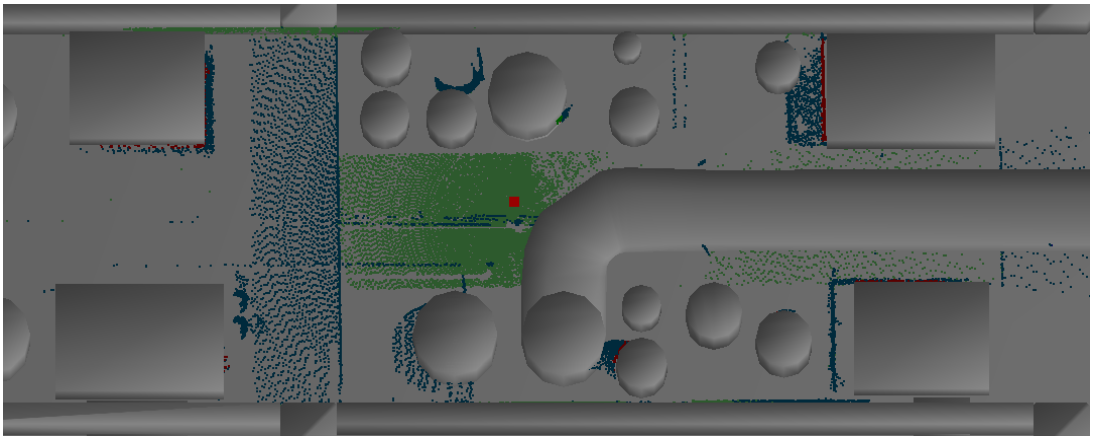

Figure 48: February 5th, 2011, Scan 4, 3D model and point-cloud after object recognition

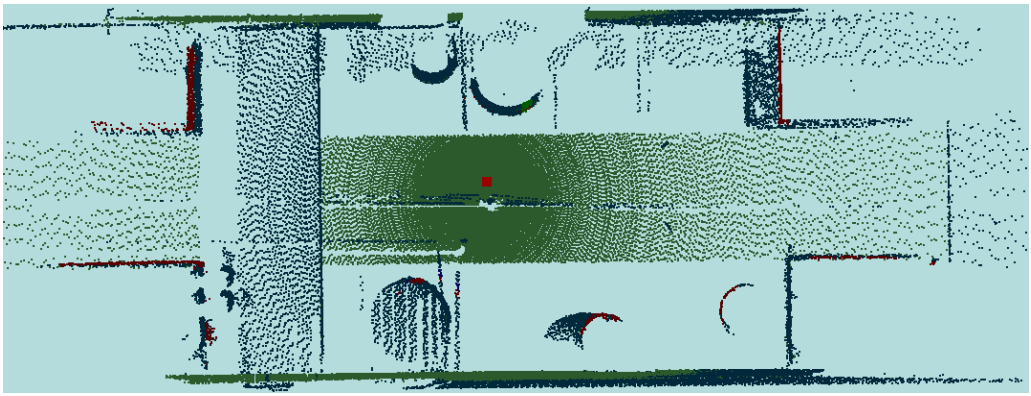

Figure 49: February 5th, 2011, Scan 4, point-cloud after object recognition

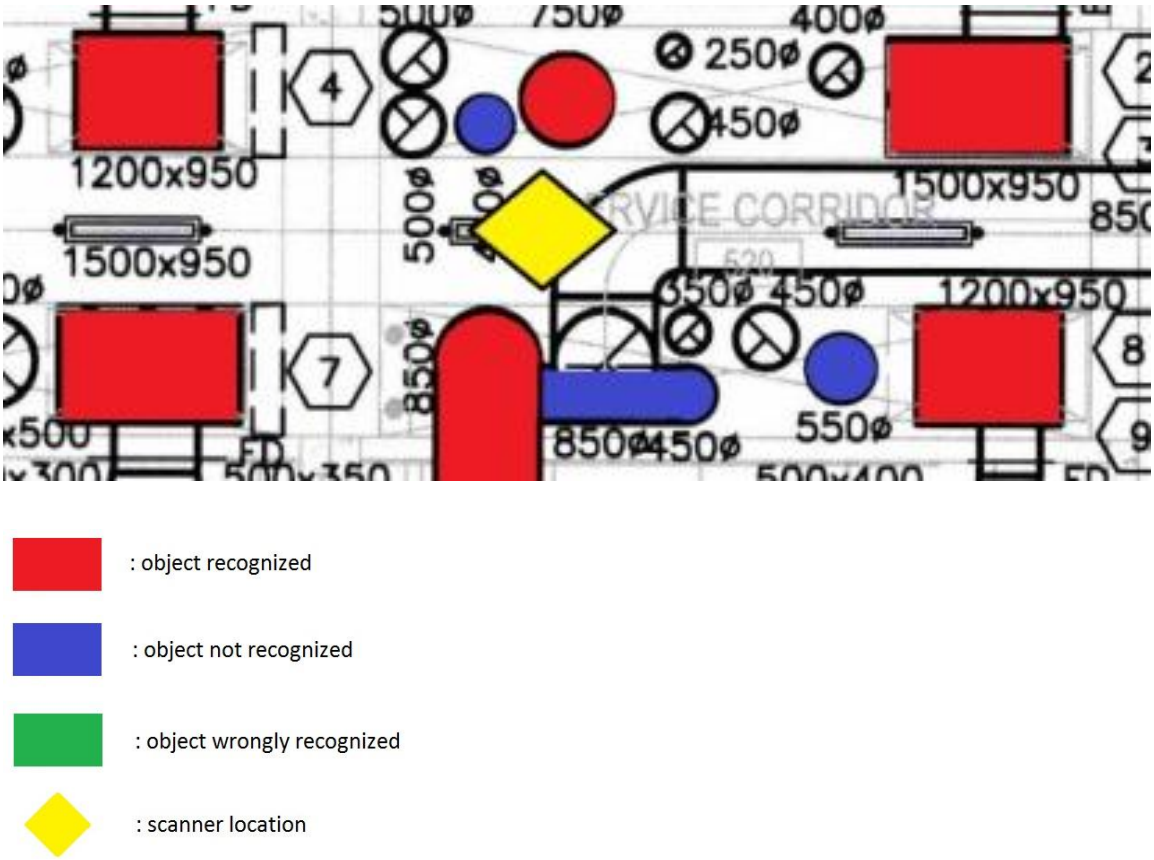

Figure 50: February 5th, 2011, Scan 4, object recognition results

5.2.6 February 5th, 2011, Scan 5

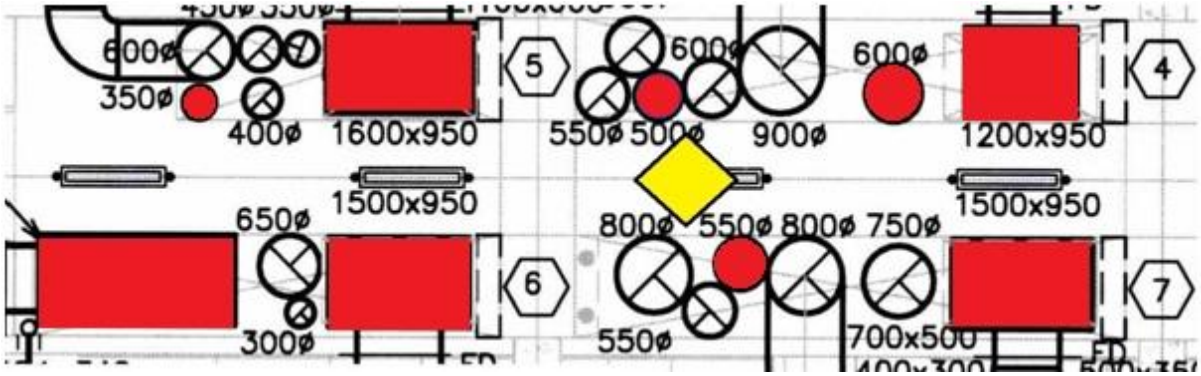

Figure 51: February 5th, 2011, Scan 5, objects built (indicated in red)

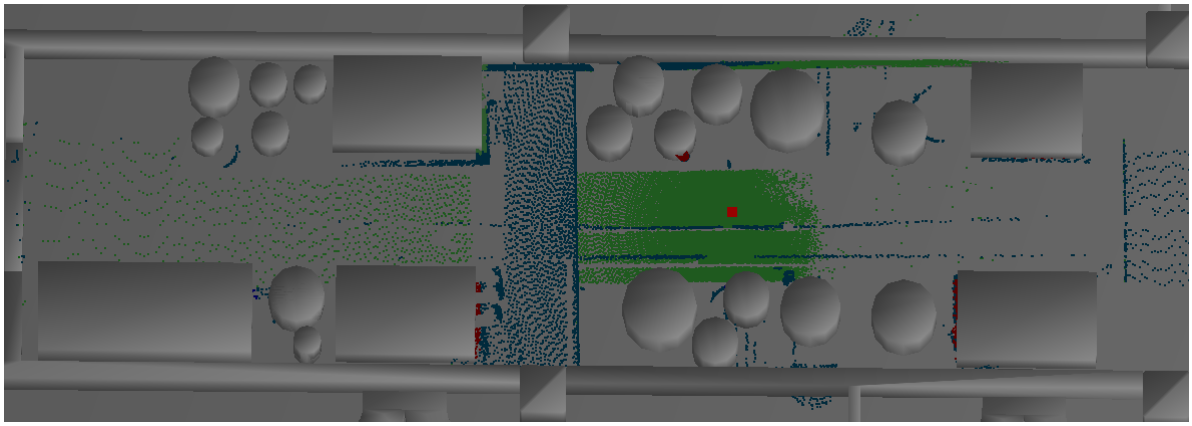

Figure 52: February 5th, 2011, Scan 5, 3D model and point-cloud after object recognition

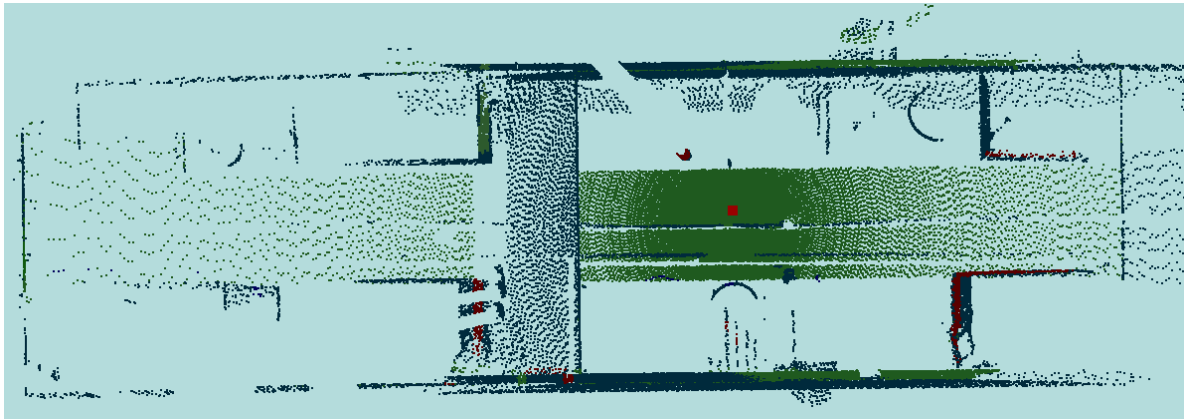

Figure 53: February 5th, 2011, Scan 5, point-cloud after object recognition

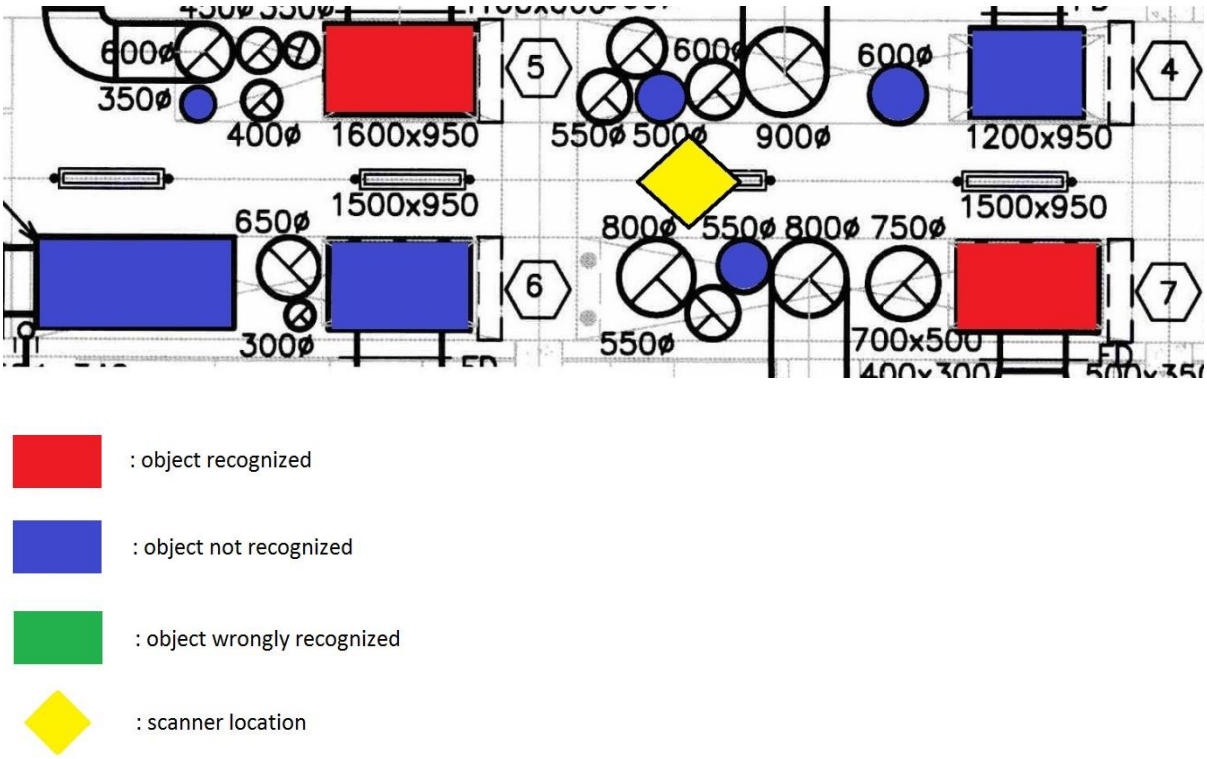

Figure 54: February 5th, 2011, Scan 5, object recognition results

5.2.7 February 5th, 2011, Scan 6

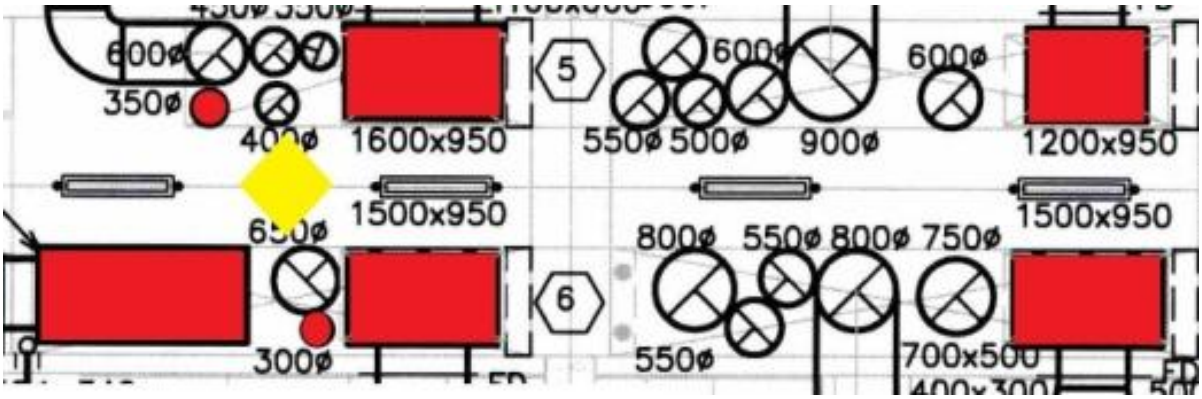

Figure 55: February 5th, 2011, Scan 6, objects built (indicated in red)

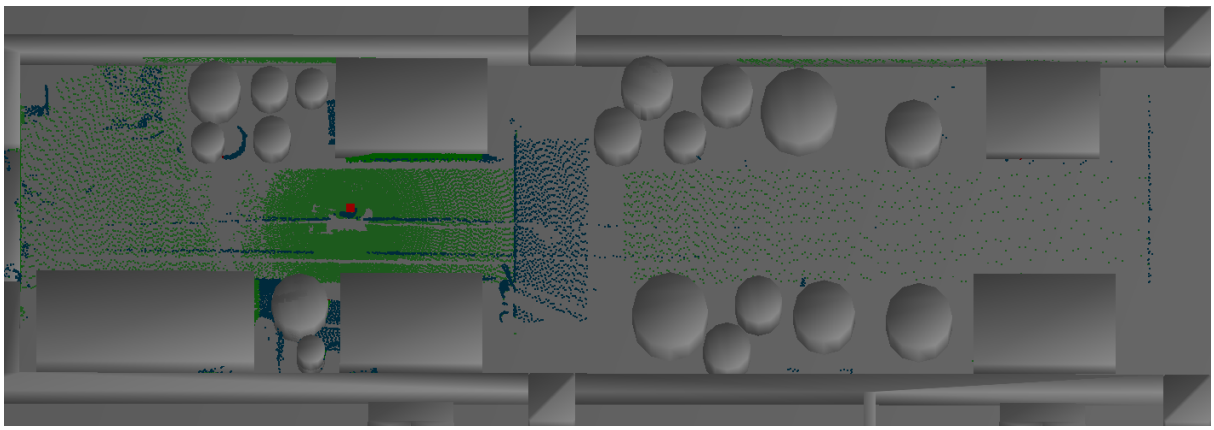

Figure 56: February 5th, 2011, Scan 6, 3D model and point-cloud after object recognition

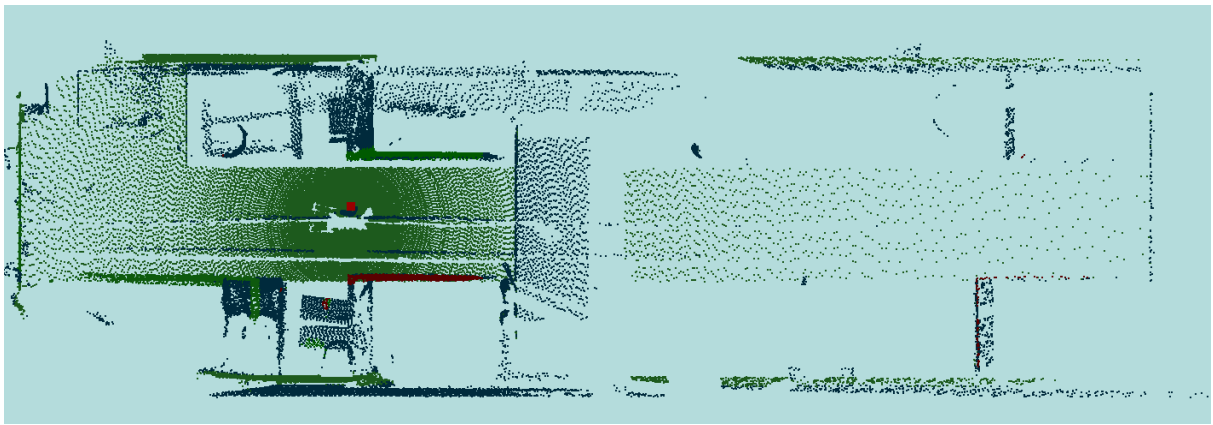

Figure 57: February 5th, 2011, Scan 6, point-cloud after object recognition

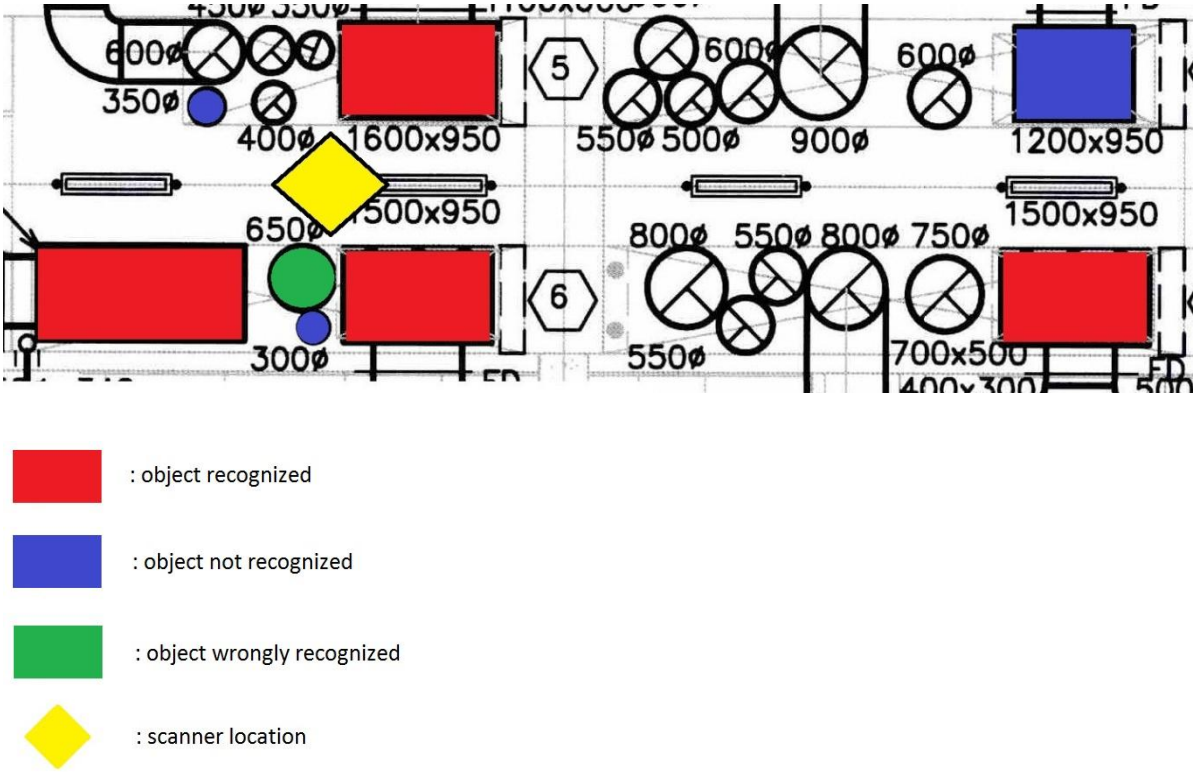

Figure 58: February 5th, 2011, Scan 6, object recognition results

5.3 Result Analysis

5.3.1 Accuracy Performance Metrics

To analyze the results presented in the preceding sections, it is important to look at the accuracy performance metrics as they are defined in Bosché (2008):

Recall: Number of model objects that truly are in the investigated scan and are located within 5 cm of where they were designed to be and are recognized, divided by the total number of model objects that truly are in the investigated scan and are located within 5 cm of where they were designed to be.

$$Recall\ Rate = \frac{n(\{Object\ in\ scan\ within\ 5\ cm\} \cap \{Object\ recognized\})}{n(\{Object\ in\ scan\ within\ 5\ cm\})}$$

Type II error rate (also called "false negative rate"): Number of objects that truly are in the investigated scan and are located within 5 cm of where they were designed to be but are not recognized, divided by the total number of model objects that truly are in the investigated scan and are located within 5 cm of where they were designed to be. This is equal to one minus the recall.

$$Type\ II\ Error\ Rate = \frac{n(\{Object\ in\ scan\ within\ 5\ cm\} \cap \{Object\ not\ recognized\})}{n(\{Object\ in\ scan\ within\ 5\ cm\})}$$

Specificity: Number of model objects that truly are not in the investigated scan within 5 cm where they were designed to be and are not recognized, divided by the total number of model objects are not in the investigated scan within 5 cm where they were designed to be.

$$Specificity\ Rate = \frac{n(\{Object\ not\ in\ scan\ within\ 5\ cm\} \cap \{Object\ not\ recognized\})}{n(\{Object\ not\ in\ scan\ within\ 5\ cm\})}$$

Type I error rate (also called "false positive rate"): Number of objects that truly are not in the investigated scan within 5cm where they were designed to be but are recognized, divided by the total number of model objects that truly are not recognized in the investigated scan within 5 cm where they were designed to be. This is equal to one minus the specificity.

$$Type\ II\ Error\ Rate = \frac{n(\{Object\ not\ in\ scan\ within\ 5\ cm\} \cap \{Object\ recognized\})}{n(\{Object\ not\ in\ scan\ within\ 5\ cm\})}$$

Precision: Number of objects that truly are in the investigated scan and are located within 5 cm of where they were designed to be and are recognized, divided by the total number of objects that are recognized.

$$Precision = \frac{n(\{Object\ in\ scan\ within\ 5\ cm\} \cap \{Object\ recognized\})}{n(\{Object\ recognized\})}$$

The 5cm limit set in all the definitions comes from the 5cm construction error parameter mentioned in Section 4.5. The use of the construction error parameter is discussed in Section 5.3.4.

5.3.2 October 19th, 2010

As seen in Section 5.2.1, the results of the object recognition leave out one duct. Figure 60 shows these results directly on the point-cloud.

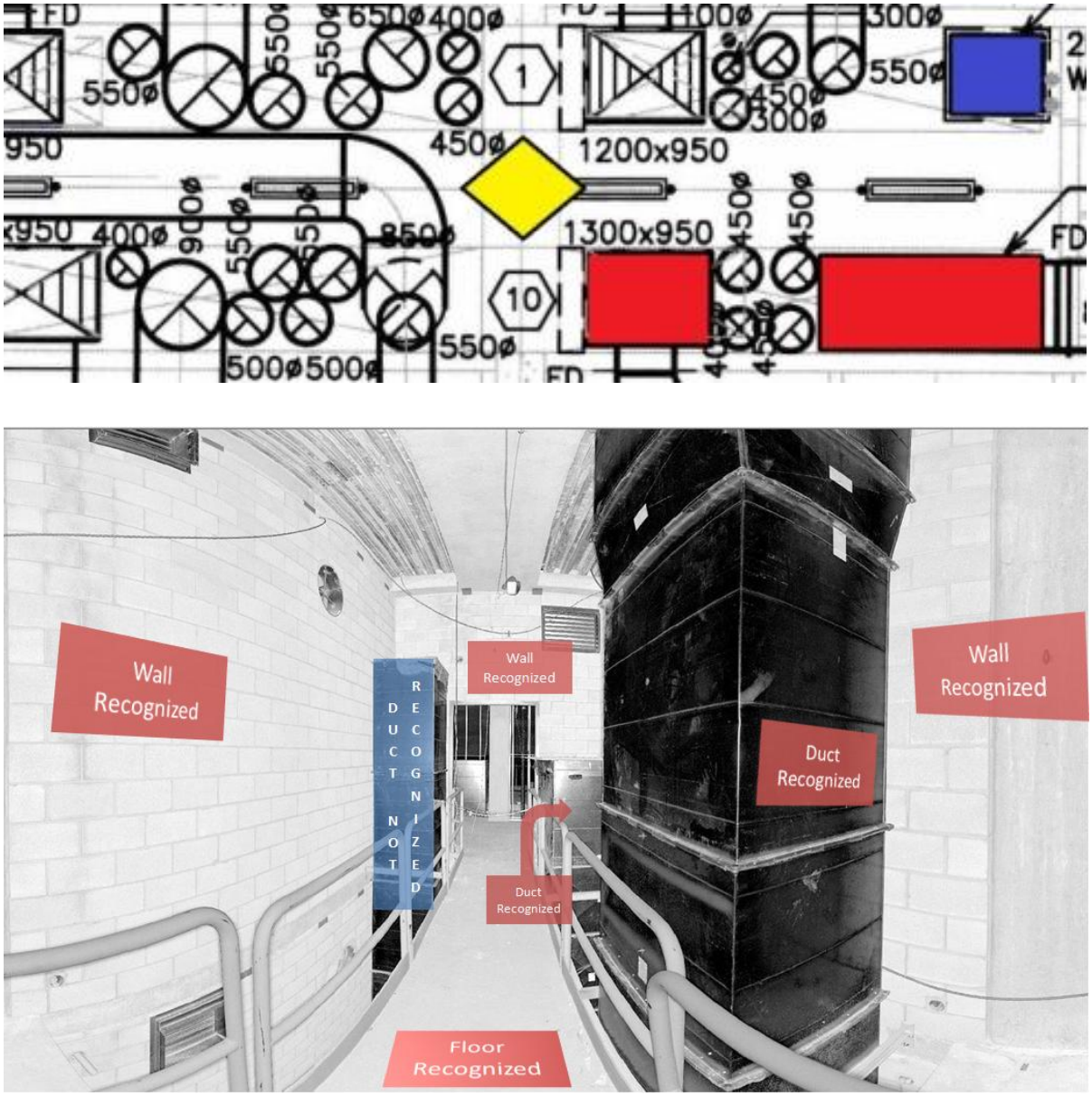

Figure 59: October 19th, 2010, object recognition analysis (colorized drawings and point-cloud)

The reason why the duct highlighted on blue in Figure 59 is not being recognized by the object recognition process is that its location on the as-planned drawings (Figure 31) was not respected due

to the fact that the object was installed in an incorrect location. One of the parameters of the object recognition that was performed during this study is called "construction error". The construction error parameter was set to 5 cm for the purpose of this study, which means that if an object is built more than 5 cm away from where it was originally supposed to be built according to the drawings, then it will not be recognized during the object recognition process. As can be seen in Figure 61, the points on the point-cloud representing the actual position of the duct are more than 5 cm away from the 3D object representing the originally planned position of the duct. If those points were within a 5 cm distance from the 3D object, then the object would be recognized. They are manifestly not, hence the object is not recognized.

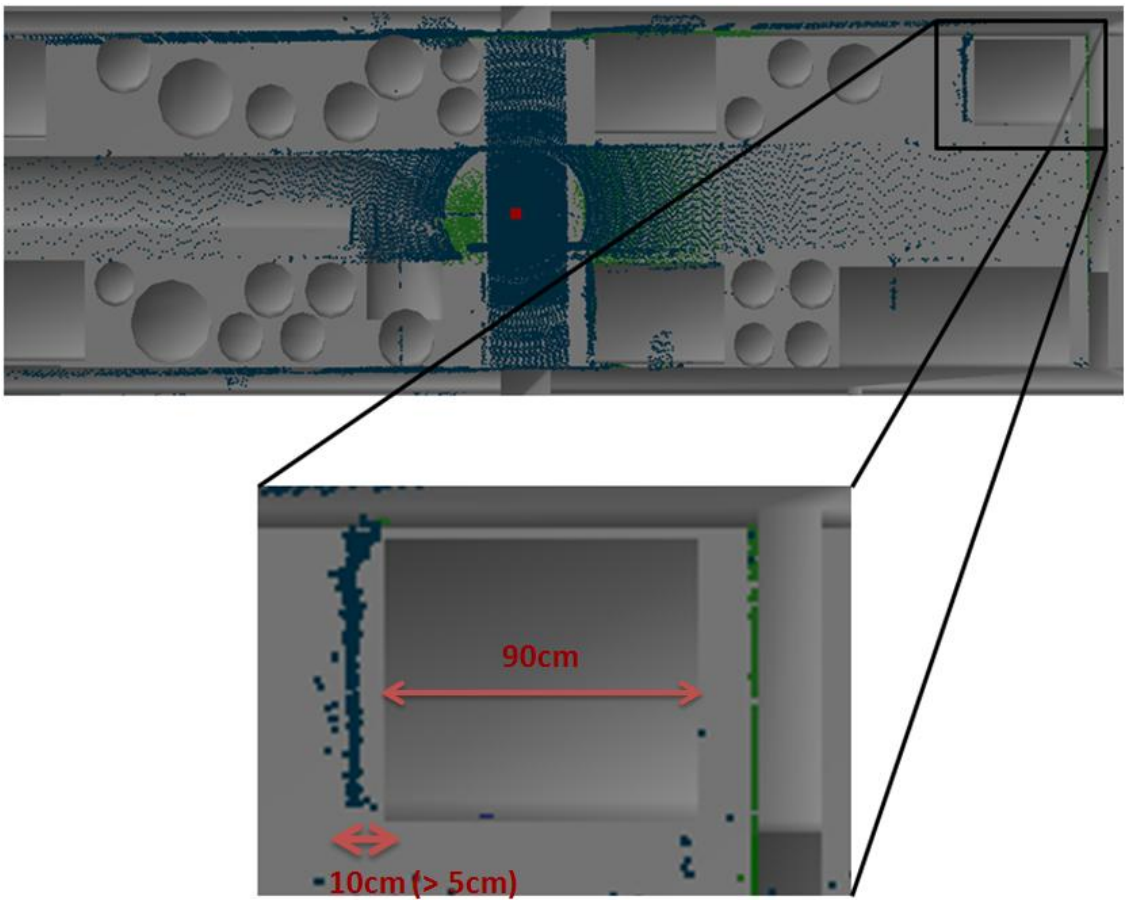

Figure 60: October 19th, 2010, duct not recognized

The recognition results and performance obtained from the data acquired on October 19th 2010 are: Recall = 100%, Specificity = 100% and Precision = 100%. The performance metrics of 100% are function of the 5 cm construction error. The object that is not recognized by the object recognition

algorithm, because not installed where it was designed to be within a 5 cm perimeter, provides information on the quality of the work that was performed. Another algorithm could be developed to enable the detection of objects installed at a location in contradiction with the original design. Research is now being conducted to study slices of point-clouds and pipe reconstruction as means to detect objects installed further away than the construction error. Such a technique would have allowed the detection of the duct in Figure 61.

5.3.3 February 5th, 2011

5.3.3.1 Overall object recognition results

Figure 62 presents the results of the study for the scans from 1 to 6 as seen in Section 5.2.

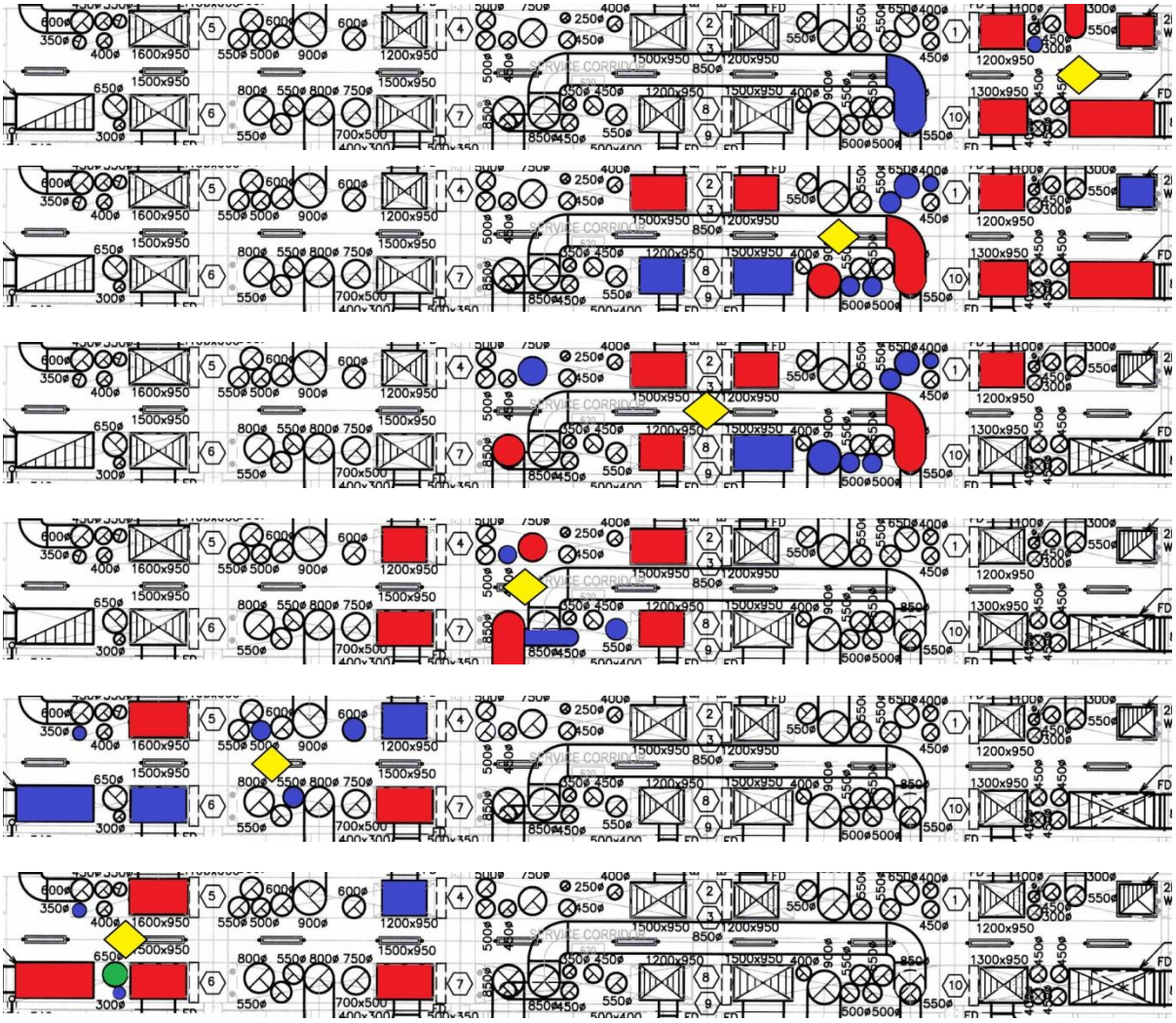

When the 6 different sets of results displayed above are merged together using a Boolean OR operation, the overall result is:

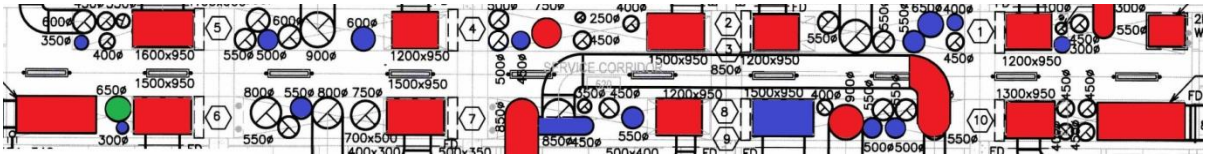

Figure 61: Object recognition overall result

Table 10 summarizes the recognition results and performances obtained for the six point-clouds.

Table 10: Febryary 5th, 2011, object recognition results

Point-cloud	Recall	Specificity	Precision
Scan 1	90%	100%	100%
Scan 2	79%	100%	100%
Scan 3	77%	100%	100%
Scan 4	83%	100%	100%
Scan 5	50%	100%	100%
Scan 6	80%	94%	89%
Overall	70%	98%	95%

There are a few explanations on why some objects are not recognized or wrongly recognized by the object recognition process: (1) wrong pipe location, (2) object not completed, (3) the range of analysis of the object recognition algorithm, (4) wrong duct shape, and (5) occlusion (which does not occur in this study because all the objects built are in the scans). These explanations are detailed in the following sections.

5.3.3.2 Objects not recognized

5.3.3.2.1 Object not recognized: Wrong object location

As can be seen in Figure 48 concerning the point-cloud (February 5th, 2011, Scan 4), one pipe was built at an entirely different location than where it was designed to be according to the original drawings (Figure 63). This results in the pipe not being recognized by the object recognition process. As discussed in Section 5.3.2, research is being conducted to allow detection of objects installed at a wrong location compared to the original design.

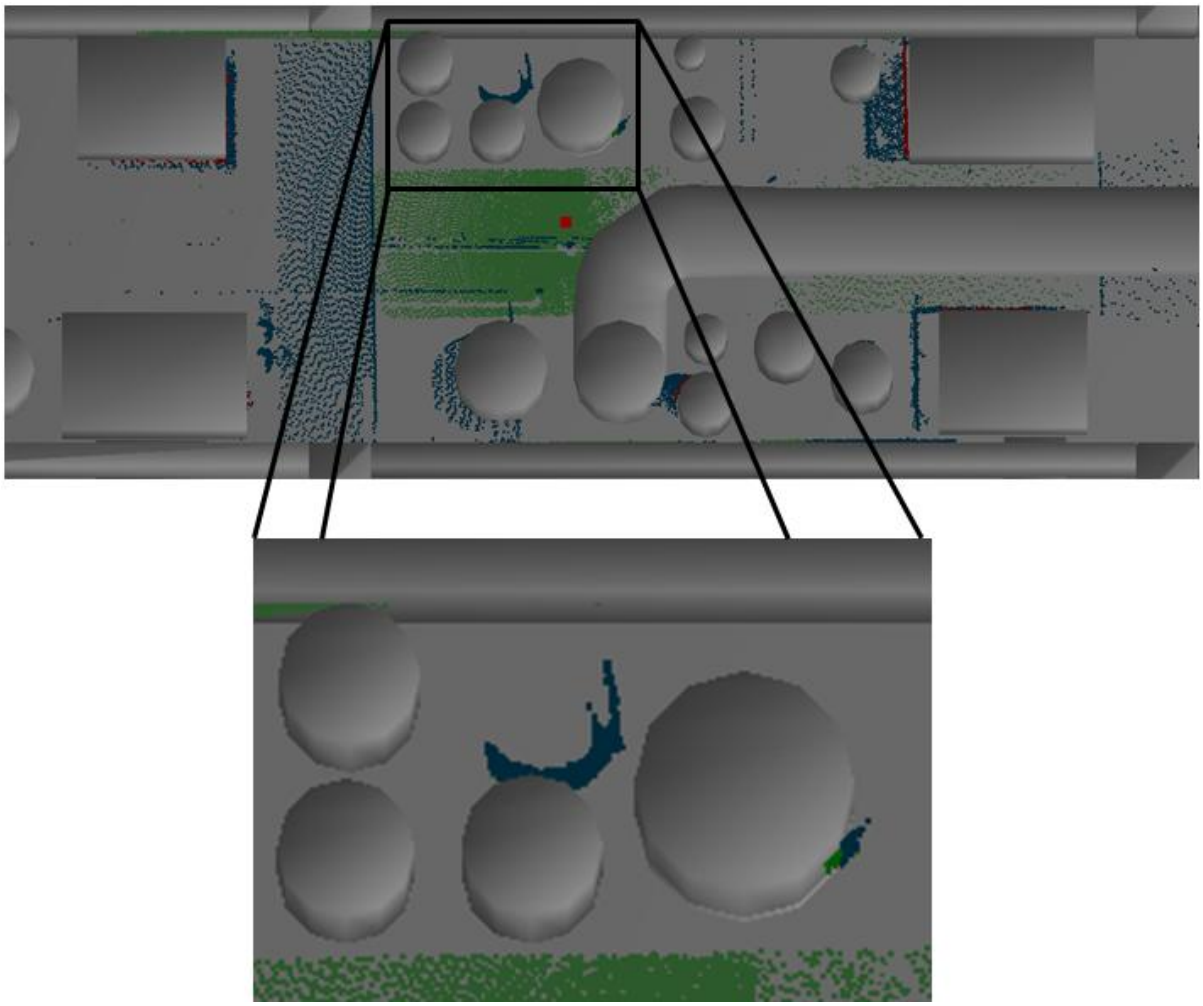

Figure 62: Object not recognized, wrong object location

5.3.3.2.2 Object not recognized: Object not completed

The second explanation for an object not to be recognized by the object recognition software is the fact that at the time of scanning some pipes or ducts may simply not be completed yet, thus reducing the number of points representing them in the as-built point-cloud. Figure 64 shows an example of this situation occurring for 2 different pipes from Figure 62 (overall result).

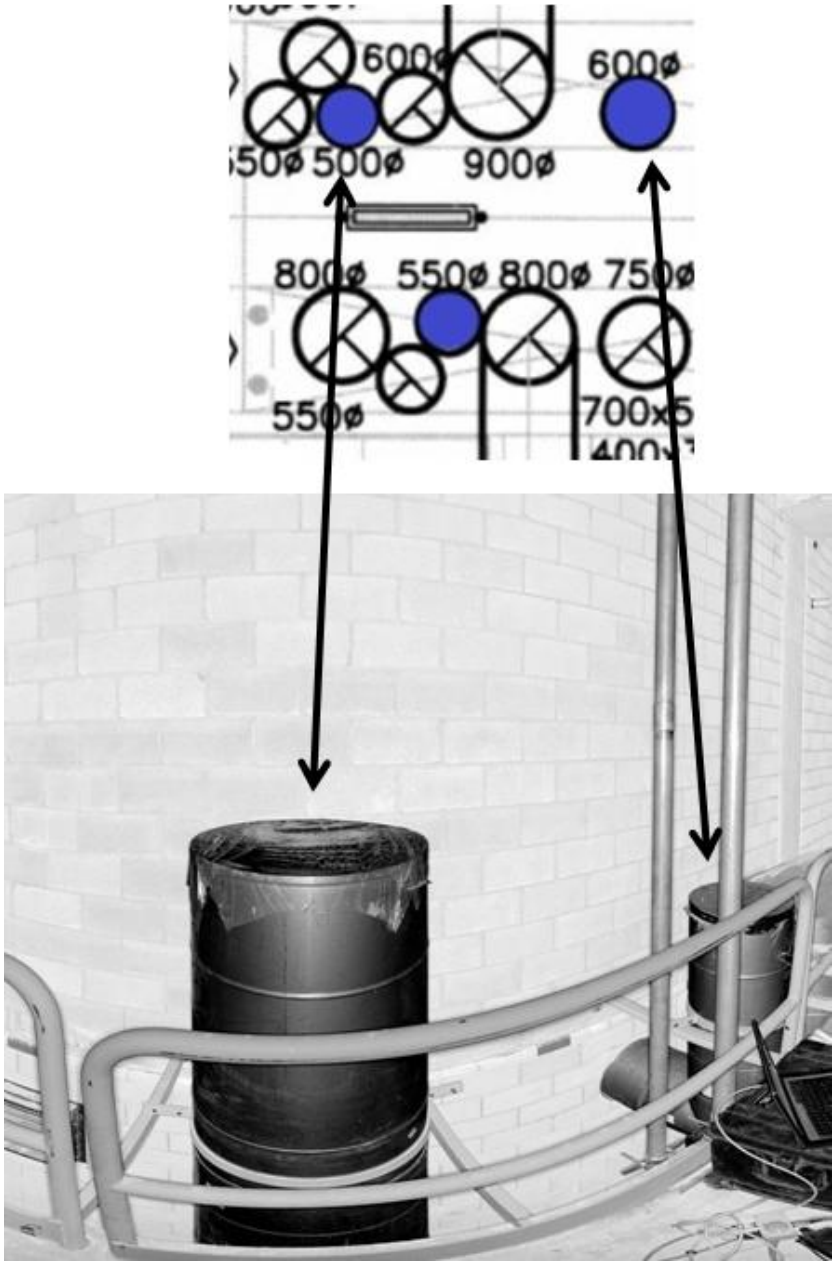

Figure 63: Object not recognized, objects not completed

5.3.3.2.3 Object not recognized: Range of analysis of the object recognition algorithm

Finally the last possible explanation for an object not to be recognized in this project is the fact that the algorithm developped by Bosché (2008) was developed for a range of point-cloud acquisition further away than the range in this study. As explained in Figure 65, Turkan (2012) used a range of acquisition from 50m to 200m whereas in this study the range was from 1m to 10m. Unfortunately, Bosché (2008) takes into account the range, called "RangeMax", which forces near objects to have a very high number of points on the point-clouds in order to be recognized.

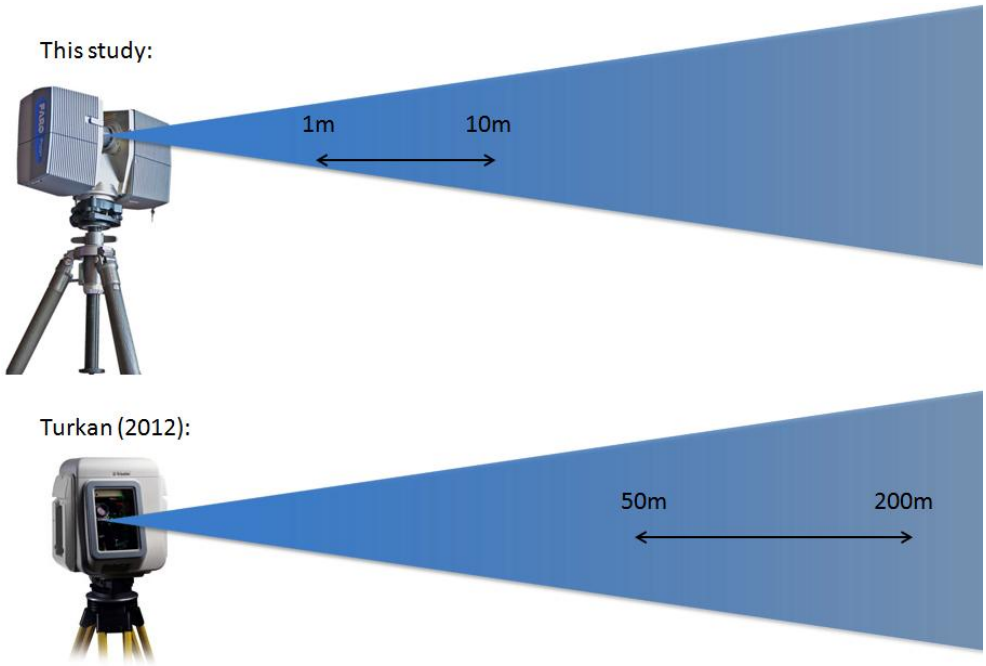

Figure 64: 5.3.2.5 Object not recognized: Range of analysis of the object recognition algorithm

Bosché (2008) is developed so that the surface the furthest way (RangeMax) on the point-cloud from the scanner location needs to be covered by at least 5 points to be recognized. As the point-clouds acquired for this study actually contain points as far as 40m away from the scanner location (which are unusable in this study as can be seen on all the results displayed in Section 5.2 where the range of recognized objects is always under 10m), it means that an object 1m away from the scanner needs to have at least 8000 points on the point-cloud to be considered recognized, which is sometimes difficult to achieve if all the previous factors (wrong object location, object not completed, occlusions) are taken into account.

5.3.3.2.4 Object not recognized: Wrong duct shape

As can be seen in Figure 56 and Figure 58, one pipe (highlighted in green) is wrongly recognized. The reason is that the duct (highlighted in red) next to it actually expands in shape at its top as can be seen in Figure 66 below representing a view in 3D from below of the 3D as-planned model and the as-built point-cloud after the object recognition process. This expansion of shape was not originally planned in the drawings, which resulted in a pipe being wrongly recognized. Figure 67 shows the actual point-cloud where this situation is occurring by simulating the pipe as it was supposed to be built.

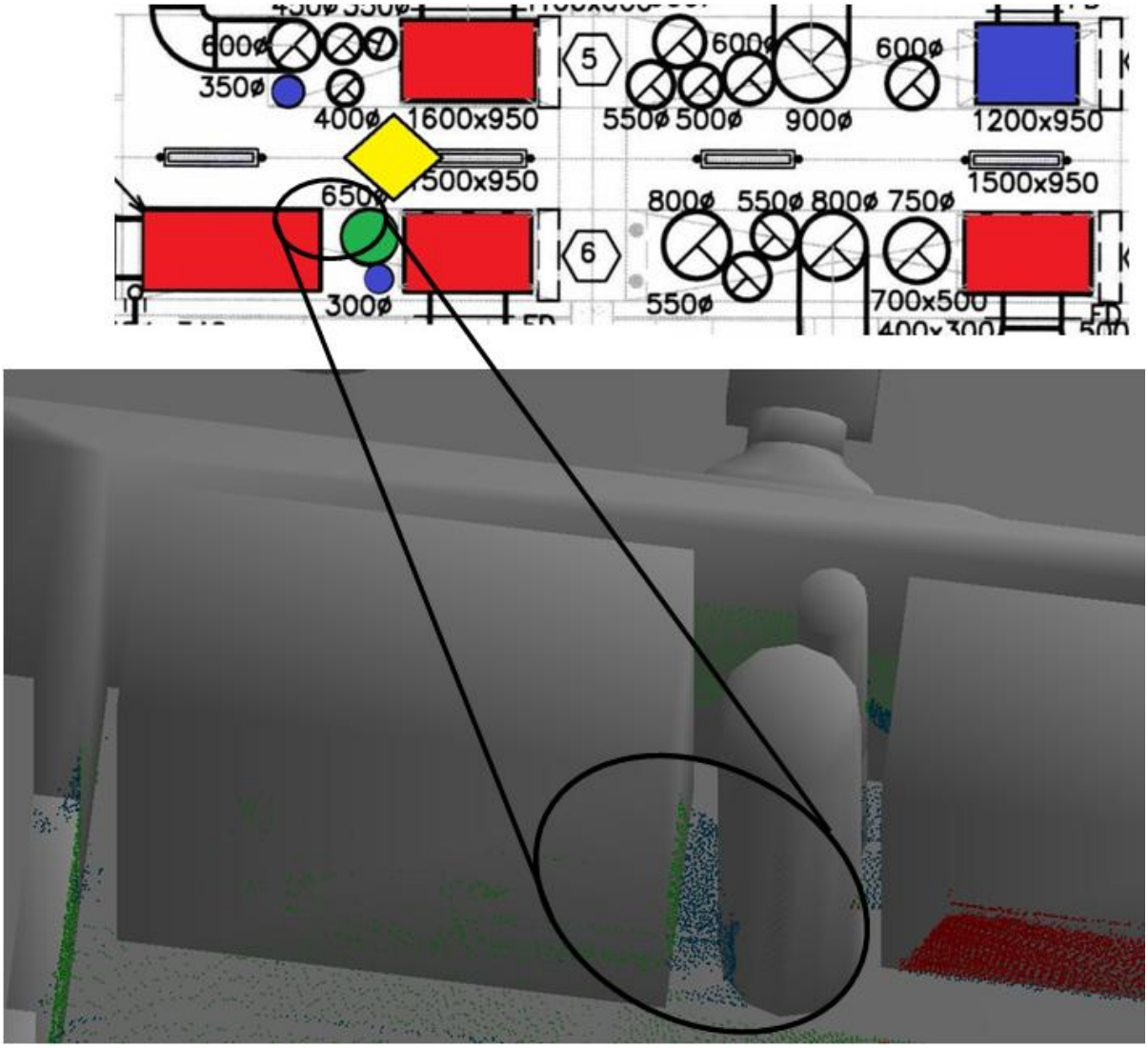

Figure 65: Object wrongly recognized: wrong duct shape (1)

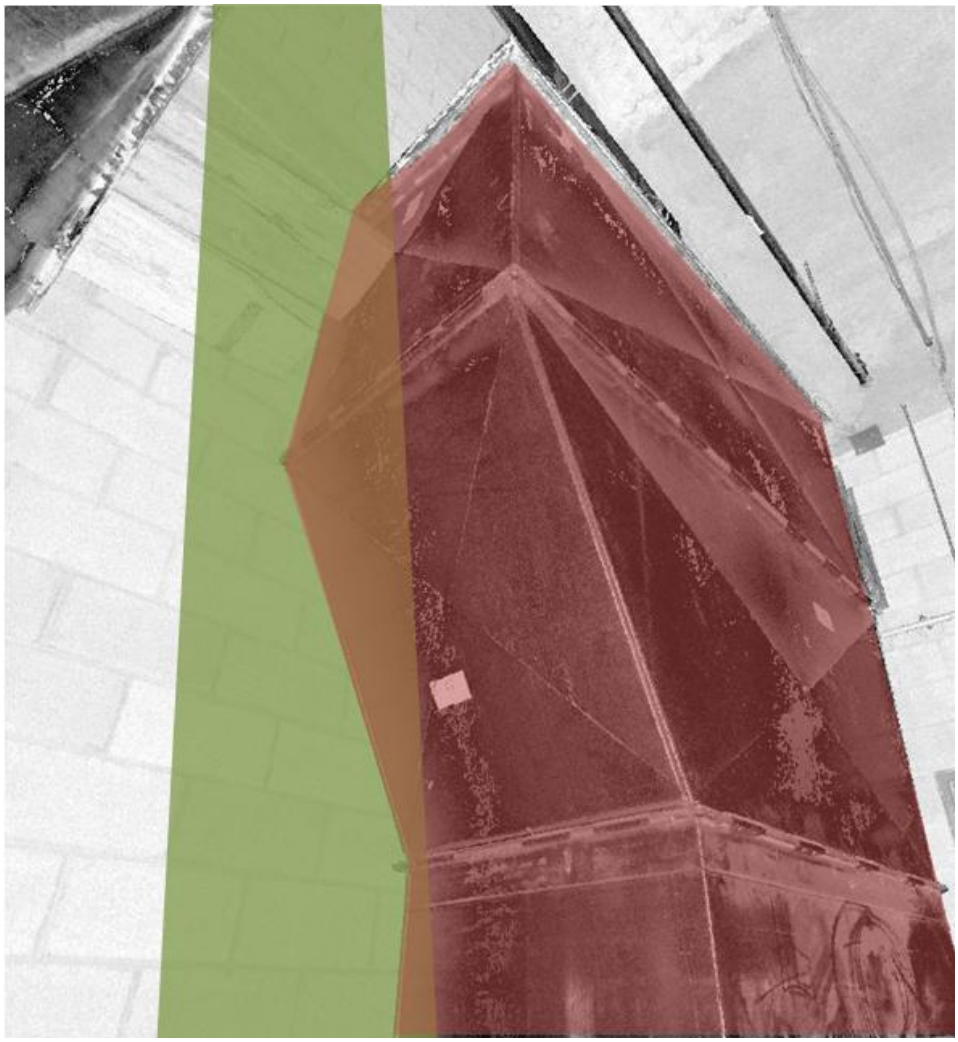

Figure 66: Object wrongly recognized: wrong duct shape (2)

5.3.3.2.5 Objects not recognized: Overall explanation

Figure 68 shows the different explanations that where responsible for objects not being recognized (highlighted in blue) or wrongly recognized (highlighted in green) on the overall results (Figure 62).

Overall objects recognized or wrongly recognized:

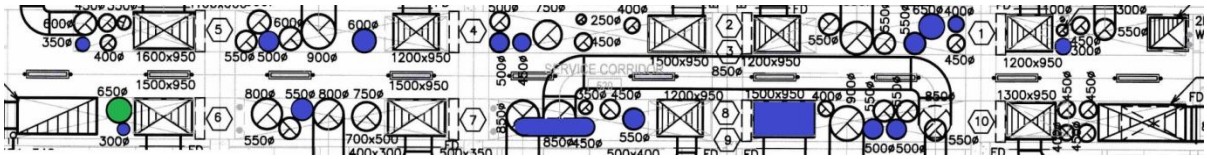

Objects not recognized or wrongly recognized by "**wrong location**" factor:

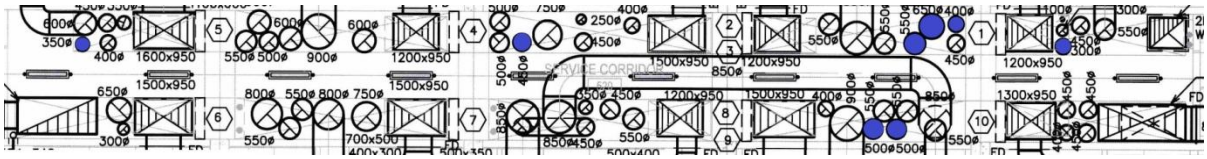

Objects not recognized or wrongly recognized by "**object not completed**" factor:

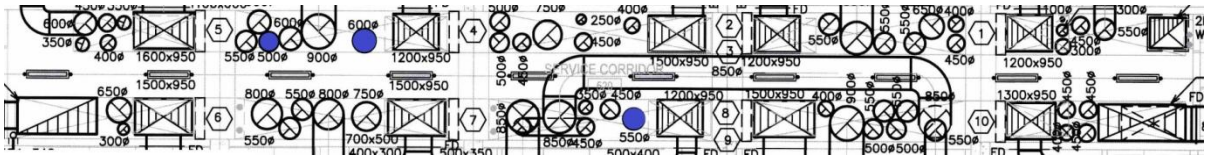

Objects not recognized or wrongly recognized by "**range of algorithm**" factor:

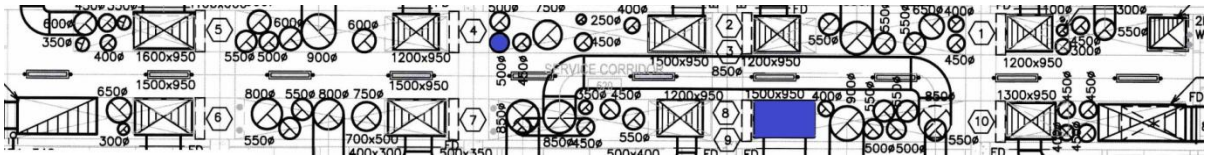

Objects not recognized or wrongly recognized by "**wrong shape**" factor:

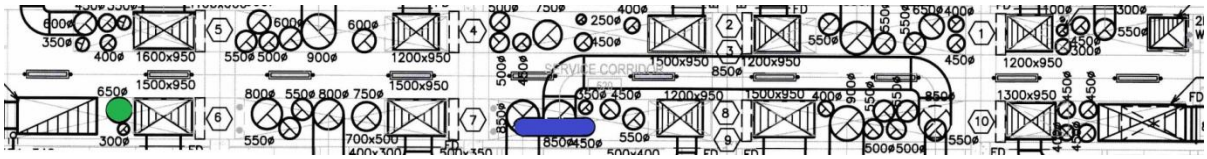

Figure 67: Object not recognized: Overall explanation

5.3.4 Construction error parameter

The previous results presented in Section 5.2 were obtained with a construction error parameter set to 5 cm, as explained in Section 4.5. The same experiments were also run for a construction error parameter set to 2 cm. The reason for this is that it sometimes is really important to know if, and by how much, an object is built at a wrong location compared to its as-planned location. By also running the object recognition process on the point-clouds at a 2 cm construction error, it is now possible to identify the objects that are built within the interval [2 cm, 5 cm] from their as-planned location by subtracting the objects recognized at 2cm construction error from those recognized at 5 cm construction error. Figure 69 shows the result of this operation for the point-cloud (October 19th, 2010), and Figure 70 for the point-clouds (February 5th, 2011).

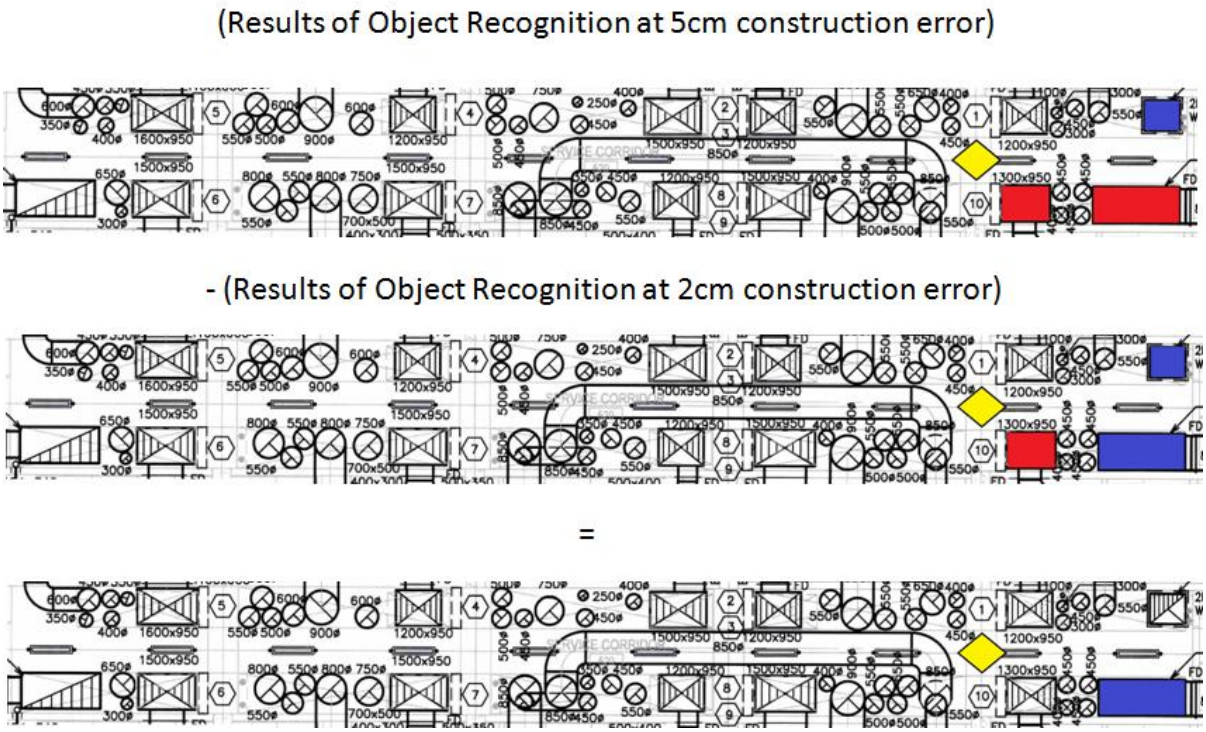

Figure 68: October 19th, 2010:
identification of objects built at wrong location within [2 cm, 5 cm]

(Results of Object Recognition at 5cm construction error)

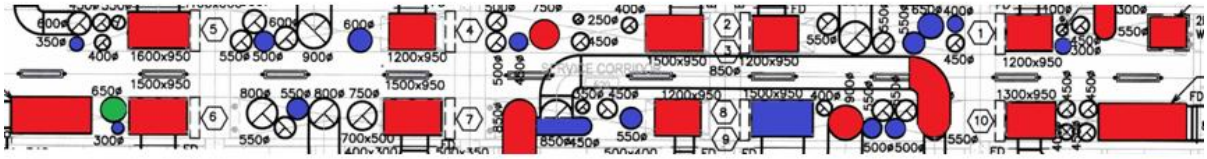

- (Results of Object Recognition at 2cm construction error)

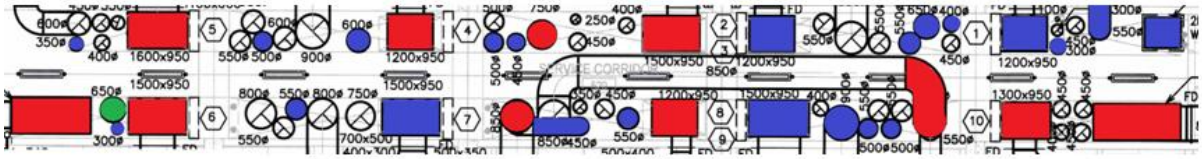

=

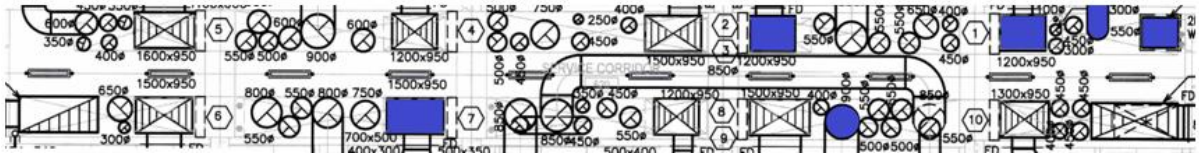

Figure 69: February 5th, 2011:
identification of objects built at wrong location within [2 cm, 5 cm]

This analysis demonstrates that the object recognition algorithm can not only be used for progress tracking, but also for quality tracking, because it gives information on objects that are installed or built at a proximate location compared to their planned location on the original design.

5.3.5 Practical differences between coarse and fine registration

As explained in Section 2.3.2, the fine registration is supposed to refine the results of the coarse registration by minimizing the distance between the as-built point-cloud and the 3D as-planned model. However, during the course of this study it sometimes was found that the output of the coarse registration was actually more accurate than the ones of the fine registration. Displayed below (Figure 71) is an example of this situation occurring.

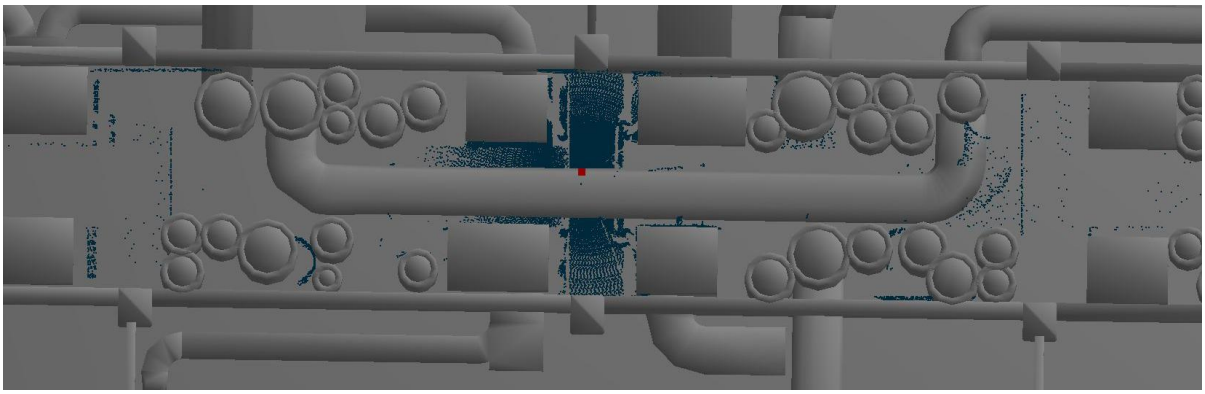

(1)

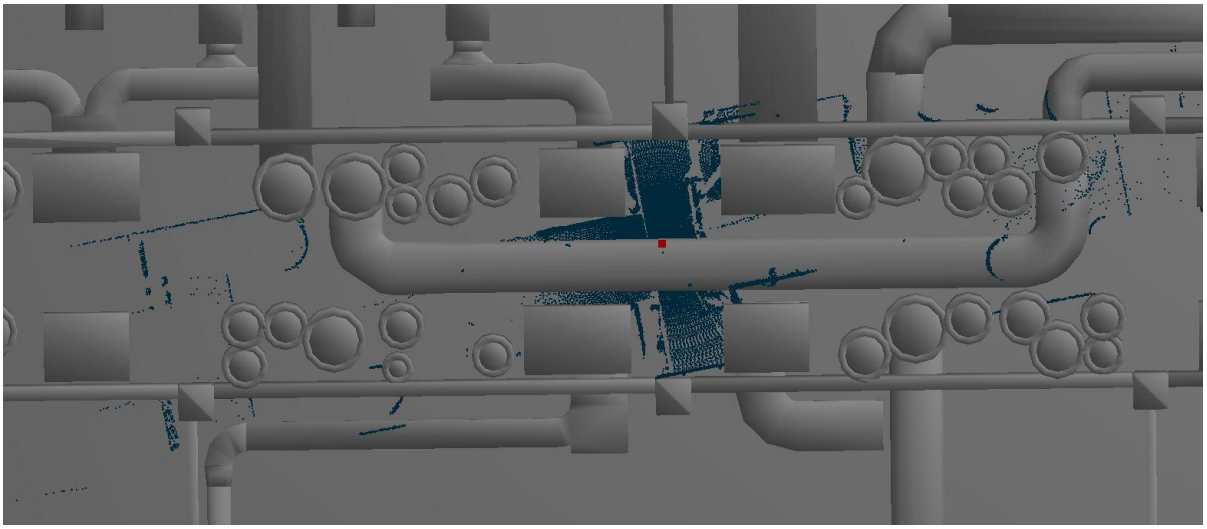

(2)

Figure 70: (1) Scan 3, February 5th, 2010, output of the coarse registration
(2) Scan 3, February 5th, 2010, output of the fine registration

In this situation, the fine registration failed to improve the output of the coarse registration, and actually caused the registration to be grossly tilted. When that case occurs, it is always preferable to use the coarse registration in the object recognition algorithm. The result of the coarse registration is always very accurate because during this operation, the points representing the walls are aligned with the objects representing those walls. The fine registration looks to optimize this placement, however an obvious error in the fine registration algorithm provokes some registrations to be grossly wrong. No guidance can be given as to when this issue may occur. Table 11 summarizes which of the two registrations was used for the different point-clouds in this study.

Table 11: Registration used for the different point-clouds

Point-cloud	Registration
October 19th, 2010	Fine
February 5th, 2011, Scan 1	Coarse
February 5th, 2011, Scan 2	Fine
February 5th, 2011, Scan 3	Coarse
February 5th, 2011, Scan 4	Fine
February 5th, 2011, Scan 5	Coarse
February 5th, 2011, Scan 6	Coarse

Chapter 6
Conclusions and Recommendations

6.1 Summary

The main purpose of this study was to apply an object recognition algorithm to enable an automated progress tracking of a building under construction. This approach already being investigated by researchers for structures such as floors, beams and columns, this study focused on reaching a smaller level of detail: pipes and ducts.

Point-clouds were acquired using the 3D laser scanning technology and were later subjected to the object recognition algorithm to determine the accuracy and efficiency of the approach.

6.2 Conclusions

Concerning the primary objective of this study, it was found that the utilization of the 3D laser scanning technology to acquire point-clouds of building under construction was excellent, although having the following constraints:

- high cost of the laser scanning technology
- bad portability
- significant labor hours
- constraints concerning the positions of the targets

Concerning the secondary objective, the use of an object recognition algorithm to automatically track the progress of pipe and ductwork installation, it was found that, although proved difficult by many factors that where individually analyzed, many of those issues can be overcome by the following methods:

- having an accurate drawing and 3D as-planned model of the building to deal with issues concerning objects installed at wrong location and wrong object shape

- acquiring enough scans in time to deal with issues of objects not completed
- acquiring enough scans in space to deal with possible occlusions and the issues of range of analysis of the object recognition algorithm

If these issues can be dealt with, the object recognition process used in this study proves to be accurate and efficient.

This study proves that Bosché (2008) can be applied to structural elements as well as mechanical systems such as ducts and pipes for progress tracking purposes. It was also found that running the object recognition algorithm at different construction error parameters enables a quality tracking by highlighting the elements that are either built or installed in incorrect locations compared to the as-planned locations.

6.3 Recommendations

It was found that the range of analysis of the object recognition algorithm may prove to be an issue for near objects. Its old design and the inappropriate area metric for ranges of 0 m to 20 m prove to be problematic. The issue should be addressed to ensure the complete success of the object recognition process for pipes and ducts.

In this study, the object recognition recall rate considers only the objects that were installed were they were designed to be on the 3D as-planned CAD model. However it was shown that objects are sometimes installed at different locations from the design and that the object recognition algorithm is enabled to detect them when it happens, this shows the limitations of the method. This study could be further improved by considering the following different status categories:

- objects built within construction error
- objects built outside construction error but proximate
- objects built in different location

By classifying the objects in these categories, different recall rates, specificity rates, and precision rates should be found. Also, a new algorithm could be designed to be able to detect the objects installed but that were not in the design.

This research could be extended by studying the earned value of the total quantity of installed pipes and ducts as it was performed in Turkan (2012). Also, some work could be done on studying the impact of the evolution of the mechanical design after the start of construction on the degradation of the automated object recognition performances, because of the difficulty of calculating the percentage of built-as-designed objects if the latest design is unavailable.

The object recognition was found to sometimes suffer from glitches. Indeed, where the fine registration is supposed to improve the output of the coarse registration, it was sometimes found that the coarse registration happened to be a lot more accurate than the fine registration. An improvement of the registration software seems in order.

Finally, this study focused on the service corridor of the fifth floor of the Engineering VI Building of the University of Waterloo, but it would be interesting to perform the same study for the point-clouds covering an entire building and in different scenarios.

References

Ahmed, M.F.M., Guillemet, A., Shahi, A., Haas, C.T., West, J.S., Haas, R.C.G., (2011), "Comparison of Point-cloud acquisition from Laser Scanning and Photogrammetry based on Field Experimentation", Proceedings, Canadian Society of Civil Engineering, 3rd International/9th Construction Specialty Conference, Ottawa, Canada.

Ahmed, M.F.M., Haas, C.T., (2011), "The Potential of Low Cost Close Range Photogrammetry towards Unified Automatic Pavement Distress Surveying", TRB 2010 Annual Meeting.

Akinci, B., Anumba, C., (2008), "Technological assessment and process implications of field data capture technologies for construction and facility/infrastructure management", ITcon Vol. 13, Special Issue Sensors in Construction and Infrastructure Management, 134-154.

American Society of Photogrammetry, (1980), "Manual of Photogrammetry Fourth Edition", Fort Bend Book Company, Sugar Land, Texas.

Besl, P.J., McKay, N.D., (1992), "A method for registration of 3D shapes", IEEE Transactions on Pattern Analysis and Machine Intelligence, 14(2), 239-256.

Biddiscombe P. (2005). "3D Laser scan tunnel inspections keep expressway infrastructure project on schedule" Trimble™ White Paper.

Blais, G., Levine, M.D., (1995), "Registering multiview range data to create 3D computer objects", IEEE Transactions on Pattern Analysis and Machine Intelligence, 17(8), 820-824.

Bosché F. (2008). Automated Recognition of 3D CAD Model Objects in Dense Laser Range Point Clouds, PhD Thesis presented to the University of Waterloo.

Bosché F., Haas C. T. (2008). "Automated retrieval of 3D CAD model objects in construction range images", Journal of Automation in Construction, Elsevier, 17(4), 499-512.

Bosché F., Haas C.T., Murray P., (2008), "Performance of Automated Project Progress Tracking with 3D Data Fusion", Proceedings, CSCE Annual Conference, Quebec, QC, Canada, June 10-13.

Bosché F., Haas C.T., Akinci B. (2009). "Performance of a new approach for automated 3D project performance tracking", ASCE Journal of Computing in Civil Engineering, Special Issue on 3D Visualization, 23(6), 311-318.

Bosché F., (2009), "Automated recognition of 3D CAD model objects and calculation of as-built dimensions for dimensional compliance control in construction", Advanced Engineering Informatics, Elsevier, 24(1), 107-118.

Chen, Y., Medioni, G., (1992), "Object modeling by registration of multiple range images", Image Vision Computing, 10(3), 145-155.

El-Omari S., Moselhi O. (2008). "Integrating 3D laser scanning and photogrammetry for progress measurement of construction work.", Journal of Automation in Construction, Elsevier, 18(1), 1-9.

Faro Laser Scanner 880 HE Handbook, (2007), Faro Technologies Inc., Lake Mary, FL, USA.

Faro Scene® Manual, (2007), Faro Technologies Inc., Lake Mary, FL, USA

Fryer, J.G, Mitchell, H.L., Chandler, J.H., (2007), "Applications of 3D Measurement from Images".

Golparvar-Fard, M., Pena-Mora, F., Savarese, S., (2009), "Application of D4AR – A 4-Dimensional augmented reality model for automating construction progress monitoring data collection, processing and communication", Journal of Information Technology in Construction, Special Issue Next Generation Construction IT: Technology Foresight, Future Studies, Road mapping, and Scenario Planning, 14, 129-153.

Greaves T., Jenkins B., (2007), "3D laser scanning market red hot: 2006 industry revenues 253 million, 43% growth", Spar Point Research LLC, SparView, 5(7).

Habib, A.F., Ghanma, M.S., Tait, M., (2004), "Integration of LIDAR and photogrammetry for close range applications", Proceedings of the XXth ISPRS congress, Istanbul, Turkey, Commission VII, 972-983.

Huber, D., Akinci, B., Tang, P., Adan, A., Okorn, B., Xiong, X., (2010), "Using Laser Scanners for Modeling and Analysis in Architecture, Engineering, and Construction".

Jacobs, G., (2008), "3D scanning: Using multiple laser scanners on projects", Professional Surveyor Magazine, 28(4).

Kiziltas S., Akinci B., (2005), "The need for prompt schedule update by utilizing reality capture technologies: A case study." Proceedings, Construction Research Congress, San Diego, CA, USA.

Liang-Chien C., Yi-Chien S., Huang-Hsaing J., Chen-Wei H., Yong-Ming T., (2006), "Measuring system for cracks in concrete using multi-temporal images", Journal of Surveying Engineering, 132 (2), 77–82.

Lijing, B., Zhengpeng, Z., (2008), "Application of point clouds from terrestrial 3D laser scanner for deformation measurements", The International Archives of the Photogrammetry, Remote Sensing and Spatial Information Sciences, Beijing 2008, Volume 37, Part B5.

Niederöst, M., Maas, H.G., (1997), "Automatic deformation measurement with a digital still video camera", Optical 3-D Measurement Techniques IV, 266-271.

Park S.Y., Subbarao M., (2003), "A fast point-to-tangent plane technique for multi-view registration." Proceedings of the Fourth International Conference on 3-D Digital Imaging and Modeling (3DIM), Banff, Canada, October 06–10.

Park, H. S., Lee H. M., Adeli H., Lee I., (2007), "A new approach for health monitoring of structures: terrestrial laser scanning", Journal of Computer Aided Civil and Infrastructure Engineering, 22 (1) 19-30.

Qui, D.W., Wu, J.G., (2008), "Terrestrial laser scanning for deformation monitoring of the thermal pipeline traversed subway tunnel engineering".

Razavi, S.N., Young, D., Nasir, H., Haas, C., Caldas, C., Goodrum, P., (2008), "Field Trial of Automated Material Tracking in Construction", Proceedings CSCE Annual Conference, Quebec City, Canada.

Rodriguez, Y., Jaselskis, E., (1994), "Automated Timekeeping and Project Information System using Bar Coding Techniques," Transactions of the American Association of Cost Engineers 38th Annual Conference, San Francisco, CA, pp. CA.3.1-CA.3.8.

Rusinkiewicz S., Levoy M., (2001), "Efficient variants of the ICP algorithm", Proceedings of the Third International Conference on 3-D Digital Imaging and Modeling (3DIM), pp. 145–152. Quebec City, QC, Canada.

Schaufelberger, J.E., Holm, L., (2002), “Quality Management”, Management of Construction Projects, 211-222, Prentice Hall, Upper Saddle River, New Jersey, Columbus, Ohio.

Song, J., Haas, C., and Caldas, C., (2006), “Tracking the location of Materials on Construction Job Sites”, Journal of Construction Engineering and Management, 132(9), 910-918, September 2006.

Stone W., Cheok G., (2001), “LADAR sensing applications for construction”, Building and Fire Research, National Institute of Standards and Technology (NIST), Gaithersburg, MD.

Teizer, J., Venugopal, M., Walia, A., (2008), "Ultra Wideband for Automated Real-time Three-Dimensional Location Sensing for Workforce, Equipment, and Material Positioning and Tracking", Transportation Research Record: Journal of the Transportation Research Board, Volume 2081.

Trimble™ GX 3D Laser Scanner Datasheet, (2007), Trimble Navigation Limited, Dayton, Ohio, USA.

Trimble™, RealWorks® Survey 6.1, Technical Notes, (2007), Trimble Navigation Limited, Dayton, Ohio, USA.

Turkan Y., Bosché F., Haas C.T., Haas R., (2010), “Towards automated progress tracking of erection of construction of concrete structures”, Proceedings, Sixth International Conference on Innovation in Architecture, Engineering and Construction (AEC), College State, PA, USA.

Turkan Y., Bosché F., Haas C.T., Haas R.G., (2011), “Automated Progress Tracking Using 4D Models and 3D Sensing Technologies”, Journal of Automation in Construction, Elsevier.

Turkan, Y., (2012), “Automated Construction Progress Tracking using 3D Sensing Technologies”, PhD Thesis, University of Waterloo, Canada.

Yen K.S., Akin K., Ravani B., (2008), “Accelerated Project Delivery: Case Studies and Field Use of 3D Terrestrial Laser Scanning in Caltrans Projects”, Advanced Highway Maintenance and Construction Technology Research Center, Research Report UCD-ARR-08-06-30-0.

Appendix A
As-Built Point-Cloud Format Conversion

The following screenshots show the different steps conducted to convert the point-clouds into an ASC format. First the point-cloud is opened on Faro Scene®:

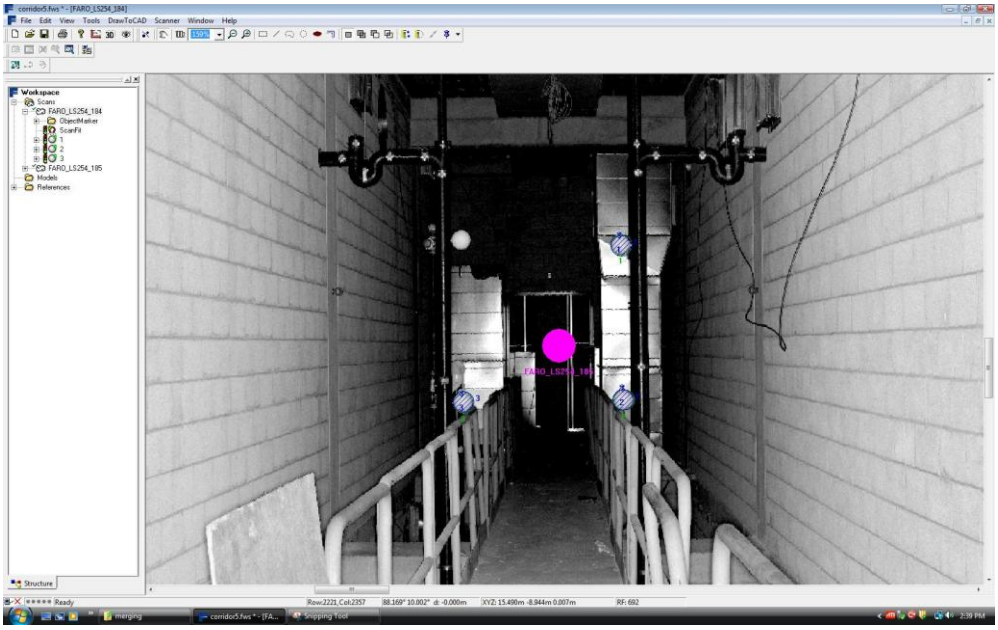

Then, the point-cloud is exported into an XYZ file via the Export Menu:

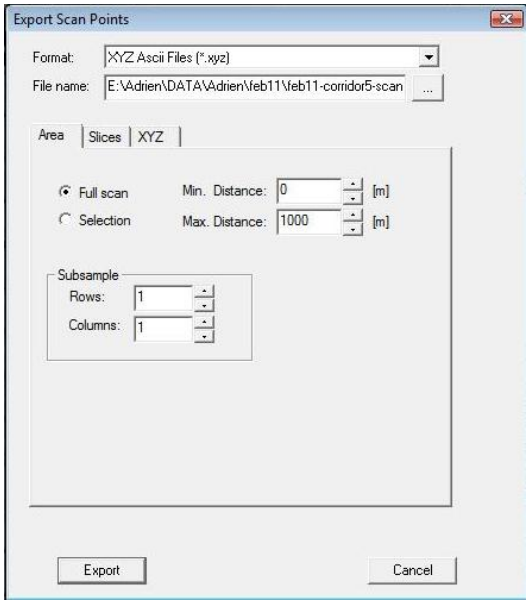

The result of this operation is a matrix, containing at every line the coordinates (X, Y, Z) and the color information (R, G, B) of every point in the point-cloud:

```
-0.02400000 -0.00540000 2.34550000 198 198 198
-0.02410000 -0.00550000 2.35800000 225 225 225
-0.02420000 -0.00550000 2.36430000 249 249 249
-0.02420000 -0.00550000 2.36080000 240 240 240
-0.02430000 -0.00550000 2.36660000 246 246 246
-0.02420000 -0.00550000 2.36250000 249 249 249
-0.02420000 -0.00550000 2.36250000 247 247 247
-0.02420000 -0.00560000 2.36550000 244 244 244
-0.02430000 -0.00570000 2.36370000 249 249 249
-0.02430000 -0.00570000 2.36550000 246 246 246
-0.02430000 -0.00580000 2.36430000 251 251 251
-0.02430000 -0.00580000 2.36490000 241 241 241
-0.02430000 -0.00580000 2.36660000 248 248 248
-0.02430000 -0.00580000 2.36350000 231 231 231
```

The point-cloud, now in XYZ format, is then imported in Trimble™ RealWorks® via the Import Menu:

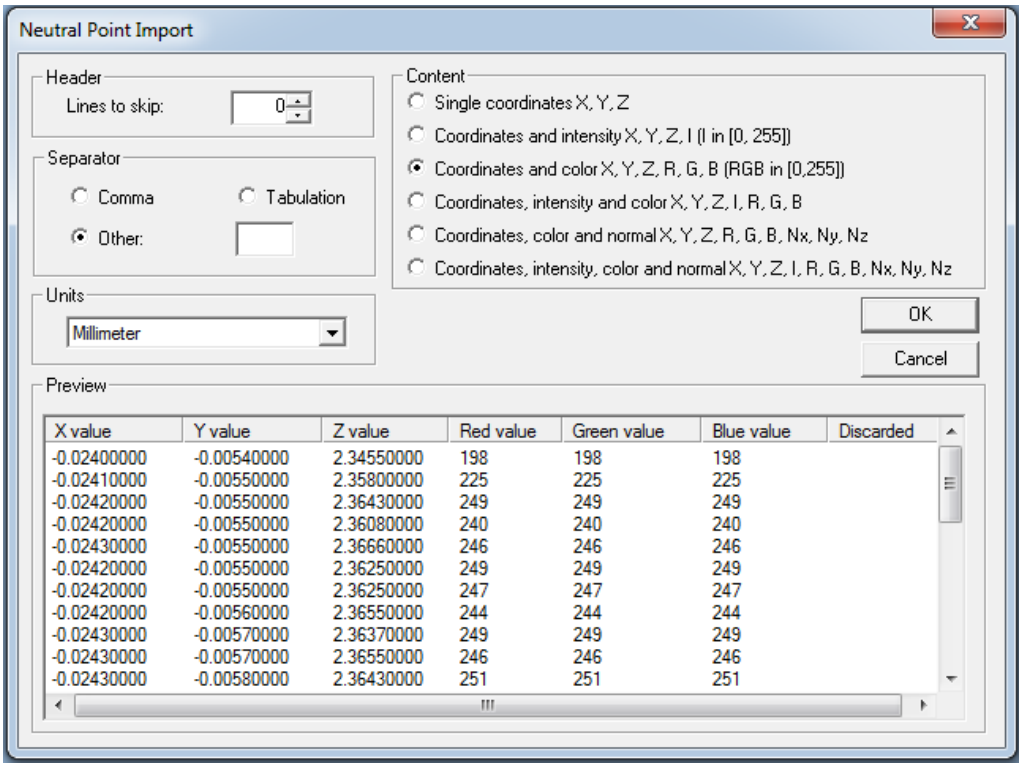

The point-cloud is now opened on Trimble™ RealWorks® :

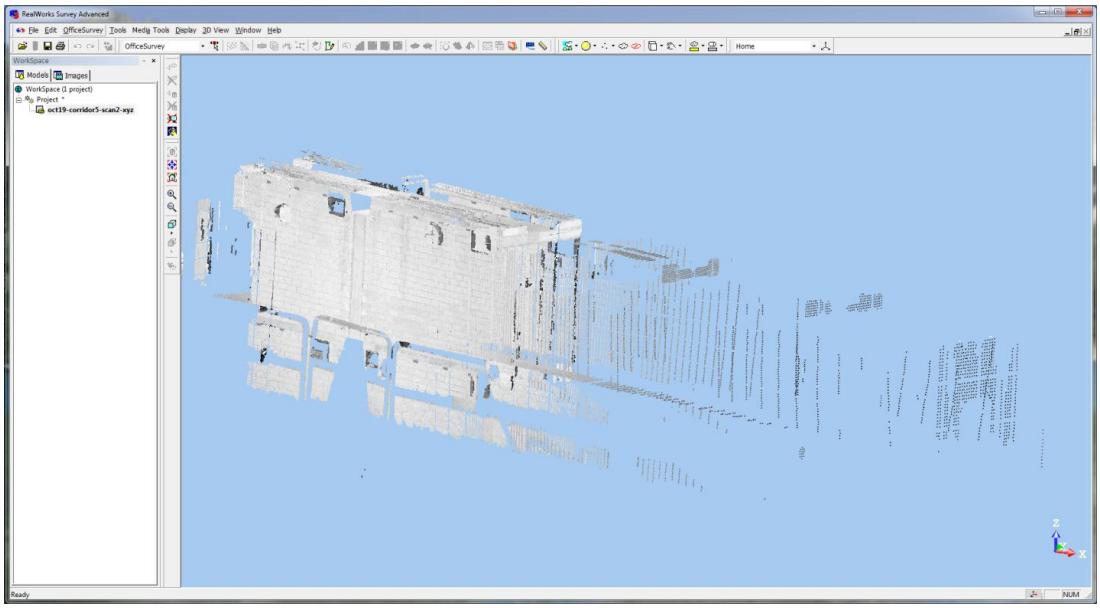

And finally, the point-cloud can now be exported into the (ASC) format needed:

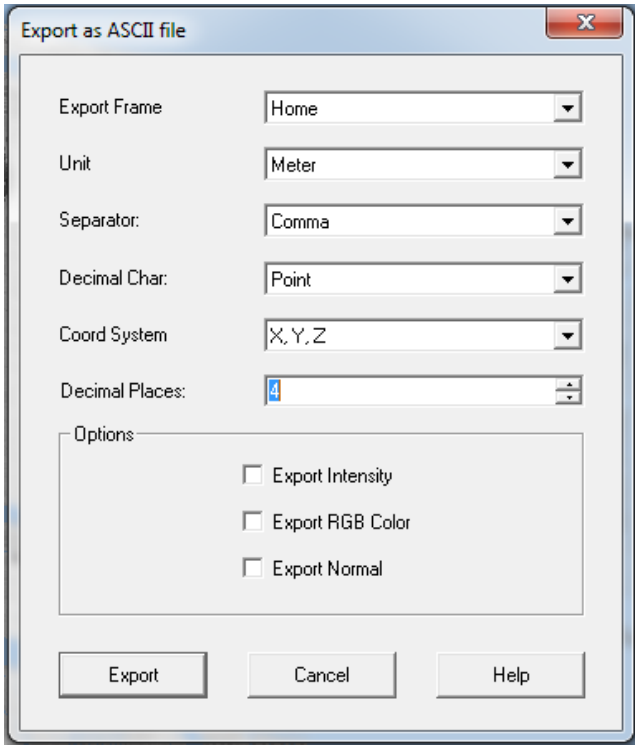

Appendix B

3D As-Built Format Conversion Menus

Autodesk 3ds Max® import menu :

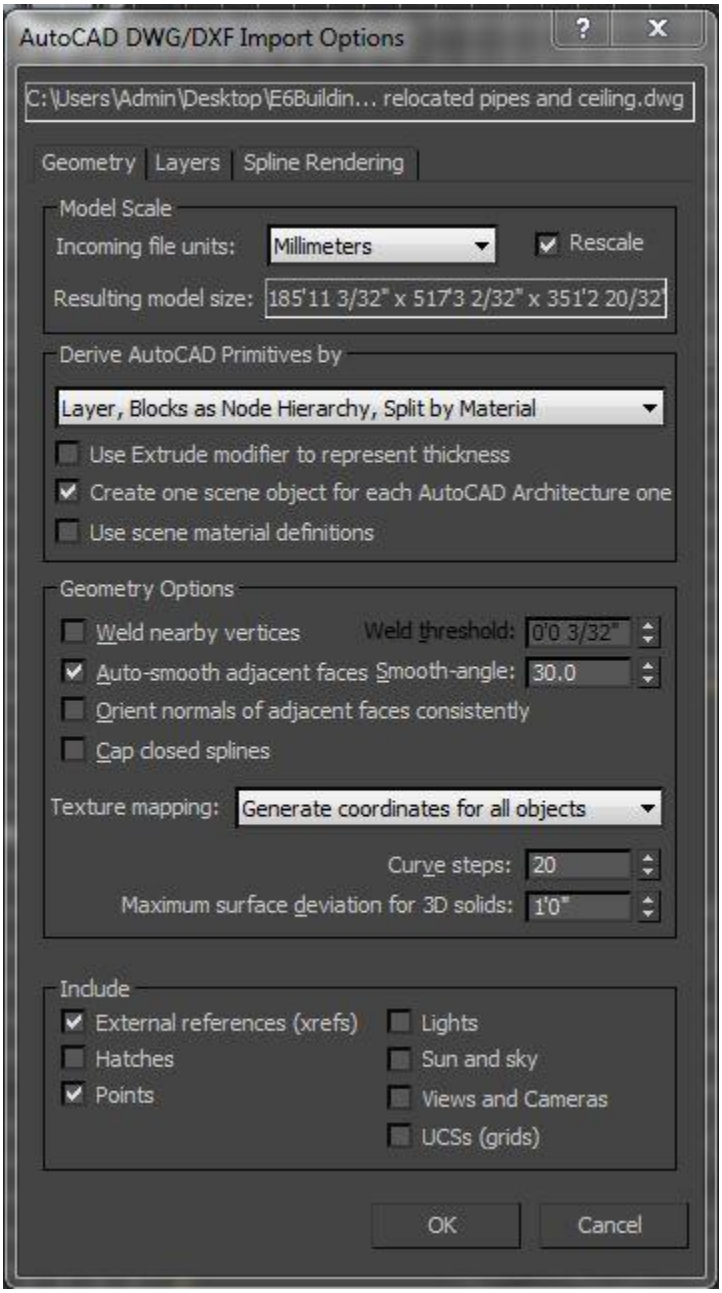

Autodesk 3ds Max® export menu :

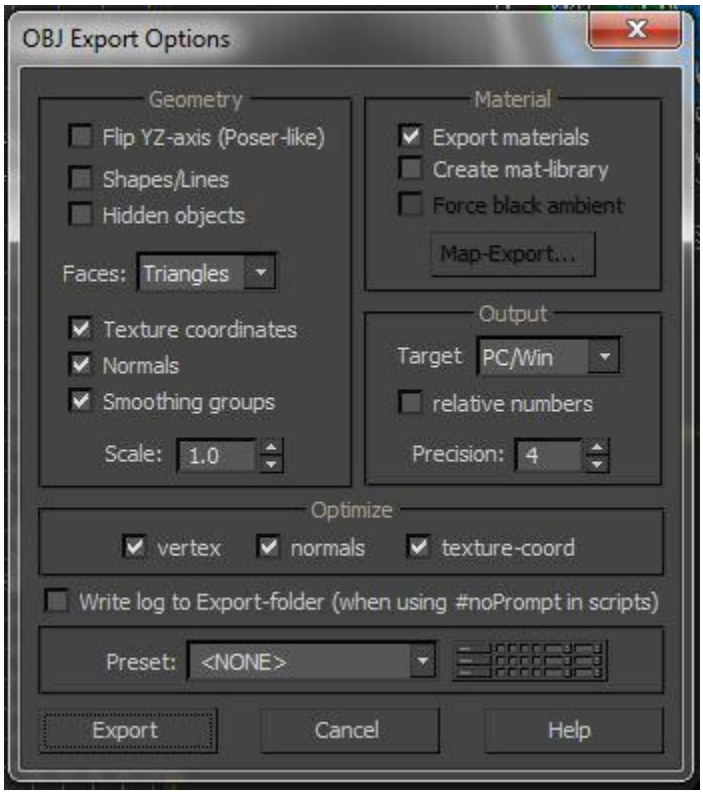

Appendix C

Registration Software

First, the models are selected through the Dialog page with their units:

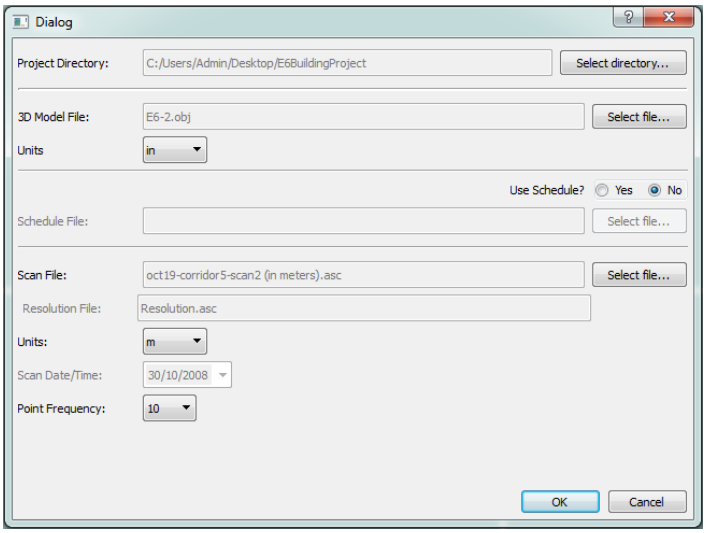

Here is what the interface look like when the 3D as-planned model and the as-built scan are open in the software.

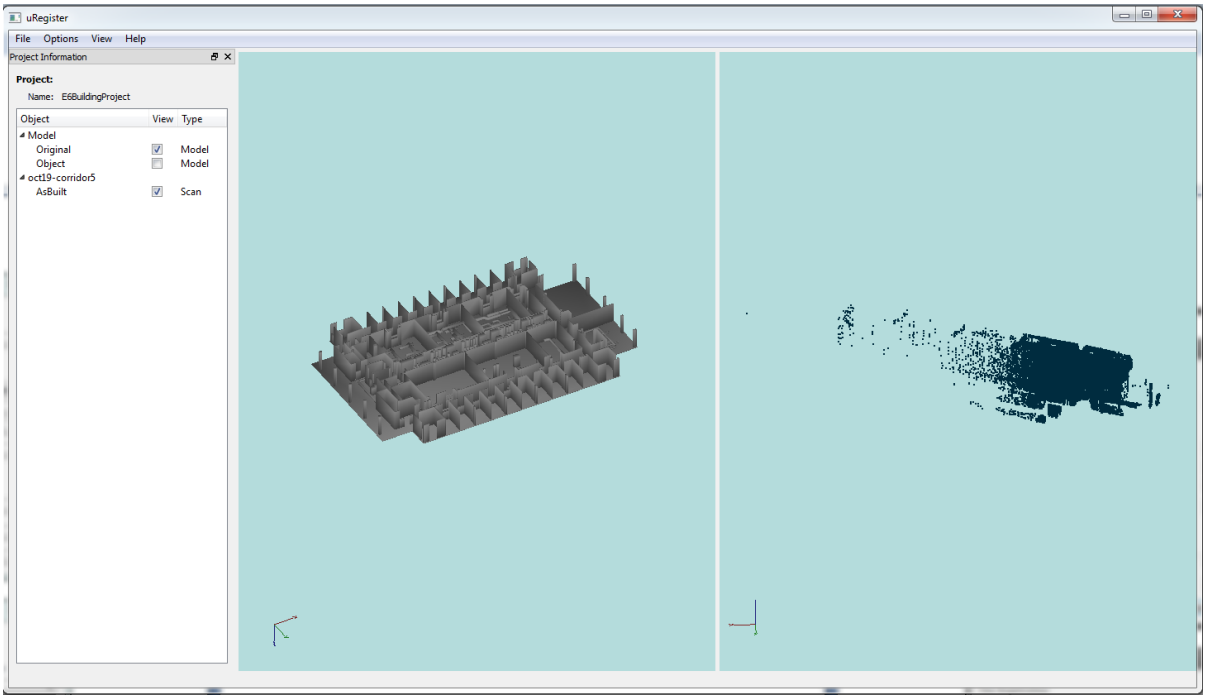

Then, three different planes (2 vertical, 1 horizontal) have to be selectedon both models to be matched up together for the coarse registration. The walls and floor are used as vertical and horizontal planes in this study.

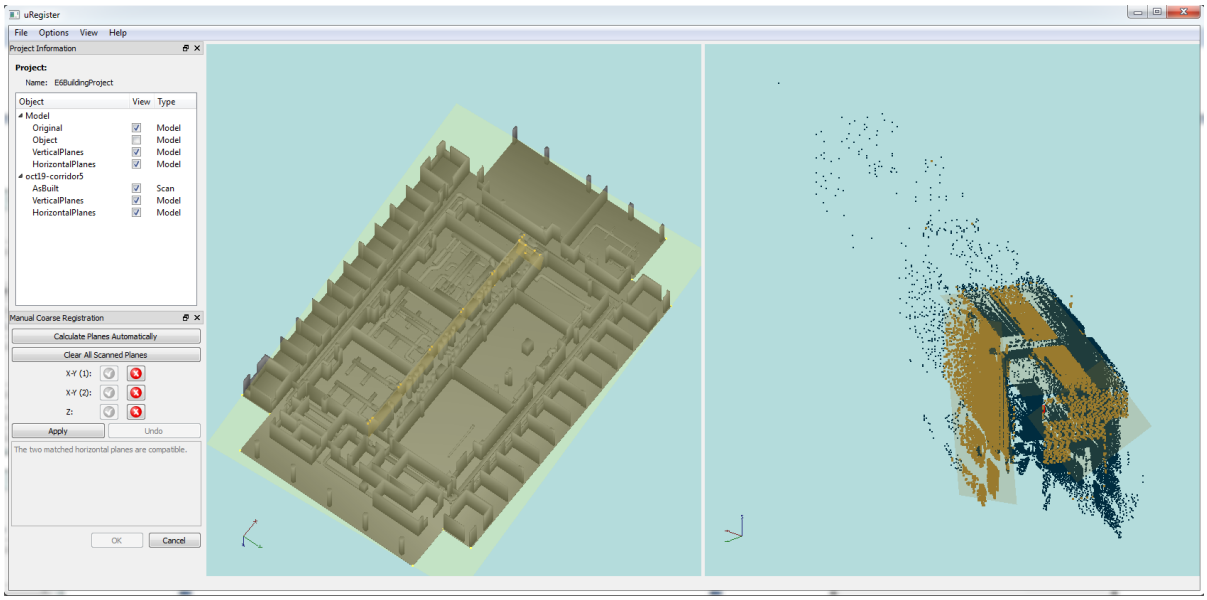

Once the coarse registration has been performed, it is necessary to perform a fine registration to enhance the registration results. The adjustable parameters for the fine registration are as follows:

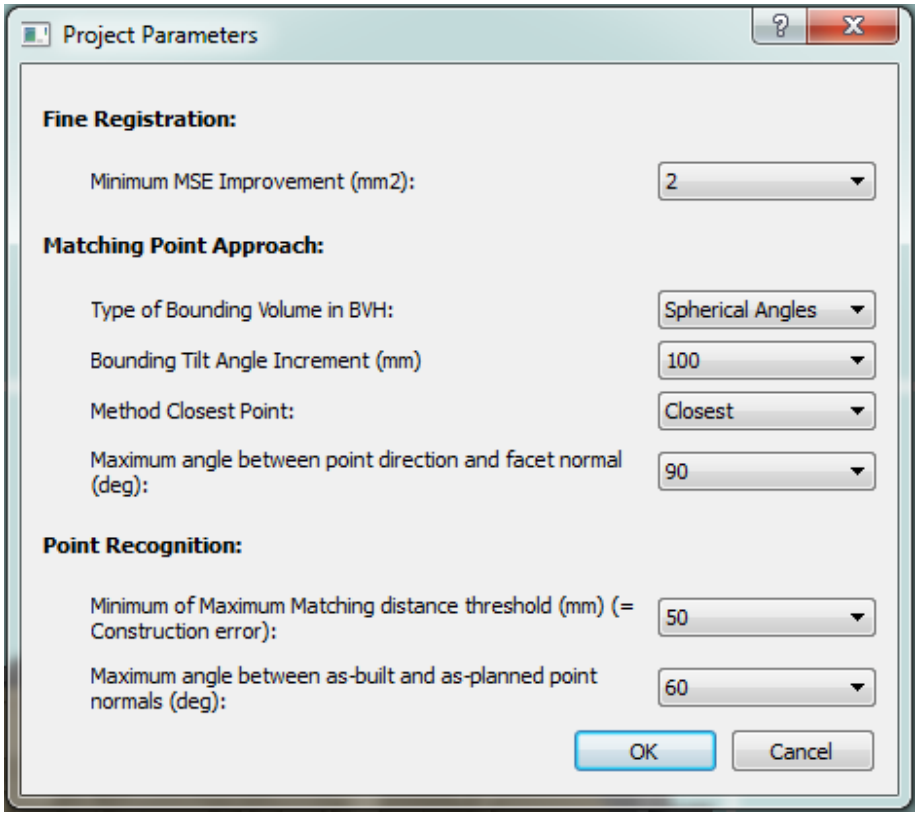

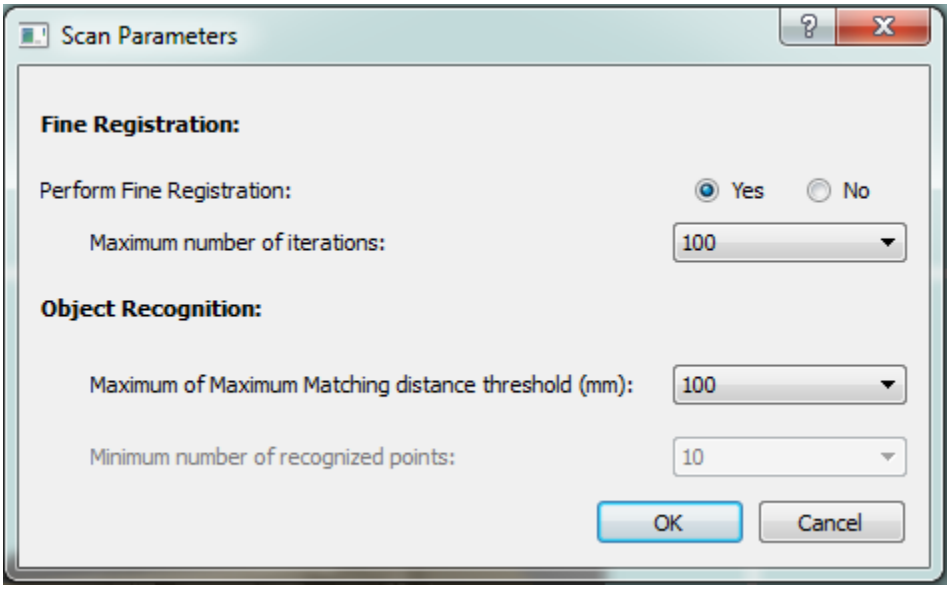

The fine registration has now been performed, and the as-built scan is now matched-up with the 3D as-planned model.

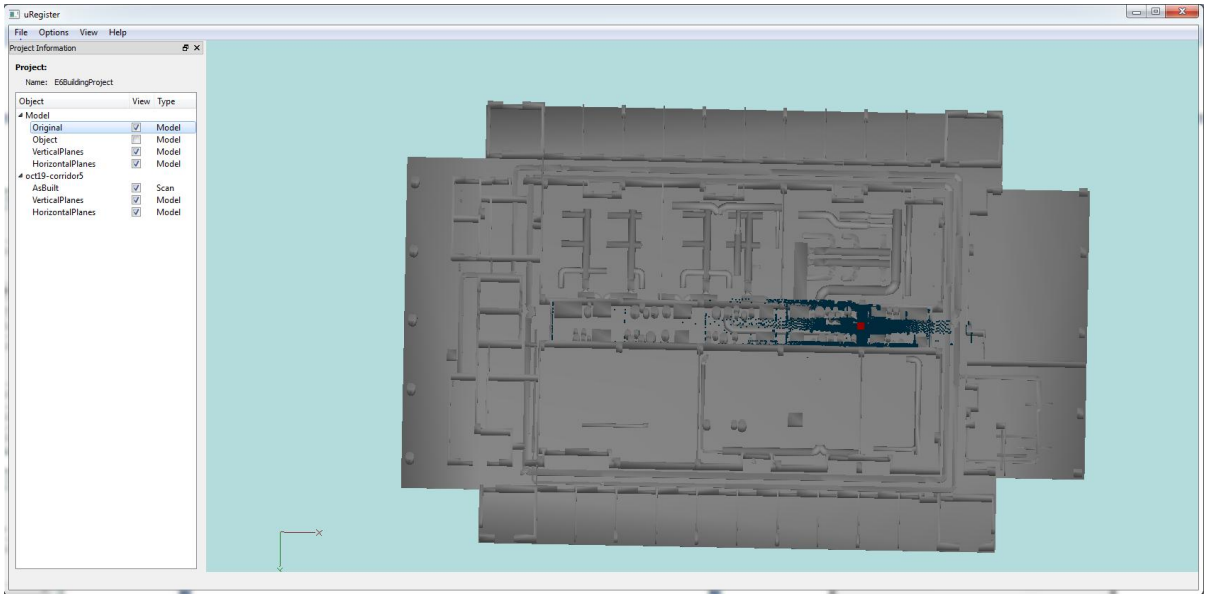

Appendix D

Object Recognition Software

Object Recognition software menus:

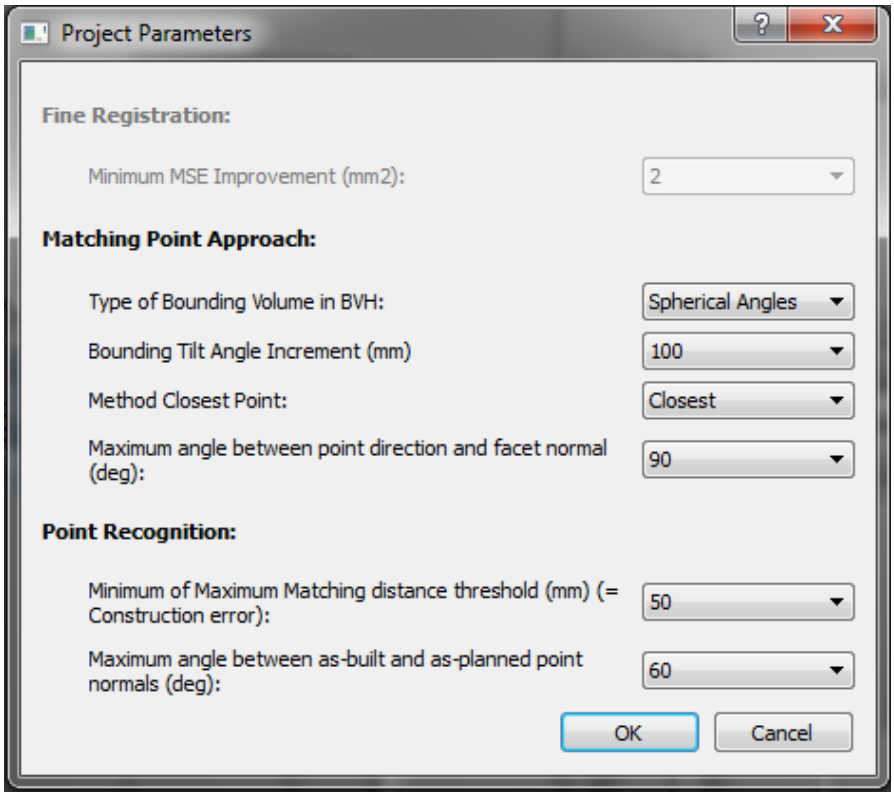

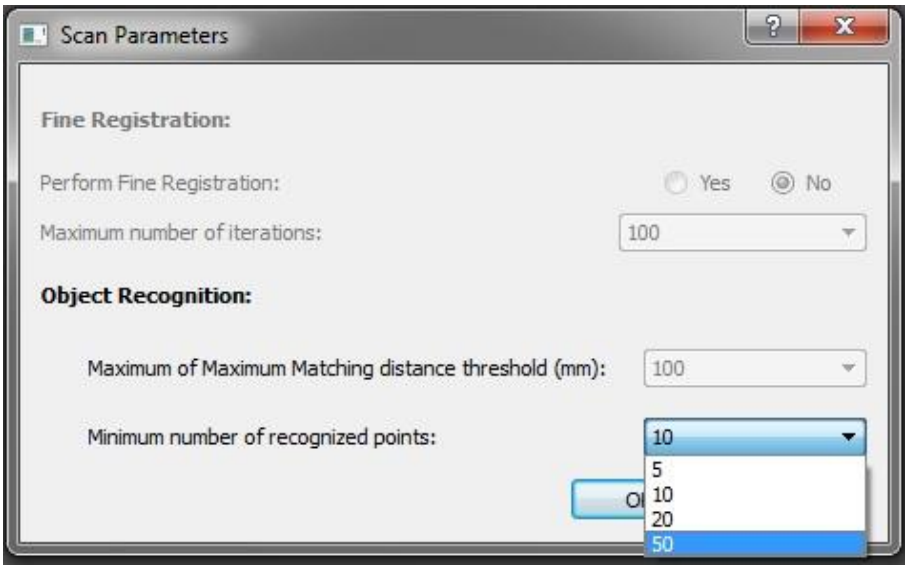

Appendix E

Excel Spreadsheet Results

RECOGNITION PARAMETERS:	
Range Max (m)	43.5714
Unit Surf (m2)	0.0003457
Nmin (pts)	10
SurfMin (1pt) (m2)	0.656386
SurfMin (Nmin pts) (m2)	6.56386

RECOGNITION STATISTICS FOR ALL OBJECTS:

Element name	PCloud (pts)	MCloud (pts)	RCloud (pts)	OCloud (pts)	VSurf (m2)	PSurf (m2)	MSurf (m2)	RSurf (m2)	OSurf (m2)	Schedule Status	Scan Planned	Recognized	Recognition Percent	Occlusion Percent
Layer_M_HVAC_DUCT_EXHS	0	0	0	0	6.277729	0	0	0	0	1	0	0	0	0
Layer_M_HVAC_DUCT_EXHS	0	0	0	0	8.199349	0	0	0	0	1	0	0	0	0
Layer_M_HVAC_DUCT_EXHS	0	0	0	0	4.61209	0	0	0	0	1	0	0	0	0
Layer_M_HVAC_DUCT_EXHS	0	0	0	0	5.579801	0	0	0	0	1	0	0	0	0
Layer_M_HVAC_DUCT_EXHS	0	0	0	0	7.442509	0	0	0	0	1	0	0	0	0
Layer_M_HVAC_DUCT_EXHS	0	0	0	0	5.579798	0	0	0	0	1	0	0	0	0
Layer_M_HVAC_DUCT_EXHS	0	0	0	0	0.472551	0	0	0	0	1	0	0	0	0
Layer_M_HVAC_DUCT_EXHS	0	0	0	0	0.472499	0	0	0	0	1	0	0	0	0
Layer_M_HVAC_DUCT_EXHS	0	0	0	0	2.049794	0	0	0	0	1	0	0	0	0
Layer_M_HVAC_DUCT_EXHS	0	0	0	0	1.569446	0	0	0	0	1	0	0	0	0
Layer_M_HVAC_DUCT_EXHS	0	0	0	0	3.202808	0	0	0	0	1	0	0	0	0
Layer_M_HVAC_DUCT_EXHS	0	0	0	0	2.594345	0	0	0	0	1	0	0	0	0
Layer_M_HVAC_DUCT_EXHS	0	0	0	0	2.049796	0	0	0	0	1	0	0	0	0
Layer_M_HVAC_DUCT_EXHS	0	0	0	0	1.569509	0	0	0	0	1	0	0	0	0
Layer_M_HVAC_DUCT_EXHS	0	0	0	0	2.594361	0	0	0	0	1	0	0	0	0
Layer_M_HVAC_DUCT_EXHS	0	0	0	0	6.645356	0	0	0	0	1	0	0	0	0
Layer_M_HVAC_DUCT_EXHS	0	0	0	0	2.049741	0	0	0	0	1	0	0	0	0
Layer_M_HVAC_DUCT_EXHS	0	0	0	0	4.61218	0	0	0	0	1	0	0	0	0

Layer_M_HVAC_DUCT_EXHS	0	0	0	0	1.153149	0	0	0	0	1	0	0	0	0
Layer_M_HVAC_DUCT_EXHS	6	14	0	0	2.161987	0.005994	0.031646	0	0	1	0	0	0	0
Layer_M_HVAC_DUCT_EXHS	24	82	54	1	2.161955	0.057322	0.37533	0.239454	0.001062	1	0	0	1	0.0185348
Layer_M_HVAC_DUCT_EXHS	0	0	0	0	2.049697	0	0	0	0	1	0	0	0	0
Layer_M_HVAC_DUCT_EXHS	0	13	13	0	2.161853	0	0.053877	0.0538769	0	1	0	0	0	0
Layer_M_HVAC_DUCT_EXHS	0	0	0	0	2.594359	0	0	0	0	1	0	0	0	0
Layer_M_HVAC_DUCT_EXHS	0	0	0	0	2.594381	0	0	0	0	1	0	0	0	0
Layer_M_HVAC_DUCT_EXHS	0	0	0	0	0.80069	0	0	0	0	1	0	0	0	0
Layer_M_HVAC_DUCT_EXHS	0	3	0	1	3.875548	0	0.037384	0	0.011671	1	0	0	0	0
Layer_M_HVAC_DUCT_EXHS	0	0	0	0	3.875639	0	0	0	0	1	0	0	0	0
Layer_M_HVAC_DUCT_EXHS	0	1	0	1	3.843535	0	0.01243	0	0.01243	1	0	0	0	0
Layer_M_HVAC_DUCT_EXHS	0	32	30	0	2.594363	0	0.370505	0.358605	0	1	0	0	0	0
Layer_M_HVAC_DUCT_EXHS	0	0	0	0	3.202866	0	0	0	0	1	0	0	0	0
Layer_M_HVAC_DUCT_EXHS	0	0	0	0	3.875548	0	0	0	0	1	0	0	0	0
Layer_M_HVAC_DUCT_EXHS	0	0	0	0	2.049762	0	0	0	0	1	0	0	0	0
Layer_M_HVAC_DUCT_EXHS	9	31	0	1	2.594349	0.135434	0.610228	0	0.000488	1	0	0	0	0.00359976
Layer_M_HVAC_DUCT_EXHS	0	0	0	0	7.206438	0	0	0	0	1	0	0	0	0
Layer_M_HVAC_DUCT_EXHS	0	0	0	0	1.220622	0	0	0	0	1	0	0	0	0
Layer_M_HVAC_DUCT_SUPP	0	0	0	0	7.350101	0	0	0	0	1	0	0	0	0
Layer_M_HVAC_DUCT_SUPP	4	1	0	1	7.350098	11.6559	2.71226	0	2.71226	1	1	0	0	0.232694
Layer_M_HVAC_DUCT_SUPP	7	6	0	6	5.160081	2.07498	0.803008	0	0.803008	1	0	0	0	0.386995
Layer_M_HVAC_DUCT_EXHS	0	0	0	0	7.206522	0	0	0	0	1	0	0	0	0
Layer_M_HVAC_DUCT_EXHS	0	3	0	3	3.875556	0	0.045192	0	0.045192	1	0	0	0	0
Layer_M_HVAC_DUCT_EXHS	0	0	0	0	0.305119	0	0	0	0	1	0	0	0	0
Layer_M_HVAC_DUCT_EXHS	0	0	0	0	0.305137	0	0	0	0	1	0	0	0	0
Layer_M_HVAC_DUCT_EXHS	0	0	0	0	0.305157	0	0	0	0	1	0	0	0	0
Layer_M_HVAC_DUCT_EXHS	0	0	0	0	0.305153	0	0	0	0	1	0	0	0	0
Layer_M_HVAC_DUCT_EXHS	45	792	761	21	3.229491	0.145337	4.87862	4.68294	0.012313	1	0	0	1	0.0847197
Layer_M_HVAC_DUCT_EXHS	0	0	0	0	2.594349	0	0	0	0	1	0	0	0	0
Layer_M_HVAC_DUCT_SUPP	245	1054	452	505	5.85	0.911811	3.7595	1.18567	2.41373	1	0	0	0	1
Layer_M_HVAC_DUCT_SUPP	121	1377	1083	26	5.16001	0.594137	3.09134	1.53069	0.054774	1	0	0	1	0.0921912
Layer_M_HVAC_DUCT_EXHS	0	0	0	0	8.199356	0	0	0	0	1	0	0	0	0
Layer_M_HVAC_DUCT_SUPP	0	0	0	0	8.1601	0	0	0	0	1	0	0	0	0
Layer_M_HVAC_DUCT_SUPP	0	0	0	0	5.160002	0	0	0	0	1	0	0	0	0
Layer_M_HVAC_DUCT_EXHS	0	0	0	0	7.206522	0	0	0	0	1	0	0	0	0
Layer_M_HVAC_DUCT_EXHS	0	0	0	0	0.211898	0	0	0	0	1	0	0	0	0
Layer_M_HVAC_DUCT_SUPP	2	3	0	0	7.350004	0.076881	0.11546	0	0	1	0	0	0	0
Layer_M_HVAC_DUCT_SUPP	1	14	5	7	8.160004	0.247423	3.87173	1.25791	2.00621	1	0	0	0	1
Layer_M_HVAC_DUCT_EXHS	0	0	0	0	8.199403	0	0	0	0	1	0	0	0	0
Layer_M_HVAC_DUCT_EXHS	0	2	0	0	2.049788	0	0.1023	0	0	1	0	0	0	0
Layer_M_HVAC_DUCT_SUPP	2675	12030	11078	294	10.58002	7.35095	26.2414	24.2692	0.747505	1	1	1	1	0.101688
Layer_M_HVAC_DUCT_SUPP	0	0	0	0	0.135014	0	0	0	0	1	0	0	0	0
Layer_M_HVAC_DUCT_SUPP	0	0	0	0	0.112514	0	0	0	0	1	0	0	0	0
Layer_M_HVAC_DUCT_EXHS	0	0	0	0	0.472555	0	0	0	0	1	0	0	0	0
Layer_M_HVAC_DUCT_EXHS	0	0	0	0	0.472551	0	0	0	0	1	0	0	0	0
Layer_M_HVAC_DUCT_SUPP	0	0	0	0	0.1125	0	0	0	0	1	0	0	0	0
Layer_M_HVAC_DUCT_SUPP	0	0	0	0	0.1125	0	0	0	0	1	0	0	0	0

Layer_M_HVAC_DUCT_SUPP	0	0	0	0	0.112514	0	0	0	0	1	0	0	0	0
Layer_M_HVAC_DUCT_SUPP	0	1	0	1	7.350103	0	0.104735	0	0.104735	1	0	0	0	0
Layer_M_HVAC_DUCT_EXHS	0	0	0	0	7.20654	0	0	0	0	1	0	0	0	0
Layer_M_HVAC_DUCT_EXHS	0	0	0	0	3.875522	0	0	0	0	1	0	0	0	0
Layer_M_HVAC_DUCT_EXHS	0	0	0	0	2.594349	0	0	0	0	1	0	0	0	0
Layer_M_HVAC_DUCT_EXHS	41	385	299	0	2.049746	0.250849	1.67974	0.863435	0	1	0	0	1	0
Layer_M_HVAC_DUCT_EXHS	116	516	294	218	17.385	1.34095	9.74669	8.05416	1.61434	1	0	1	0	1
Layer_M_HVAC_DUCT_EXHS	0	0	0	0	1.175084	0	0	0	0	1	0	0	0	0
Layer_M_HVAC_DUCT_EXHS	0	0	0	0	1.175076	0	0	0	0	1	0	0	0	0
Layer_M_HVAC_DUCT_EXHS	0	0	0	0	2.162038	0	0	0	0	1	0	0	0	0
Layer_M_HVAC_DUCT_EXHS	0	0	0	0	2.162038	0	0	0	0	1	0	0	0	0
Layer_M_HVAC_DUCT_SUPP	0	0	0	0	2.56	0	0	0	0	1	0	0	0	0
Layer_M_HVAC_DUCT_EXHS	0	0	0	0	3.875559	0	0	0	0	1	0	0	0	0
Layer_M_HVAC_DUCT_EXHS	0	0	0	0	3.202801	0	0	0	0	1	0	0	0	0
Layer_M_HVAC_DUCT_EXHS	0	0	0	0	3.875656	0	0	0	0	1	0	0	0	0
Layer_M_HVAC_DUCT_EXHS	0	0	0	0	3.875522	0	0	0	0	1	0	0	0	0
Layer_M_HVAC_DUCT_EXHS	0	0	0	0	2.594367	0	0	0	0	1	0	0	0	0
Layer_M_HVAC_DUCT_EXHS	0	0	0	0	5.412785	0	0	0	0	1	0	0	0	0
Layer_M_HVAC_DUCT_EXHS	0	0	0	0	3.202817	0	0	0	0	1	0	0	0	0
Layer_M_HVAC_DUCT_EXHS	0	0	0	0	3.202863	0	0	0	0	1	0	0	0	0
Layer_M_HVAC_DUCT_EXHS	0	0	0	0	3.202808	0	0	0	0	1	0	0	0	0
Layer_M_HVAC_DUCT_EXHS	3	10	3	7	3.202808	0.035056	0.119281	0.0390081	0.080272	1	0	0	0	1
Layer_M_HVAC_DUCT_EXHS	0	0	0	0	3.202808	0	0	0	0	1	0	0	0	0
Layer_M_HVAC_DUCT_EXHS	1	54	0	0	0.960942	0.001405	0.031382	0	0	1	0	0	0	0
Layer_M_HVAC_DUCT_EXHS	0	0	0	0	0.176244	0	0	0	0	1	0	0	0	0
Layer_M_HVAC_DUCT_EXHS	187	421	107	209	393.5116	35.9185	70.7875	2.30122	67.3039	1	1	0	0	1
Layer_M_HVAC_DUCT_SUPP	0	0	0	0	90.82179	0	0	0	0	1	0	0	0	0
Layer_M_HVAC_DUCT_EXHS	0	0	0	0	2.452248	0	0	0	0	1	0	0	0	0
Layer_M_HVAC_DUCT_EXHS	0	0	0	0	1.56948	0	0	0	0	1	0	0	0	0
Layer_M_HVAC_DUCT_EXHS	0	0	0	0	3.202833	0	0	0	0	1	0	0	0	0
Layer_M_HVAC_DUCT_SUPP	0	0	0	0	5.160077	0	0	0	0	1	0	0	0	0
Layer_M_HVAC_DUCT_EXHS	0	0	0	0	6.277729	0	0	0	0	1	0	0	0	0
Layer_M_HVAC_DUCT_EXHS	0	0	0	0	8.199349	0	0	0	0	1	0	0	0	0
Layer_M_HVAC_DUCT_EXHS	0	0	0	0	2.452248	0	0	0	0	1	0	0	0	0
Layer_M_HVAC_DUCT_EXHS	0	0	0	0	4.61209	0	0	0	0	1	0	0	0	0
Layer_M_HVAC_DUCT_EXHS	0	0	0	0	5.579801	0	0	0	0	1	0	0	0	0
Layer_M_HVAC_DUCT_EXHS	0	0	0	0	7.442509	0	0	0	0	1	0	0	0	0
Layer_M_HVAC_DUCT_EXHS	0	0	0	0	5.579798	0	0	0	0	1	0	0	0	0
Layer_M_HVAC_DUCT_EXHS	0	0	0	0	0.472551	0	0	0	0	1	0	0	0	0
Layer_M_HVAC_DUCT_EXHS	0	0	0	0	0.472499	0	0	0	0	1	0	0	0	0
Layer_M_HVAC_DUCT_EXHS	0	0	0	0	2.049794	0	0	0	0	1	0	0	0	0
Layer_M_HVAC_DUCT_EXHS	0	0	0	0	1.569446	0	0	0	0	1	0	0	0	0
Layer_M_HVAC_DUCT_EXHS	0	0	0	0	3.202808	0	0	0	0	1	0	0	0	0
Layer_M_HVAC_DUCT_EXHS	0	0	0	0	2.594345	0	0	0	0	1	0	0	0	0
Layer_M_HVAC_DUCT_EXHS	0	0	0	0	2.049796	0	0	0	0	1	0	0	0	0
Layer_M_HVAC_DUCT_EXHS	0	0	0	0	1.569509	0	0	0	0	1	0	0	0	0
Layer_M_HVAC_DUCT_EXHS	0	0	0	0	2.594361	0	0	0	0	1	0	0	0	0

Layer_M_HVAC_DUCT_EXHS	0	0	0	0	6.645356	0	0	0	0	1	0	0	0	0
Layer_M_HVAC_DUCT_EXHS	0	0	0	0	2.049741	0	0	0	0	1	0	0	0	0
Layer_M_HVAC_DUCT_EXHS	0	0	0	0	4.61218	0	0	0	0	1	0	0	0	0
Layer_M_HVAC_DUCT_EXHS	0	0	0	0	1.153149	0	0	0	0	1	0	0	0	0
Layer_M_HVAC_DUCT_EXHS	0	0	0	0	1.569498	0	0	0	0	1	0	0	0	0
Layer_M_HVAC_DUCT_EXHS	0	0	0	0	3.202833	0	0	0	0	1	0	0	0	0
Layer_M_HVAC_DUCT_EXHS	3	14	0	0	2.161987	0.013097	0.018387	0	0	1	0	0	0	0
Layer_M_HVAC_DUCT_EXHS	27	26	0	3	2.161955	0.058299	0.107116	0	0.002996	1	0	0	0	0.0513982
Layer_M_HVAC_DUCT_EXHS	0	0	0	0	2.049697	0	0	0	0	1	0	0	0	0
Layer_M_HVAC_DUCT_EXHS	0	0	0	0	2.161853	0	0	0	0	1	0	0	0	0
Layer_M_HVAC_DUCT_EXHS	0	0	0	0	2.594359	0	0	0	0	1	0	0	0	0
Layer_M_HVAC_DUCT_EXHS	0	0	0	0	2.594381	0	0	0	0	1	0	0	0	0
Layer_M_HVAC_DUCT_EXHS	0	0	0	0	0.80069	0	0	0	0	1	0	0	0	0
Layer_M_HVAC_DUCT_EXHS	0	0	0	0	3.875548	0	0	0	0	1	0	0	0	0
Layer_M_HVAC_DUCT_EXHS	0	0	0	0	3.875639	0	0	0	0	1	0	0	0	0
Layer_M_HVAC_DUCT_EXHS	0	3	0	3	3.843535	0	0.037338	0	0.037338	1	0	0	0	0
Layer_M_HVAC_DUCT_EXHS	0	2	0	0	2.594363	0	0.011272	0	0	1	0	0	0	0
Layer_M_HVAC_DUCT_EXHS	0	0	0	0	3.202866	0	0	0	0	1	0	0	0	0
Layer_M_HVAC_DUCT_EXHS	1	0	0	0	3.875548	0.024829	0	0	0	1	0	0	0	0
Layer_M_HVAC_DUCT_EXHS	0	0	0	0	2.049762	0	0	0	0	1	0	0	0	0
Layer_M_HVAC_DUCT_EXHS	0	0	0	0	2.594349	0	0	0	0	1	0	0	0	0
Layer_M_HVAC_DUCT_EXHS	0	0	0	0	7.206438	0	0	0	0	1	0	0	0	0
Layer_M_HVAC_DUCT_EXHS	0	0	0	0	1.220622	0	0	0	0	1	0	0	0	0
Layer_M_HVAC_DUCT_SUPP	0	0	0	0	7.350101	0	0	0	0	1	0	0	0	0
Layer_M_HVAC_DUCT_SUPP	0	0	0	0	7.350098	0	0	0	0	1	0	0	0	0
Layer_M_HVAC_DUCT_SUPP	1	4	0	4	5.160081	0.636956	0.155999	0	0.155999	1	0	0	0	0.244913
Layer_M_HVAC_DUCT_EXHS	0	0	0	0	7.206522	0	0	0	0	1	0	0	0	0
Layer_M_HVAC_DUCT_EXHS	0	2	0	2	3.875556	0	0.028023	0	0.028023	1	0	0	0	0
Layer_M_HVAC_DUCT_EXHS	0	0	0	0	0.305119	0	0	0	0	1	0	0	0	0
Layer_M_HVAC_DUCT_EXHS	0	0	0	0	0.305137	0	0	0	0	1	0	0	0	0
Layer_M_HVAC_DUCT_EXHS	0	0	0	0	0.305157	0	0	0	0	1	0	0	0	0
Layer_M_HVAC_DUCT_EXHS	0	0	0	0	0.305153	0	0	0	0	1	0	0	0	0
Layer_M_HVAC_DUCT_EXHS	49	26	0	12	3.229491	0.20433	0.194526	0	0.007164	1	0	0	0	0.0350622
Layer_M_HVAC_DUCT_EXHS	0	0	0	0	2.594349	0	0	0	0	1	0	0	0	0
Layer_M_HVAC_DUCT_SUPP	207	544	0	450	5.85	0.784497	2.30343	0	2.14308	1	0	0	0	1
Layer_M_HVAC_DUCT_SUPP	97	279	0	32	5.16001	0.522104	1.40933	0	0.065773	1	0	0	0	0.125977
Layer_M_HVAC_DUCT_EXHS	0	0	0	0	8.199356	0	0	0	0	1	0	0	0	0
Layer_M_HVAC_DUCT_SUPP	0	0	0	0	8.1601	0	0	0	0	1	0	0	0	0
Layer_M_HVAC_DUCT_SUPP	0	0	0	0	5.160002	0	0	0	0	1	0	0	0	0
Layer_M_HVAC_DUCT_EXHS	0	0	0	0	7.206522	0	0	0	0	1	0	0	0	0
Layer_M_HVAC_DUCT_EXHS	0	0	0	0	0.211898	0	0	0	0	1	0	0	0	0
Layer_M_HVAC_DUCT_SUPP	4	1	0	0	7.350004	0.154411	1.09001	0	0	1	0	0	0	0
Layer_M_HVAC_DUCT_SUPP	0	4	0	0	5.160002	0	1.65919	0	0	1	0	0	0	0
Layer_M_HVAC_DUCT_SUPP	3	2	0	2	8.160004	0.731795	0.651063	0	0.651063	1	0	0	0	0.88968
Layer_M_HVAC_DUCT_EXHS	2	0	0	0	2.049788	0.101956	0	0	0	1	0	0	0	0
Layer_M_HVAC_DUCT_SUPP	1838	497	0	123	10.58002	4.93276	1.01564	0	0.200969	1	0	0	0	0.0407418
Layer_M_HVAC_DUCT_SUPP	0	0	0	0	0.135014	0	0	0	0	1	0	0	0	0

Layer_M_HVAC_DUCT_SUPP	0	0	0	0	0.112514	0	0	0	0	1	0	0	0	0
Layer_M_HVAC_DUCT_EXHS	0	0	0	0	0.472555	0	0	0	0	1	0	0	0	0
Layer_M_HVAC_DUCT_EXHS	0	0	0	0	0.472551	0	0	0	0	1	0	0	0	0
Layer_M_HVAC_DUCT_SUPP	0	0	0	0	0.1125	0	0	0	0	1	0	0	0	0
Layer_M_HVAC_DUCT_SUPP	0	0	0	0	0.1125	0	0	0	0	1	0	0	0	0
Layer_M_HVAC_DUCT_SUPP	0	0	0	0	0.112514	0	0	0	0	1	0	0	0	0
Layer_M_HVAC_DUCT_SUPP	0	1	0	1	7.350103	0	0.105003	0	0.105003	1	0	0	0	0
Layer_M_HVAC_DUCT_EXHS	0	0	0	0	7.20654	0	0	0	0	1	0	0	0	0
Layer_M_HVAC_DUCT_EXHS	0	0	0	0	3.875522	0	0	0	0	1	0	0	0	0
Layer_M_HVAC_DUCT_EXHS	7	25	0	1	2.594349	0.199362	0.535709	0	0.000727	1	0	0	0	0.00364689
Layer_M_HVAC_DUCT_EXHS	120	246	0	243	17.385	1.36186	1.75977	0	1.69958	1	0	0	0	1
Layer_M_HVAC_DUCT_EXHS	0	0	0	0	1.175084	0	0	0	0	1	0	0	0	0
Layer_M_HVAC_DUCT_EXHS	0	0	0	0	1.175076	0	0	0	0	1	0	0	0	0
Layer_M_HVAC_DUCT_EXHS	0	0	0	0	2.162038	0	0	0	0	1	0	0	0	0
Layer_M_HVAC_DUCT_EXHS	0	0	0	0	2.162038	0	0	0	0	1	0	0	0	0
Layer_M_HVAC_DUCT_SUPP	0	0	0	0	2.56	0	0	0	0	1	0	0	0	0
Layer_M_HVAC_DUCT_EXHS	0	0	0	0	3.875559	0	0	0	0	1	0	0	0	0
Layer_M_HVAC_DUCT_EXHS	0	0	0	0	3.202801	0	0	0	0	1	0	0	0	0
Layer_M_HVAC_DUCT_EXHS	0	0	0	0	3.875648	0	0	0	0	1	0	0	0	0
Layer_M_HVAC_DUCT_EXHS	0	0	0	0	3.875522	0	0	0	0	1	0	0	0	0
Layer_M_HVAC_DUCT_EXHS	0	0	0	0	2.594367	0	0	0	0	1	0	0	0	0
Layer_M_HVAC_DUCT_EXHS	0	0	0	0	5.412785	0	0	0	0	1	0	0	0	0
Layer_M_HVAC_DUCT_EXHS	0	0	0	0	3.202817	0	0	0	0	1	0	0	0	0
Layer_M_HVAC_DUCT_EXHS	0	0	0	0	3.202863	0	0	0	0	1	0	0	0	0
Layer_M_HVAC_DUCT_EXHS	0	0	0	0	3.202808	0	0	0	0	1	0	0	0	0
Layer_M_HVAC_DUCT_EXHS	1	3	0	3	3.202808	0.009633	0.031787	0	0.031787	1	0	0	0	1
Layer_M_HVAC_DUCT_EXHS	0	0	0	0	3.202808	0	0	0	0	1	0	0	0	0
Layer_M_HVAC_DUCT_EXHS	35	58	0	0	0.960942	0.023632	0.041587	0	0	1	0	0	0	0
Layer_M_HVAC_DUCT_EXHS	0	0	0	0	0.176244	0	0	0	0	1	0	0	0	0
Layer_M_HVAC_DUCT_RTUN	0	0	0	0	42.22152	0	0	0	0	1	0	0	0	0
Layer_0	0	0	0	0	7.47805	0	0	0	0	1	0	0	0	0
Layer_7661A_5F_0_A_STRC	63	142	102	0	200.2499	1.77723	1.50671	1.08482	0	1	0	0	0.610398	0
Layer_M_HVAC_DUCT_EXHS	0	0	0	0	6.277836	0	0	0	0	1	0	0	0	0
Layer_7661A_5F_0_A_WALL	11992	45017	36790	5008	4071.918	66.6827	222.034	140.03	69.3648	1	1	1	0	1
Layer_7661A_5F_0_A_WALL	935	3044	2870	157	171.9338	5.78165	14.7412	11.3154	3.36657	1	0	1	1	0.582285
Layer_M_HAVC_INSULATION	10282	24091	4114	3616	570.6567	34.7224	86.6866	18.1853	27.5659	1	1	1	1	0.793893
	29154	90876	58055	10962	6215.74	179.526	465.705	215.452	183.351	195	5	5	1	1